



TECHNISCHE UNIVERSITÄT MÜNCHEN

TUM School of Life Sciences

A contribution to the harmonization of microplastic  
analysis in beverages and food

**Jana Weißer**

Vollständiger Abdruck der von der TUM School of Life Sciences der Technischen Universität München zur Erlangung des akademischen Grades einer

**Doktorin der Naturwissenschaften (Dr. rer. nat.)**

genehmigten Dissertation.

Vorsitzender:

Prof. Dr. Jürgen Geist

Prüfer\*innen der Dissertation:

1. Prof. Dr. Thomas F. Hofmann

2. Priv.-Doz. Dr. Natalia P. Ivleva

3. Prof. Dr. Jes Vollertsen

Die Dissertation wurde am 16.08.2022 bei der Technischen Universität München eingereicht und durch die TUM School of Life Sciences Weihenstephan am 25.01.2023 angenommen.

*Für die, auf die es ankommt. Aber auch für mich.*

# Danksagung

Es gäbe diese Doktorarbeit nicht, hätten mich nicht viele Menschen dabei auf unterschiedlichste Art und Weise unterstützt.

Großer Dank gebührt meinem Doktorvater, Prof. Dr. Thomas Hofmann für das mir entgegengebrachte Vertrauen sowie die gewährte wissenschaftliche Freiheit in der Bearbeitung meines Forschungsprojektes.

Dem Leiter der Arbeitsgruppe Wassertechnologie, Dr. Karl Glas, danke ich von Herzen für die unermüdliche Unterstützung in jedweder Angelegenheit. Selbst die größten Herausforderungen konnte ich dank deiner Hilfe, Karl, überwinden. Ohne die vielen von dir „vom Eis geholten Kühe“ wäre meine Arbeit nicht in dieser Form möglich gewesen.

Auch meiner Mentorin und zweiten Prüferin, PD Dr. Natalia P. Ivleva möchte ich herzlich danken für ihre fachliche Unterstützung, sowie die wertvollen durch sie zustande gekommenen Kontakte.

Für die anregenden Diskussionen im des Rahmen Projekts MiPAq möchte ich mich beim gesamten Konsortium bedanken. Vor allem Dr. Hannes Imhof hatte stets viele wertvolle Tipps für mich auf Lager. Der Bayerischen Forschungstiftung danke ich sehr für die finanzielle Förderung unseres Projektes. Dass der Kontakt zu Prof. Dr. Jürgen Geist auch über das Projekt hinaus bestehen blieb und er den Vorsitz der Prüfungskommission übernimmt, freut mich sehr. Auch hierfür danke ich herzlich.

Die Kolleginnen und Kollegen in der Arbeitsgruppe Wassertechnologie haben nicht nur durch fachbezogene Diskussionen zum Gelingen dieser Arbeit erheblich beigetragen, sondern auch ganz besonders durch die angenehme, kollegiale Arbeitsatmosphäre. Besonderer Dank gilt Sarah Brunschweiler, die mir ein Vorbild war in Durchhaltevermögen, strukturiertem Arbeiten, und positivem Denken. Danke, Sarah, dass du mich immer wieder bestärkt hast!

Vom fachlichen Austausch mit Benedikt Hufnagl und Prof. Dr. Hans Lohninger hat meine Arbeit ganz wesentlich profitiert, wofür ich vielmals danke. Das Etablieren des *Random Decision Forests* an unserem Lehrstuhl ging mir durch die aufschlussreichen Gespräche deutlich leichter von der Hand. Nicht zu vergessen, dass mir für ein Jahr eine kostenfreie Softwarelizenz zur Verfügung gestellt wurde, wofür ich mich ebenfalls herzlich bedanke.

So kurz mein Aufenthalt an der Aalborg Universität, Dänemark, war, so war er doch von unschätzbarem Wert. Jes Vollertsen, thank you very much for having me as a guest at your chair. Alwise Vianello, thank you so much for letting me join your workshop and answering all my stupid questions. Nikki van Alst, it was a pleasure to meet you! Your advices for dealing with the sometimes tricky FTIR machine were really precious.

Großer Dank gilt außerdem dem Werkstattteam im Lebensmitteltechnikum, die nicht nur hilfreiche Tipps zur Umsetzung meiner Ideen hatten, sondern auch jede Sonderanfertigung mit größter Präzision durchführten.

Es gab viel zu tun – darum bin ich sehr froh und dankbar, dass insgesamt 15 Studierende mit großem Engagement ihre Abschlussarbeiten oder Forschungspraktika bei mir im „Mikroplastik-Labor“ durchgeführt haben. Eure Arbeiten haben wesentlich zu meiner Forschung beigetragen und es hat mir viel Spaß gemacht, ein kleines Team um mich zu haben. Dazu haben auch die fleißigen Hiwis gehört, denen ich ebenfalls herzlich für Ihre Mitarbeit danken möchte.

Meine Freunde mussten einiges hinnehmen während meiner Promotion. Gerade in der heißen Phase gen Ende hatte ich nicht immer Zeit für euch oder war mit dem Kopf ständig bei der „Diss“. Das habt ihr geduldig ertragen und mich immer wieder auf andere Gedanken gebracht. Das Leben ist eben nicht nur Wissenschaft. Ich bin so froh, euch schon so viele Jahre an meiner Seite zu wissen! Ihr wisst, wen ich meine.

Gleiches gilt für meine Familie, die alle Hochs und Tiefs miterlebt und ertragen hat. Aber nicht nur dafür möchte ich von Herzen danken, sondern noch weit darüber hinaus: MaPi, wäre ich nicht von euch immer wieder bestärkt und gefördert worden, so wäre ich sicher nicht da, wo ich heute stehe. Fabia, du hast mich nach Kräften auch aus den fernen USA moralisch unterstützt und meine Arbeit sprachlich poliert. Ich kann euch gar nicht genug danken! Ich hab euch lieb.

Mein wichtigster moralischer und manchmal auch fachlicher Unterstützer war stets ganz nah bei mir: Michi, was wäre ich nur ohne dich! Du hast alle Hochs und Tiefs miterlebt, mir zugehört, mich ermutigt, mich inspiriert. Und das, obwohl du selbst denselben Stress durchmachst. Wir sind ein großartiges Team und ich bin unendlich dankbar, dich in meinem Leben zu haben. Auf unsere Zukunft!

## **Vorbemerkung**

Der praktische Teil dieser Arbeit wurde von September 2017 bis Juni 2022 in der Arbeitsgruppe Wassertechnologie unter der Leitung von Dr. Karl Glas am Lehrstuhl für Lebensmittelchemie und molekulare Sensorik unter der Leitung von Prof. Dr. Thomas Hofmann beziehungsweise Prof. Dr. Corinna Dawid (ab 01. Oktober 2019) an der School of Life Sciences Weihenstephan der Technischen Universität München durchgeführt.

Die wissenschaftlichen Veröffentlichungen und Abbildungen wurden mit Genehmigung der jeweiligen wissenschaftlichen Journale abgedruckt beziehungsweise bedürfen keiner gesonderten Genehmigung zum Abdruck, da sie unter Creative Commons CC-BY Lizenz veröffentlicht wurden.

## Publications

Parts of this work have already been published elsewhere:

### Peer reviewed articles as the main author

**Weisser J**, Pohl T, Ivleva NP, Hofmann T, Glas K. Know what you don't know: assessment of overlooked microplastic particles in FTIR images. *Microplastics*. 2022;1(3):359. DOI 10.3390/microplastics1030027

**Weisser J**, Pohl T, Heinzinger M, Ivleva NP, Hofmann T, Glas K. The identification of microplastics based on vibrational spectroscopy data – A critical review of data analysis routines. *TrAC Trends in Analytical Chemistry*. 2022;148:116535. DOI 10.1016/j.trac.2022.116535

**Weisser J**, Beer I, Hufnagl B, Hofmann T, Lohninger H, Ivleva NP, Glas, K. From the Well to the Bottle: Identifying Sources of Microplastics in Mineral Water. *Water*. 2021;13(6):841. DOI 10.3390/w13060841

The editorial board of *Water* chose this article as the cover story for the journal's issue number 6 in volume 13.

### Peer reviewed articles as a co-author

Schymanski D, Oßmann BE, Benismail N, Boukerma K, Dallmann G, von der Esch E, Fischer D, Fischer F, Gilliland D, Glas K, Hofmann T, Käßler A, Lacorte S, Marco J, Rakwe MEL, **Weisser J**, Witzig C, Zumbülte N, Ivleva NP. Analysis of microplastics in drinking water and other clean water samples with micro-Raman and micro-infrared spectroscopy: minimum requirements and best practice guidelines. *Analytical and Bioanalytical Chemistry*. 2021;413:5969-94. DOI 10.1007/s00216-021-03498-y

Al-Azzawi MSM, Kefer S, **Weißer J**, Reichel J, Schwaller C, Glas K, Knoop O, Drewes JE. Validation of Sample Preparation Methods for Microplastic Analysis in Wastewater Matrices—Reproducibility and Standardization. *Water*. 2020;12(9):2445. DOI 10.3390/w12092445

Brunschweiger S, Ojong ET, **Weisser J**, Schwaferts C, Elsner M, Ivleva NP, Haseneder R, Hofmann T, Glas K. The effect of clogging on the long-term stability of different carbon fiber brushes in microbial fuel cells for brewery wastewater treatment. *Bioresource Technology Reports*. 2020;11:100420. DOI 10.1016/j.biteb.2020.100420

von der Esch E, Lanzinger M, Kohles A, Schwaferts C, **Weisser J**, Hofmann T, Glas K, Elsner M, Ivleva NP. Simple Generation of Suspensible Secondary Microplastic Reference Particles via Ultrasound Treatment. *Frontiers in Chemistry*. 2020;8. DOI 10.3389/fchem.2020.00169

## Non-peer reviewed articles

Imhof HK, Al-Azzawi MSM, Bartonitz A, Beggel S, Drewes JE, Elsner M, von der Esch E, Glas K, Ivleva NP, Kefer S, Knoop O, Langowski HC, Miesbauer O, Reichel J, Schwaferts C, **Weisser J**, Geist J. Der Eintrag von Mikroplastik in Lebensmittel und die Aquatischen Umwelt und seine Folgen – aktuelle Fragen und Antworten. Mitteilungen der Fachgruppe Umweltchemie und Ökotoxikologie – Gesellschaft deutscher Chemiker GdCh, 26. Jahrgang. 2020/ Nr. 2.

Al-Azzawi MSM, **Weißer J**, Kefer S, Knoop O, Drewes JE. Microplastic contamination in the aquatic environments: Validation and reproducibility of sample preparation methods. Gesellschaft Deutscher Chemiker, Fachgruppe Wasserchemische Gesellschaft, Kurzreferate zur Wasser 2020. S. 45-49.

**Weißer J**, Mödinger M, Glas K. Mikroplastik – Bedrohung der Umwelt und unserer Lebensmittel? Der Weihenstephaner, Nr.2, 208 (86. Jahrgang), S. 82-84.

## Standards

**DIN/TS 10068 Vornorm: 2022-09, Lebensmittel - Bestimmung von Mikroplastik - Analytische Verfahren**

Elaborated by NA 057 DIN-Normenausschuss Lebensmittel und landwirtschaftliche Produkte (NAL), NA 057-08-05 AAH Arbeitsausschuss Bestimmung von Mikroplastik in Lebensmitteln. **Jana Weißer** has been a member of this standardization body since its foundation in December 2019.

## Conference papers

**Weisser J**, Pohl T, Ivleva NP, Hofmann T, Glas K. Finding microplastics in hyperspectral images – a guide through current methods. SETAC Europe 2022 Meeting abstract book. ONLINE ISSN 2310-3043. <https://europe2022.setac.org/wp-content/uploads/2022/05/SE-2022-abstract-book-v1.pdf>

Al-Azzawi MSM, **Weißer J**, Kefer S, Knoop O, Drewes JE. Microplastic contamination in the aquatic environments: Validation and reproducibility of sample preparation methods. Paper No. V 010. Kurzreferate zur Wasser 2020. Gesellschaft Deutscher Chemiker, Fachgruppe Wasserchemische Gesellschaft.

## Oral presentations at conferences

**Weisser J**, Ivleva NP, Hofmann T, Glas K. Finding microplastics in hyperspectral images – a guide through current methods. SETAC Europe 2022. 16.05.2022. Hybrid event in Copenhagen, Denmark, plus web attendance.

**Weisser J**, Murer L, Bramberger A. Analysis and Occurrence of Microplastics in Connection with Food Contact Materials (invited talk). Symposium Food Contact Materials. 22.12.2021. Web conference.

**Weisser J**. Challenges in analyzing microplastics (invited talk). ILSI Europe Webinar: Consumer questions about microplastics in food - the science perspective. 29.11.2021. Web conference.

**Weisser J**. Approaches for the Detection of Microplastics through Spectroscopy with a Focus on FTIR imaging (invited talk). Agilent Microplastics in the Environment Virtual Symposium 2021. 30.09.2021. Web conference.

**Weisser J**. Entry of Microplastics into Packaged Food and Beverages – the Example of Bottled Mineral Water. EFSA Scientific Colloquium N° 25, A coordinated approach to assess the human health risks of micro- and nanoplastics in food. 06.05.2021. Web conference.

**Weisser J**. Microplastics in Food: Occurrence, Consequences and Solutions. BIOFACH/VIVANESS eSPECIAL. 18.02.2021. Web conference.

**Weisser J**, Glas K. Analyse pflanzlicher Lebensmittel und Getränke mittels FTIR Imaging und Random Decision Forests. Durchführung des § 64 LFGB, hier: Kick-off-Meeting zum Thema Mikroplastik in Lebensmitteln, Bundesamt für Verbraucherschutz und Lebensmittelsicherheit. 03.12.2020. Web conference.

**Weisser J**. Mikroplastik in Getränken: Methoden zur Probenvorbereitung und Analyse. Seminar Mikroplastik der Qualitätsgemeinschaft Bio-Mineralwasser e.V.. 17.11.2020. Web conference.

**Weisser J**. Erkenntnisse bisheriger Mineralwasseruntersuchungen im Rahmen des Projekts "Mikropartikel in der Aquatischen Umwelt und in Lebensmitteln". Seminar Mikroplastik der Qualitätsgemeinschaft Bio-Mineralwasser e.V.. 17.11.2020. Web conference.

**Weisser J**, Glas K. Mikroplastik in Getränken – ein Update zum Stand der Wissenschaft. 53. Technologisches Seminar. 13.02.2020. Freising.

**Weisser J**. Microplastics in Drinking Water. BIOFACH 2020. 12.02.2020. Nürnberg.

**Weisser J**. Nachweis von Mikroplastik in Lebensmitteln. Workshop Automatisierungsansätze in der Mikroplastikanalytik, Landesamt für Umwelt. 17.12.2019. Wielenbach.

**Weisser J.** Mikroplastik in Getränken – ein Update zum Stand der Wissenschaft. 13. Weihenstephaner Seminar für Wassertechnologie. 12.09.2019. Freising.

**Weisser J.** Mikro(plastik)-Partikel in Trinkwasser – Stand des Wissens und Analysemethoden. 13. Bad Kissinger Mineralwassertag, Institut Romeis. 27.09.2018. Bad Kissingen.

### **Poster presentations at conferences**

Al-Azzawi MSM, **Weißer J**, Kefer S, Reichel J, Schwaller C, Knoop O, Drewes JE. Microplastic contamination in the aquatic environments: validation and reproducibility of sample preparation methods. Wasser 2021. 10.05.2021. Web conference.

**Weisser J**, Glas K. Systemanalyse der Lebensmittelproduktion und –verpackung. BIOFACH 2020. 12.-15.02.2020. Nürnberg.

**Weißer J**, Glas K. Aus der Natur auf den Teller und von der Quelle in die Flasche? - Entwicklung eines matrixabhängigen Verfahrens zur Isolierung von Mikroplastik aus Getränken und Nahrungsmitteln. Umwelt 2018. 10.-12.09.2018. Münster.

## List of Abbreviations

|                 |  |
|-----------------|--|
| ( $\mu$ )FTIR   | Fourier-Transform Infrared (micro)spectroscopy |
| AAH             | Ascorbic acid                                  |
| Acc             | Accuracy                                       |
| CV              | Cross Validation                               |
| DAR             | Data Analysis Routine                          |
| DW              | Dry Weight                                     |
| EtOH            | Ethanol  |
| EvOH            | Ethylene Vinyl Alcohol                         |
| FN              | False Negative                                 |
| FP              | False Positive                                 |
| FP              | False Positive                                 |
| FPA             | Focal Plane Array                              |
| KOH             | Potassium Hydroxyde                            |
| MCCV            | Monte Carlo Cross Validation                   |
| MCT             | Mercury Cadmium Telluride                      |
| MIR             | Mid Infrared                                   |
| ML              | Machine Learning                               |
| MP              | Microplastic(s)                                |
| NA              | Numerical Aperture                             |
| NER             | Non-Error-Rate                                 |
| NP              | Nanoplastic(s)                                 |
| PA              | Polyamide                                      |
| PC              | Polycarbonate                                  |
| PE              | Polyethylene                                   |
| PEST            | Polyester                                      |
| PET             | Polyethylene terephthalate                     |
| PLA             | Polylactic acid                                |
| PMMA            | Polymethyl methacrylate                        |
| PP              | Polypropylene                                  |
| Pr              | Average Precision                              |
| Pr <sub>g</sub> | Precision of class g                           |
| PS              | Polystyrene                                    |
| PTFE            | Polytetraflourethylene                         |
| PUR             | Polyurethane                                   |
| PVC             | Polyvinylchloride                              |
| QA              | Quality Assurance                              |
| QC              | Quality Control                                |
| RDF             | Random Decision Forest                         |
| RefIMP          | Reference Image of MicroPlastics               |
| RM              | Raman Microspectroscopy                        |
| RR              | Recovery Rate                                  |
| SDS             | Sodium dodecyl sulfate                         |
| Sn <sub>g</sub> | Sensitivity of class g                         |
| Sp <sub>g</sub> | Specificity of class g                         |
| TP              | True Positive                                  |

# Table of Contents

|   |      |
|---|------|
| Danksagung .....  | III  |
| Vorbemerkung.....   | V    |
| Publications.....   | VI   |
| Peer reviewed articles as the main author .....   | VI   |
| Peer reviewed articles as a co-author .....   | VI   |
| Non-peer reviewed articles .....  | VII  |
| Standards .....   | VII  |
| Conference papers .....   | VII  |
| Oral presentations at conferences .....   | VII  |
| Poster presentations at conferences.....  | IX   |
| List of Abbreviations .....   | X    |
| Table of Contents .....   | XI   |
| Kurzfassung .....   | XIII |
| Executive Summary .....   | XIII |
| 1. Introduction .....   | 1    |
| 1.1. Microplastics – an emerging pollutant of the environment, beverages, and food .....                              | 1    |
| 1.1.1. Microplastic particles: definition.....  | 2    |
| 1.1.2. Occurrence of microplastics in beverages and food .....  | 3    |
| 1.1.3. Potential impacts of micro- and nanoplastics on (human) health .....   | 4    |
| 1.2. Harmonizing and standardizing microplastics research .....   | 5    |
| 1.3. A pipeline for the analysis of microplastics .....   | 7    |
| 1.3.1. Sampling of microplastics in food and beverages.....   | 7    |
| 1.3.2. Sample preparation.....  | 8    |
| 1.3.3. Suitable filters for microplastics analysis .....  | 11   |
| 1.4. Fourier-transform infrared imaging for the analysis of microplastics .....                                       | 12   |
| 1.5. Random Decision Forest Classifiers for machine-learning assisted microplastic identification in FTIR images..... | 15   |
| 1.6. Quality assurance and quality control in microplastics research .....  | 17   |
| 1.6.1. Contamination prevention and assessment.....   | 17   |
| 1.6.2. Particle loss assessment.....  | 18   |
| 1.6.3. Sample analyzability.....  | 19   |
| 1.6.4. Data analysis routine performance evaluation .....   | 19   |
| 2. Aims of the project.....   | 21   |
| 3. Results.....   | 22   |
| 3.1. Sample preparation of beverages and plant-based food products for microplastic analysis.....                     | 22   |

|        |   |    |
|--------|---|----|
| 3.1.1. | Sample matrix-dependent degradation methods and analysis filters .....  | 22 |
| 3.1.2. | Quality assurance and quality control during sampling and sample preparation<br>25  |    |
| 3.2.   | The identification of microplastics based on vibrational spectroscopy data – A critical<br>review of data analysis routines ..... | 28 |
| 3.3.   | Know what you don't know: assessment of overlooked microplastic particles in FTIR<br>images.....                                  | 30 |
| 3.4.   | From the Well to the Bottle: Identifying Sources of Microplastics in Mineral Water .  | 32 |
| 3.5.   | Entry paths for microplastics during the production and preparation of selected foods<br>34                                       |    |
| 4.     | Discussion.....   | 38 |
| 4.1.   | Proceedings in matrix-dependent sample preparation for MP analysis.....   | 38 |
| 4.2.   | Quality assurance and quality control in sampling and sample preparation .....  | 40 |
| 4.3.   | Quality assurance and quality control in data analysis.....   | 45 |
| 4.3.1. | QA/QC in database matching programs .....   | 45 |
| 4.3.2. | Reference images for DAR evaluation .....   | 46 |
| 4.3.3. | DAR evaluation using RefIMP and MPVal.....  | 47 |
| 4.3.4. | Potential reasons for class confusion .....   | 49 |
| 4.3.5. | Up- and downsides of RefIMP and MPVal.....  | 50 |
| 4.3.6. | Advanced recovery rates for improving DAR QA/QC.....  | 51 |
| 4.4.   | Entry paths for microplastics into beverages and food.....  | 52 |
| 4.4.1. | Food preparation equipment .....  | 52 |
| 4.4.2. | Food packaging.....   | 54 |
| 5.     | Conclusions and future perspectives .....   | 57 |
| 6.     | References.....   | 61 |
| 7.     | Appendix A: Raw Data of unpublished data presented.....   | 72 |
| 8.     | Appendix B: Peer-reviewed publications .....  | 78 |

## **Kurzfassung**

Probenahme, -vorbereitung und Partikeldetektion sind die Eckpunkte der Analyse von Mikroplastik (MP). Um diese zu harmonisieren, ist das Befolgen strenger Maßnahmen zur Qualitätssicherung und –kontrolle (QS/QK) notwendig. Diese wurden jedoch bisher insbesondere für die Analyse von Hyperspektralen MP-Datensätzen vernachlässigt. Um diese Lücke zu schließen wird eine transparente, detaillierte Methode zur QS/QK basierend auf der automatisierten Evaluierung eines Referenzdatensatzes vorgestellt.

Des Weiteren wurden Protokolle zur Vorbereitung von Proben pflanzlicher Lebensmittel und Getränke entwickelt und optimiert. Schlussendlich wurden die Haupteintragspfade für MP in ausgewählte Lebensmittel und Getränke untersucht. Beispielsweise wurde gezeigt, dass MP in abgefülltem Mineralwasser mehrheitlich durch Abrieb am Flaschendeckel entsteht.

## **Executive Summary**

Sampling, sample preparation and particle detection are the key steps in microplastics (MP) analysis. In order to harmonize MP analysis, implementing strict measures for quality assurance and control (QA/QC) for all steps is key. However, especially QA and QC for the analysis of hyperspectral MP data has remained widely neglected. To fill this gap, a transparent and detailed QA/QC method for data analysis based on the automated evaluation of a ground truth reference image is presented.

Moreover, sample preparation protocols for plant-based food and drinks were elaborated and optimized. Lastly, the main entry paths of MP into selected foods and beverages were investigated. For instance, it was shown that the majority of MP particles in bottled mineral water are generated through abrasion from bottle caps.

# 1. Introduction

In order to introduce the reader to the topic, section 1.1 summarizes the theoretical background knowledge about microplastics, its occurrence in beverages and food and concerns connected therewith. The challenges in harmonizing MP research and progress made therein are outlined in section 1.2. Focusing on the methods applied, sections 1.3 to 1.5 describe the analysis of microplastics as carried out during the experimental part of this thesis. Concluding with section 1.6, the measures taken for quality assurance and quality control are described, which are crucial for pushing forward the harmonization of MP analysis.

## 1.1. Microplastics – an emerging pollutant of the environment, beverages, and food

Life in 2022 is unthinkable without plastic – the probably most versatile material ever invented is used for the production of vehicles, electronics, food packaging, and much more. Whilst plastic has become essential for us, it is cheap and thus often treated carelessly as soon as it is no longer needed. Out of the estimated 367 Mt produced in 2020, at least 23% did not end up in recycling facilities or incineration, but in landfills or in the environment (Plastics Europe's Market Research and Statistics Group 2021). It is estimated that at least 8 Mt of plastic enter the world's oceans each year, where it accumulates (Ritchie and Roser 2018).

While plastic pollution of the oceans is a long-known problem, early reports on millimeter-sized plastic pieces by Carpenter and Smith (1972) did not receive much attention. In 2013, however, a report was published about alleged findings of small plastic pieces in honey and sugar (Liebezeit and Liebezeit 2013), followed by a report on so-called 'microplastic' in beer (Liebezeit and Liebezeit 2014). This was the starting point for intensive research, revealing that microplastic (MP) is present all across the globe, not only in the sea, but also in rivers and lakes, and even in remote areas with sparse human activity (Wang, Lai *et al.* 2021). This shows that plastic items in the oceans are not only the result of on-sea littering, but are also land-based and that they are transported by the currents of water and wind. Moreover, mulching films or contaminated compost and sewage sludge, used as fertilizers, release MP into agricultural soils. Rainfall can then wash the particles out and into aquatic systems (Yang, Zhang *et al.* 2021). Even snow and bird feces contribute to the distribution of MP (Abbasi, Alirezazadeh *et al.* 2022; Bourdages, Provencher *et al.* 2021).

Animals can mistake MP particles for food, as was first shown for copepods and other zooplankton by Cole, Lindeque *et al.* (2013). Meanwhile, MP has been detected in the guts of fishes (Rochman, Tahir *et al.* 2015), avifauna (Bourdages, Provencher *et al.* 2021), and mammals (Eriksson and Burton 2003) who ingested it either directly or indirectly with their prey. Furthermore, plants were shown to take up plastic particles in the nanometer range via their roots (Li, Gao *et al.* 2021). The potential impacts of MP uptake on living organisms has been and still is subject of intensive research, which probably is illustrated best by the fact that a new scientific journal, called 'Microplastics', was founded in July 2021 (Kalogerakis 2022).

Plastic is capable of adsorbing chemicals, especially hydrophobic substances such as phenanthrene. Because of their high surface-to-volume ratio, MP particles can adsorb relatively high amounts. The impacts of which on aquatic organisms, however, remain disputed (Tang 2021). Further, it has been observed that biofilms can form on MP particles, turning them into potential vectors for pathogenic germs (Bowley, Baker-Austin *et al.* 2021).

While it has become clear that MP is abundant, the exact concentrations, its behavior, and its effects remain only partially understood to date. This is the case also because the methods for

MP analysis are yet to be standardized. In fact, highly specialized methods for sampling, sample preparation, instrumental analysis, and data evaluation had to be established, stretching further to new experimental design for assessing sorption, uptake by animals and plants, and (eco-) toxicological effects. The methods are continuously refined by researchers across the globe and first steps have been made towards a standardization of methods in national and international boards.

### 1.1.1. Microplastic particles: definition

MP particles in the environment can be distinguished based on their origin: ‘Primary MP’ are MP particles that were intentionally produced in the size range of 1 to 1,000  $\mu\text{m}$ , such as pellets that serve as raw materials for the production of plastic items, or microbeads for cosmetics. Their usage, however, has meanwhile been banned in Canada (Microbeads in Toiletries Regulations 2017) and the European Union is planning to forbid intentionally added MP in any kind of product (European Chemicals Agency 2018). ‘Secondary’ MP, in turn, are the result of plastic items breaking down into smaller fragments under the influence of UV radiation, thermal and mechanical stress. They make up for the largest part of MP in the environment (Hale, Seeley *et al.* 2020). While primary MP are mostly spherical, secondary MP particles have irregular shapes: fragmental structures can be found as well as fibers (length : width  $\geq 3 : 1$ , (Vianello, Jensen *et al.* 2019)).

Reflecting the broad variety of plastic materials in various sizes and shapes, MP are a very heterogeneous group of analytes as shown exemplarily in Figure 1. MP types reflect the broad variety of plastic materials, including polyolefins, polyesters and rubbers as well as so-called ‘bioplastics’. In fact, the distribution of MP types in the environment reflects the plastic types’ production shares (Huppertsberg and Knepper 2018). While some definitions include even water-soluble artificial polymers, these are excluded in this thesis according to Braun (2021), DIN/TS 10068 and ISO/NP 16094-1 (draft stage).

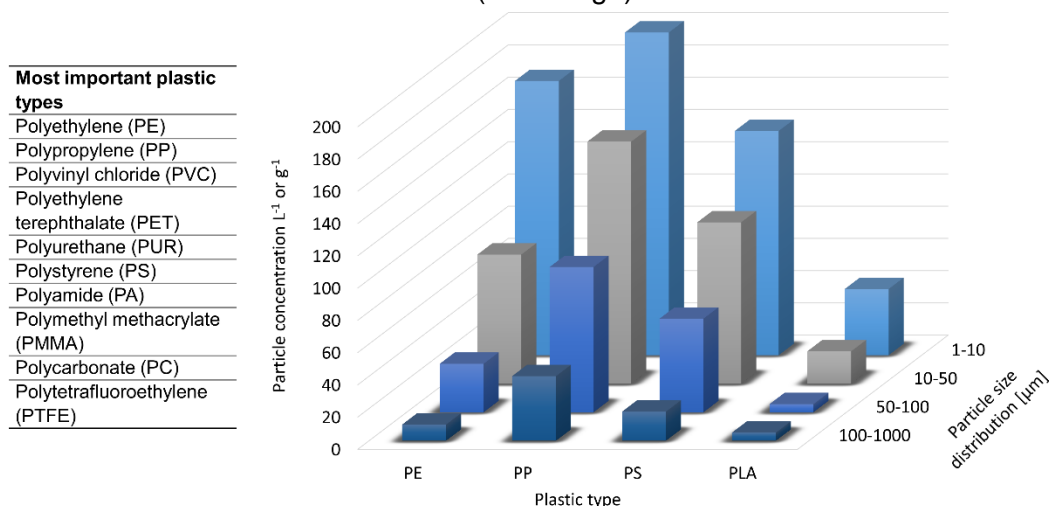


Figure 1. Most important plastic types and an exemplarily illustration of target variables of MP analysis: plastic types, particle concentrations, and particle size distributions.

Early research classified MP as particles and fibers < 5 mm, however, it soon became clear that even nano-scaled plastic particles existed, so the term ‘nanoplastics’ (NP) was introduced for particles sized 1-1000 nm (Hartmann, Hüffer *et al.* 2019). The definition most probably seen as a consensus in the debate on MP size categories can be found in Braun (2021), DIN/TS 10068 and ISO/NP 16094-1 (draft stage), all of which define plastic particles between 1 and 5 mm as ‘large MP’ and plastic particles between 1 and 1000  $\mu\text{m}$  as ‘MP’. Typically, MP particle numbers increase exponentially with decreasing particle sizes (Kooi and Koelmans 2019).

### 1.1.2. Occurrence of microplastics in beverages and food

Even though the very first reports of MP findings in honey and sugar (Liebezeit and Liebezeit 2013, 2015), and in beer (Liebezeit and Liebezeit 2014) have faced harsh criticism (Lachenmeier, Kocareva *et al.* 2015), the case has become one of the *hot topics* of food safety. Especially consumers are worried about potential health impacts of MP when ingested: in the latest 'Verbrauchermonitor', published by the German Federal Institute for Risk Assessment, 55% of consumers stated that they were '(very) worried' about MP in food. Leaving behind concerns such as antibiotic resistance in meat or coronavirus particles on food, MP is the most worrying food safety issue for German consumers (BfR 2022a).

Until today, a broad variety of beverages and food has been analyzed for MP. Out of which, drinking water is the best-studied sustenance as it contains very few solids that can disturb the analysis, making it comparably easy to analyze. The first peer-reviewed study in 2018 dealt with mineral water in glass and polyethylene terephthalate (PET) bottles. Particles  $\geq 5 \mu\text{m}$  were analyzed by means of Raman microspectroscopy (RM). With  $118 \pm 88$  MP particles  $\text{L}^{-1}$ , returnable PET bottles showed the highest MP concentrations. Opposed to this, results from single-use PET did not differ from the blank values. As 84% of the MP in returnable PET bottles was identified as PET, it was assumed that these were generated during bottle usage and cleaning. In glass bottles, a broader variety of plastic types, summing up to  $50 \pm 52$  MP  $\text{L}^{-1}$  were present, hinting at the bottle cleaning process as the main entry path (Schymanski, Goldbeck *et al.* 2018). Similar findings were made in another study, detecting MP concentrations of  $6,292 \pm 10,521$  MP  $\text{L}^{-1}$  for glass bottles and  $4,889 \pm 5,432$  MP  $\text{L}^{-1}$  for returnable PET bottles. The concentrations were significantly higher in this study because particles down to a size of  $1 \mu\text{m}$  were analyzed. Along with the MP particles, pigmented particles were found, potentially originating from the bottle labels (Oßmann, Sarau *et al.* 2018). Note the high standard deviations of the findings, the reasons for which may lie in sample heterogeneity, sampling and analysis methods, or a combination of all three. Thus, general statements about MP concentration in bottled water are not possible to date.

When sourcing drinking water from rivers or lakes that are contaminated with MP, water treatment (such as flocculation and/or filtration, for instance) cannot completely remove the particles. Depending on the treatment process, between 40 and 88% of MP can be removed (Pivokonský, Pivokonská *et al.* 2020). In contrast, ground water was shown to be nearly free of MP particles (Mintenig, Löder *et al.* 2019). This shows that the contamination of natural mineral water sold in the European Union (which needs to be sourced from ground water by law (2009/54/EC)) must occur during bottling. Winkler, Santo *et al.* (2019) showed that repeated twisting of polypropylene (PP) caps on the necks of PET bottles caused abrasion. To finally answer the question of how the majority of MP gets into bottled water, the bottling process was analyzed step-by-step during this thesis (see section 3.4.).

In beer, no MP could be detected by means of RM (Wiesheu, Anger *et al.* 2016), contradicting the findings by Liebezeit and Liebezeit (2014). In another study, an average of  $28 \pm 5$  MP  $\text{L}^{-1}$  was identified in beer (Shruti, Pérez-Guevara *et al.* 2020). None of these studies, however, conducted a fully quantitative analysis but instead analyzed subsamples or manually chosen particles and fibers only, indicating that MP particles potentially were overlooked (Pérez-Guevara, Roy *et al.* 2022). The variance between the studies may result from the different methodologies, but also from variations in the bottle manufacturing and filling processes.

Originating from the oceans, sea salt can contain up to  $19,800$  MP  $\text{kg}^{-1}$  (Renzi and Blašković 2018). Salt, however, is not consumed in large amounts, making it less relevant for human exposure to MP. Like sea salt, fish and seafood seem to be a very likely source of MP at first glance. In fish, however, MP have mostly been identified in the digestive tracts, which are

usually not consumed. Similarly, MP in crustaceans seem to be present predominantly in their digestive tract, however, their guts are not always removed before consumption. Lastly, mollusks have been shown to contain  $1 \pm 3$  MP g<sup>-1</sup> tissue, which would be ingested when the mollusk is eaten as a whole. Depurating them before consumption, however, lowers the MP concentration to  $< 1$  MP g<sup>-1</sup> (Dawson, Santana *et al.* 2021).

Packaging materials pose another potential source of MP contamination. Opening a package, using scissors, or simply tearing, can generate MP. The amount of MP generated seems to depend on the plastic's material properties such as stiffness or density (Sobhani, Lei *et al.* 2020). Meat packaged in polystyrene (PS) trays was found to be contaminated with up to 19 PS particles kg<sup>-1</sup> (Kedzierski, Lechat *et al.* 2020). As only particles  $\geq 300$   $\mu\text{m}$  were analyzed, higher numbers are to be expected when including lower size ranges. A report on MP generation from PET and nylon teabags claimed that per cup of tea, billions of MP and NP were released during brewing (Hernandez, Xu *et al.* 2019). This study, however, was broadly criticized concerning the methods applied that possibly over-estimated the number of MP particles (Busse, Ebner *et al.* 2020). Furthermore, plastic kitchenware may be another source of MP in food. Cutting meat on plastic boards, for instance, can cause up to  $7 \pm 5$  MP g<sup>-1</sup> (Habib, Poulouse *et al.* 2022). This result, however, is to be seen with caution because the blank values were not reported.

This short summary shows that even though until today dozens of studies on MP in beverages and food have been published, they need to be interpreted with care. The methods applied are often questionable (Oßmann 2021; Koelmans, Mohamed Nor *et al.* 2019; Oßmann, Schymanski *et al.* 2019; Busse, Ebner *et al.* 2020), stressing the urgent need for a harmonization of MP research methods.

### 1.1.3. Potential impacts of micro- and nanoplastics on (human) health

To date, there is no doubt that humans ingest MP, but also egest it at least partly, as analyses of MP  $\geq 50$   $\mu\text{m}$  in stool samples have shown (Schwabl, Köppel *et al.* 2019). In general, it is estimated that only particles smaller than 10  $\mu\text{m}$  can be taken up by human intestinal cells, making small MP and NP the most relevant for potential toxic effects (Paul, Stock *et al.* 2020). Indeed, the presence of NP has been confirmed in samples from human placenta (Braun, Ehrlich *et al.* 2021; Ragusa, Svelato *et al.* 2021) and human blood (Leslie, van Velzen *et al.* 2022), showing the bioavailability of NP. Note that NP in blood do not necessarily stem from oral uptake but may have been translocated from lung tissue after inhalation (Fournier, D'Errico *et al.* 2020).

In small organisms such as zooplankton, MP particles may block guts and physically damage intestinal tissues (Wright, Thompson *et al.* 2013). For larger organisms such as humans, this is not the case. However, it is known that the smaller an orally delivered PS particle is (sizes 50 nm to 3  $\mu\text{m}$ ), the more likely is its uptake into the liver of rats (Jani, Halbert *et al.* 2011). *In vitro* studies with human colorectal cells (Caco-2) showed that PS particles between 25 and 500 nm were taken up and that specifically the uptake of 100 nm PET particles increased over time (Magri, Sánchez-Moreno *et al.* 2018).

The first conclusion that can be drawn is that particle sizes seem to drive MP and NP uptake into cells. Uptake alone, however, does not *per se* cause damage. In fact, MP and NP toxicity is still disputed as studies contradict each other and/or were conducted under doubtful conditions (Paul, Stock *et al.* 2020). One reason for this ambiguity lays in the lack of standardized testing materials. As a recent study shows, testing material from different suppliers can have different impacts on cells, even though they are nominally identical, based on their specifications. Using PS beads with 3  $\mu\text{m}$  diameter from two suppliers, Ramsperger, Jasinski *et al.* (2022) showed that murine cell metabolism and proliferation decreased for

particles with lower zeta potential and higher content of styrene monomers. Recently, plastic monomers from ingested polyethylene (PE) MP were shown to be bioaccessible in standardized tests (Lopez-Vazquez, Rodil *et al.* 2022). Acute exposure to PE MP further seems to impair the growth of water fleas and insects (Castro, Bernegossi *et al.* 2022).

Altogether, it is to date not possible to draw a conclusion about the toxicity or harmlessness of MP and NP. Nevertheless, under the precautionary principle, research should be pushed ahead further (Leslie and Depledge 2020; Ramsperger, Jasinski *et al.* 2022). Especially because we can expect rising MP and NP concentrations in the environment (Hale, Seeley *et al.* 2020), and therefore also in beverages, food, and in the air we breathe.

### 1.2. Harmonizing and standardizing microplastics research

Methods for MP analysis need to be harmonized in order to gather reliable and comparable data on the occurrence of MP in the environment, in beverages, and in food. Especially for the implementation of future legal regulations, standard methods are a prerequisite.

Early MP research was often done with simplistic methods, such as light microscopy, considering colored particles to be plastic (Liebezeit and Liebezeit 2013). Unsurprisingly, this method can lead to high error rates (Song, Hong *et al.* 2015). Consequently, more reliable methods were developed that enabled to identify a particle's chemical composition, and are meanwhile in the process of becoming standard for MP analysis (ISO/DIS 24187, ISO/NP 16094-2 and -3 (draft stage)). To date, the most important methods are RM, Fourier-transform Infrared microspectroscopy ( $\mu$ FTIR) (more details in section 1.4), and thermo-analytical methods; the latter is an umbrella term for pyrolysis-gas chromatography-mass spectrometry (Pyr-GC-MS) and thermal extraction desorption (TED)-GC-MS. While all these methods are in principle capable of determining plastic types in a sample, they complement each other in some aspects. In contrast to the microspectroscopic methods, thermo-analytical methods destroy MP samples during the analysis and therefore, particle sizes and shapes of the analyzed sample cannot be determined. Size-fractionating the samples beforehand can partly solve this problem (Bannick, Szewzyk *et al.* 2019). The limit of detection, in theory, is one particle within the analyzable particle size range for the spectroscopic methods ( $\sim 1 \mu\text{m}$  for RM and  $\sim 10 \mu\text{m}$  for  $\mu$ FTIR). For thermo-analytical methods, the limit of detection, however, depends on the plastic type and ranges from  $0.06 \mu\text{g}$  for styrene butadiene rubber up to  $2.2 \mu\text{g}$  for PE, corresponding to a minimum of, for example, 10 PE particles with  $75 \mu\text{m}$  diameters. The strength of the thermo-analytical methods in turn, is their speed and capability of analyzing the polymer type simultaneously with additives and adsorbed substances (Braun 2021). For both method families, however, non-plastic sample matrix constituents can pose a major challenge, making sample preparation before the analysis indispensable (Primpke, Fischer *et al.* 2020).

Much effort has been put into sample preparation methods, yielding multi-step chemical and enzymatic digestion protocols, tailored for many different sample types (see sections 1.3 and 3.1.1) and with enhanced quality assurance (Al-Azzawi, Kefer *et al.* 2020; Schymanski, Oßmann *et al.* 2021). Because there is no 'one-fits-all' solution, it is inherently necessary to have a variety of methods at hand. The aspect of harmonization here lays rather in the evaluation of the sample preparation methods (Schymanski, Oßmann *et al.* 2021) than in the methods themselves. Thus, the harmonization committees have agreed that any method applied must be tested for compatibility with the plastic types targeted to avoid particle damage or even destruction (ISO/DIS 24187, DIN/TS 10068). A series of measures for quality assurance (QA) and quality control (QC) should be followed as outlined in section 1.6.

Even though the harmonization of sampling, sample preparation, and instrumental analysis methods has made progress, inter-laboratory comparisons show that there is still a ‘substantial lack of inter-laboratory reproducibility’ (Belz, Bianchi *et al.* 2021). One reason may be the challenge in preparing homogeneous test samples, as becomes evident in the report of an inter-laboratory study initiated by the European Union’s Joint Research Centre, where a rather large indicative range of the test samples provided to the participants is given with 500-1,100 PET particles L<sup>-1</sup> (Belz, Bianchi *et al.* 2021).

While progress in the development of standard MP particles is undoubtedly urgent, this thesis aims to draw attention to the method gap that remains at the end of the analysis pipeline: the interpretation of data gained through instrumental analysis. Especially the hyperspectral imaging techniques (here RM, FTIR and Near infrared (NIR) microspectroscopy) produce large amounts of data, the interpretation of which is not trivial and requires automated data analysis routines (DARs). Database matching and machine learning techniques have been shown to be capable of this task (Primpke, Cross *et al.* 2020; Hufnagl, Steiner *et al.* 2019). Yet, method harmonization at this point suffers two-fold: First, methods often are not reported in full transparency, as shown through a literature review during this thesis, summarized in Figure 2. Focusing only on studies using FTIR, about a quarter of studies did not report how spectra were interpreted. From the 62% using database matching, where a substance is identified by comparing its spectrum with a known reference, again about a quarter did not report which database was used. Concerning the algorithm that computes the similarity between a query and a reference spectrum, three quarters of studies failed to deliver this information (Weisser, Pohl, Heinzinger *et al.* 2022).

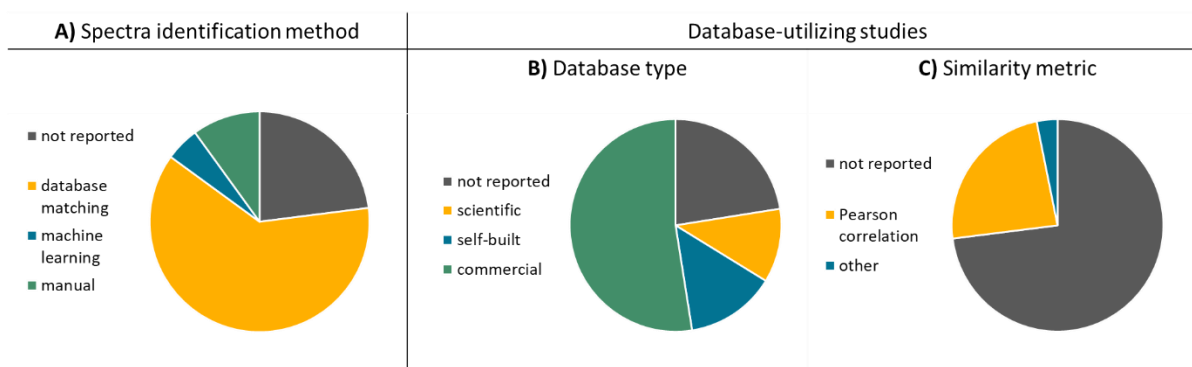


Figure 2. Summary of an assessment of 100 studies on microplastic utilizing Fourier-transform Infrared spectroscopy regarding A) spectra identification methods, B) databases and C) similarity metrics used (Reprint from Weisser, Pohl, Heinzinger *et al.* (2022) with permission from the publisher).

The second issue hampering method harmonization is the inconsistency in DAR evaluation. If DARs are evaluated in the literature (which is not always the case), arbitrary methods and metrics are used to do so, see section 1.6.4. Consequently, the evaluation remains superficial, incomplete, biased, or all three combined. In ISO/NP 16094-2 (draft stage), the importance of ensuring accuracy of database matching for MP identification is mentioned, and that a maximum of 20% false positive and 20% false negative results should be aimed for. Further, in DIN/TS 10068, the importance of tailoring DARs for the respective sample type and laboratory conditions is stressed. However, clear definitions are lacking, as well as a description of how this can be achieved. A more detailed explanation can be found in the annex A of ISO/DIS 24187, where the importance of separate test data sets is highlighted and basic metrics for DAR evaluation are proposed. Nevertheless, some questions remain unanswered as discussed extensively in section 4.3.

### 1.3. A pipeline for the analysis of microplastics

The fact that MP analysis deals with a group of solid analytes instead of soluble substances leads to some challenges for sampling and sample preparation. Crucially, MP particles need to be isolated from the sample matrix to avoid interferences during instrumental analysis. Depending on the presence or absence of inorganic and organic substances, different strategies can be pursued as described in section 1.3.2.

After sample preparation, the remaining particles were concentrated on an analysis filter as described in section 1.3.3 to undergo FTIR imaging, followed by data analysis. During all steps (summarized in Figure 3), measures for quality assurance and quality control were followed, see section 1.6.

MP concentrations were determined during this thesis for bottled mineral water, bread, tea, and fruit purees, including raw materials.

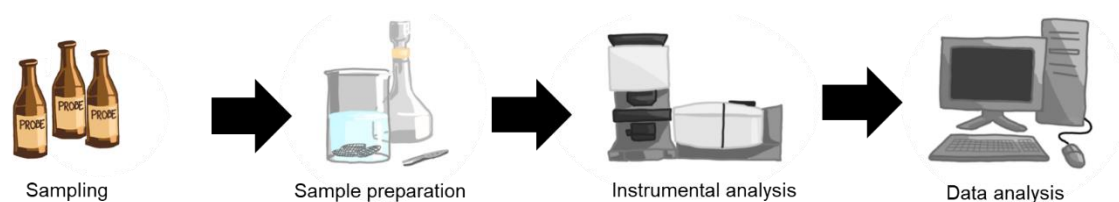


Figure 3. Schematic representation of a microplastic analysis pipeline, Illustrations created by Teresa Pohl with kind permission to use here.

#### 1.3.1. Sampling of microplastics in food and beverages

For the analysis of MP in beverages and food, preferably a whole unit of consumption, such as one whole bottle of mineral water, was sampled. However, for samples with a higher content of solids, for example fruit purees, the analysis of a whole container was not possible. Despite the multi-step degradation process, matrix residues would have covered potential MP particles. In such cases, the sample was homogenized through stirring before sampling. Homogenization was necessary for a second reason: in contrast to water-soluble analytes, MP particles cannot be considered to be homogeneously distributed in a sample (Braun 2021). For instance, low-density polymers such as PE ( $0.92 \text{ g cm}^{-3}$ ) float at the water surface, while others, such as polyvinyl chloride (PVC,  $1.36 \text{ g cm}^{-3}$ ), tend to sink (Domininghaus 2012). Moreover, MP particles tend to aggregate in water (Eitzen, Paul *et al.* 2019). Both causes inhomogeneous distribution of MP.

The sample volume or mass further depends on the expected number of MP particles in the targeted size range. For instance, Schymanski, Goldbeck *et al.* (2018) found that mineral water from reusable PET bottles contained  $\sim 50 \pm 30$  MP particles  $\geq 10 \mu\text{m L}^{-1}$ , while another  $68 \pm 58$  MP particles between 5 and  $10 \mu\text{m}$  were present. Hence, even when only the size range  $\geq 10 \mu\text{m}$  is targeted, a considerable amount of MP particles can be expected in a 1 L-bottle. In contrast, MP ( $\geq 50 \mu\text{m}$ ) concentrations below  $1 \text{ L}^{-1}$  are to be expected in ground water (Mintinig, Löder *et al.* 2019), making it necessary to sample at least  $1 \text{ m}^3$  in order to gain a representative sample (Braun 2021). For reasons of practicability, groundwater was filtered *in-situ* through stainless steel cartridge filters (see Figure 4 A; mesh sizes 5 and  $50 \mu\text{m}$  to avoid clogging (Lenz and Labrenz 2018)) to reach a sample size of  $\sim 1,000 \text{ L}$ . All particles  $> 5 \mu\text{m}$  thereby were concentrated on the filters.

Bottled water did not require any sample pretreatment, but could be filtered directly through an analysis filter. Empty bottles were flushed twice with a 0.02% sodium dodecyl sulfate (SDS) solution and once more with 30% ethanol to extract as many particles as possible.

When having the goal of identifying the sources of MP contamination into a (food) product, it is advisable to assess the end product and to take additional samples step-by-step along the production process as is described in Weisser, Beer *et al.* (2021). To account for the high variances typical in MP research, at least triplicate samples are required (Schymanski, Oßmann *et al.* 2021).

### 1.3.2. Sample preparation

Depending on the sample's physical state (solid/liquid), water content, and content of organic and inorganic substances, the preparation steps described in the following are suitable to isolate MP from the sample matrix. The success of sample matrix degradation here was evaluated first by determining the sample's dry mass reduction. This was necessary for all sample types, except for water samples. Dry mass was determined after 24 h drying at 60°C to avoid thermal damaging of the polymers (Löder, Imhof *et al.* 2017). Importantly, dry mass reduction was determined in relation to the filtered, but untreated sample, instead of in relation to the unfiltered sample to avoid misinterpretation caused by dissolved substances. Sample treatments were tested using model food matrices (e.g. fruit puree, flour, and cellulose).

#### Solid-liquid separation and size classification

Filtering through stainless-steel filters allows to remove the liquid share of a sample or to fractionate it into particle size categories. Fractionation can be relevant either to exclude particles below the analytical method's detection limit in terms of particle size, or, when a sample contains large particles that might superimpose smaller MP particles. For example, in the present work, particles < 5 µm were discarded by filtering through stainless steel sieves while particles > 1 mm were analyzed with Attenuated Total Reflection-FTIR spectroscopy instead of FTIR imaging (see section 1.4).

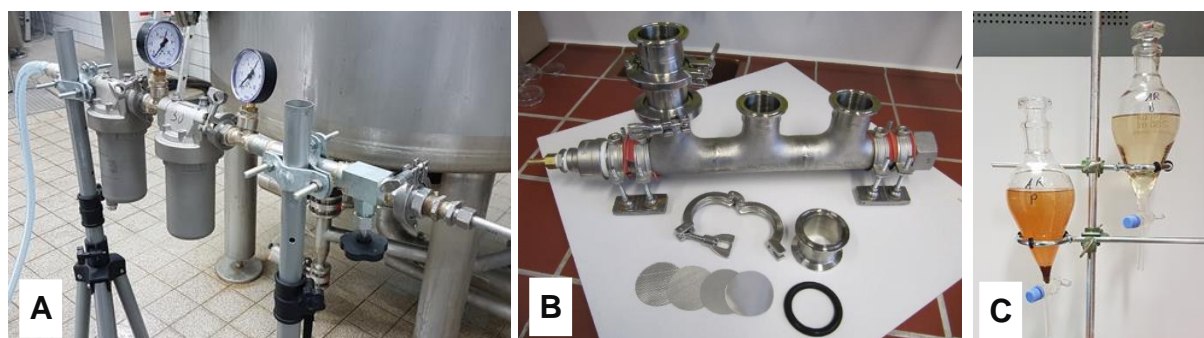


Figure 4. Sampling, fractionation and separation methods for MP. A. Stainless steel cartridge filters for *in-situ* filtration of groundwater samples. B. Customized filtering device, stainless steel sieves and Viton gasket. C. Particulate matter from a groundwater sample (left) and corresponding blank sample (right) undergoing density separation. Photos by Jana Weißer.

For size fractionation and sample volume reduction, a customized filtering device (see Figure 4 B) was commissioned using 2" Tri-Clamp ferrules enabling up to three samples to be vacuum-filtered in parallel through cascades of up to four stainless steel sieves each. The sieve mesh sizes (5, 10, 50, and 100 µm, Rolf Körner GmbH, Germany) were chosen depending on the sample's solids content to avoid filter clogging. Black Viton® gaskets were used because black materials are hardly analyzable with FTIR. This way, confusion with sample MP particles was avoided.

#### Density separation

To separate inorganic substances from a sample, density separation in a 60% (w/w) zinc chloride ( $\text{ZnCl}_2$ ) solution with a density of 1.75 g cm<sup>-3</sup> for 24 h at room temperature was

employed. The settled particles were discarded through the valve at the lower end of the separation funnel. The floating particles, including MP particles with densities  $<1.75 \text{ g cm}^{-3}$ , were processed further. As can be seen in Figure 4 C, inorganic particles, mostly ferric oxides, were separated from the sample this way. During the work on this thesis, density separation was necessary only for sea salt (Hubin 2020) and ground water samples (Weisser, Beer *et al.* 2021).

### Enzymatic sample preparation for plant-based samples

After successful enzymatic matrix degradation described by Löder, Imhof *et al.* (2017), their protocol was adapted. Enzymes summarized in Table 1 were acquired from ASA Spezialenzyme GmbH, Germany, and tested for their suitability to degrade high polysaccharides in plant-based beverages and food. Enzymes were chosen that yield soluble products, like mono- or disaccharides.

Table 1. Enzymes tested for beverage and food matrix degradation.

| Product name                               | Function   | Enzyme Commission number   |
|--|--|----------------------------|
| <b>Cellulase TXL</b>                       | endo-1,4- $\beta$ -glucanase                                       | EC 3.2.1.4                 |
| <b>Amylases Thermo and TXL</b>             | 1,4- $\alpha$ -D-glucanohydrolases                                 | EC 3.2.1.1                 |
| <b>Pektinase L-40</b>                      | endo-polygalacturonase   | EC 3.2.1.15                |
| <b>Xylanase 2x<br/>(mixed preparation)</b> | endo-1,4- $\beta$ -D-xylanase and<br>endo-1,3- $\beta$ -D-xylanase | EC 3.2.1.8 and EC 3.2.1.32 |

*Cellulase TXL* was tested as it was expected to be versatile for the degradation of any plant-based beverages and food. It breaks down the insoluble cellulose into soluble  $\beta$ -D-glucose as shown in Figure 5 (Je Yoo, Feng *et al.* 2017).

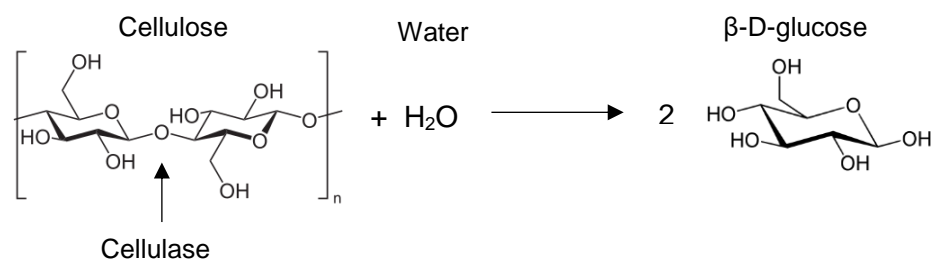


Figure 5. Hydrolytic cleavage of 1,4- $\beta$ -D glucosidic bonds in cellulose by cellulase.

For degradation of starch-containing samples, both *Amylase Thermo* and *Amylase TXL* were tested, yielding dextrans and maltose. Amylases play a major role during the saccharification of malt during beer brewing, for example (Je Yoo, Feng *et al.* 2017). Adding 100 ppm of calcium was recommended by the supplier for stabilizing the enzyme at temperatures  $>60^\circ\text{C}$ . For the degradation of pectin in fruit purees, *Pektinase L-40* was tested. In the food industry, pectinases play a role in liquefaction and viscosity decrease of fruit mashes and juices (Je Yoo, Feng *et al.* 2017). Lastly, *Xylanase 2x* was tested for the degradation of plant and yeast cell walls as it comprises the hemicellulase activities of mannanase, xylanase, and  $\beta$ -glucanase. It is used, for example, to enhance the availability of complex substrates in industrial fermentation processes (Hu, Arantes *et al.* 2011).

First experiments resulted in denaturing of the enzymes despite usage of buffer systems and reaction temperatures as described by Löder, Imhof *et al.* (2017) who followed the manufacturer's recommendations. Therefore, suitable reaction systems had to be established for each enzyme, aiming to keep the enzymes stable. For reasons of practicability, a reaction

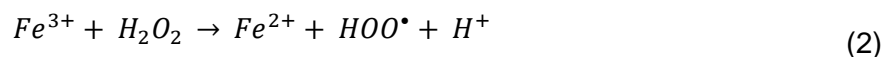
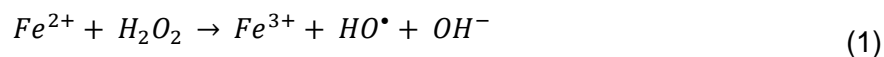
time of  $\geq 24$  h was targeted. Four buffer systems (sodium-acetate, sodium hydroxide-citric acid, sodium-phosphate, and trisodium citrate-citric acid) were tested at concentrations of 0.1, 0.5, and 1.0 M. Further, the influence of temperature (40 to 80°C) and pH (5.0, 6.0, and 7.0) were investigated. For *Amylase Thermo* and *Xylanase 2x*, the addition of 100 ppm  $\text{Ca}^{2+}$  as a stabilizing agent was tested, following the enzyme manufacturer's suggestion (Dunkel 2018).

### Chemical sample preparation

Usage of aggressive chemical reactants was kept at a minimum to avoid degradation of MP particles. The chemical digestion methods described below were tested towards their effects on MP particles and found to not cause any significant effects as is described in section 3.1.2.

Residual mineral precipitates after density separation of ground water samples were dissolved in 30 mL of citric acid (0.55 M) at room temperature for 24 h.

Fenton's reaction (Fenton 1894), was employed for degradation of all samples except water. It is a relatively mild, yet effective method for the degradation of organic compounds (Tagg, Harrison *et al.* 2017; Al-Azzawi, Kefer *et al.* 2020; Bolobajev, Trapido *et al.* 2015; Hou, Huang *et al.* 2018), where ferric ions ( $\text{Fe}^{2+}$ ) catalyze the formation of hydroperoxyl ( $\text{HO}_2$ ) and hydroxyl ( $\text{OH}$ ) radicals from hydrogen peroxide ( $\text{H}_2\text{O}_2$ ) as described in formulae 1 and 2. Formula 3 is the net outcome:



The formed radicals act as reductants for organic compounds present in the sample, thereby cleaving molecular bonds. While first experiments followed a protocol proposed by Masura, Baker *et al.* (2015), adaptations were necessary after the formation of iron precipitates was observed. To avoid this, the relation between  $\text{H}_2\text{O}_2$  (30%) and  $\text{FeSO}_4$  (0.05 M) was increased from 1:1 to 40:5, and the reaction temperature was kept between 20 and 30°C in a water bath, following Simon, van Alst *et al.* (2018). This procedure further considerably reduced the formation of foam and overflowing of vessels. Depending on the sample amount (up to 6.500 mg), usually 100 mL of  $\text{H}_2\text{O}_2$  were needed for a satisfying result.

Aiming to quench the formation of radicals before starting the next degradation step as recommended by Martin Elsner (Institute of Hydrochemistry and Chair of Analytical Chemistry and Water Chemistry, TUM), a solution of ascorbic acid (AAH, 200 g  $\text{L}^{-1}$ ) was added after two hours in a ratio of 10:40 to  $\text{H}_2\text{O}_2$ .

### Method assessment with model foods

To assess the suitability of enzymatic and Fenton + AAH treatments, tests were conducted with approximately 6 g of a) an apple puree with strawberry, banana, and raspberry added (10, 9, and 4%, respectively) and b) a mixed pear and apple puree (ratio 70 to 30%). These model foods will in the following be referred to as 'strawberry puree' and 'pear puree', respectively. Both purees were dissolved in 300 mL of demineralized water, vacuum-filtered through a cascade of stainless steel filter disks (100, 50, 10, and 5  $\mu\text{m}$ ). Next, they underwent treatment with Fenton's reagent for three hours in triplicates. The samples were re-filtered and their dry mass determined. The experiment was repeated, but after two hours, AAH was added. To determine the samples' initial dry mass, they were dissolved in 300 mL of water and filtered through the stainless steel filters without further treatment.

### 1.3.3. Suitable filters for microplastics analysis

The final sample preparation step was the deposition of the remaining particles on a substrate suitable for the analysis by means of FTIR imaging (described in detail in section 1.4).

As shown by Löder, Kuczera *et al.* (2015), FTIR imaging in transmission mode poses a quick and reliable method for identifying MP particles  $\geq 10 \mu\text{m}$ . This requires to deposit the particles on a substrate that is infrared (IR) transparent, i.e. that does not interfere with IR light. For this purpose, IR-transparent filters are available that are made from inorganic compounds (Löder, Kuczera *et al.* 2015). When choosing filters with a pore size similar to the analysis method's detection limit ( $\sim 10 \mu\text{m}$  for FTIR imaging), smaller particles pass the filter and cannot form a filter cake that interferes with potentially present MP particles. Finally, targeting an analysis time of e.g. maximum 4 h per sample, the filters' diameter should not be too big. A sample area of approximately  $10 \times 10 \text{ mm}^2$  to be measured by FTIR imaging was found acceptable here.

The filter of choice for samples with low contents of suspended solids, i.e. drinking water, was Anodisc (Whatman, Buckinghamshire, UK), made from aluminum oxide with a diameter of 25 mm and a pore diameter of  $0.2 \mu\text{m}$ . Anodisc membranes are available with a PP support ring, which considerably eases their handling. Without the ring, the membranes tend to break easily. No remarkable number of PP particles was found in blank samples, indicating that no or only very few contamination through the support ring occurred. Filtration took place under vacuum in a glass filtration unit. To concentrate the sample particles in a squared area of approximately  $100 \text{ mm}^2$ , a spacer made from the paper interlaying the filters in their box was used.

Similarly, for reflection FTIR imaging experiments, particle suspensions were filtered through gold-coated polycarbonate (PC) membrane filters (Analytische Produktions-, Steuerungs- und Controllgeräte GmbH, Germany) with diameters of 25 mm and a pore size of  $0.8 \mu\text{m}$ .

For FTIR imaging, samples on both Anodisc and PC membranes were placed on  $\text{BaF}_2$  windows and into custom-made filter holders (Figure 6 A) to hold them flat and even as proposed by Primpke, Dias *et al.* (2019). Its influence on filter flatness was kindly evaluated by Elisabeth von der Esch, TUM (section 3.1.1).

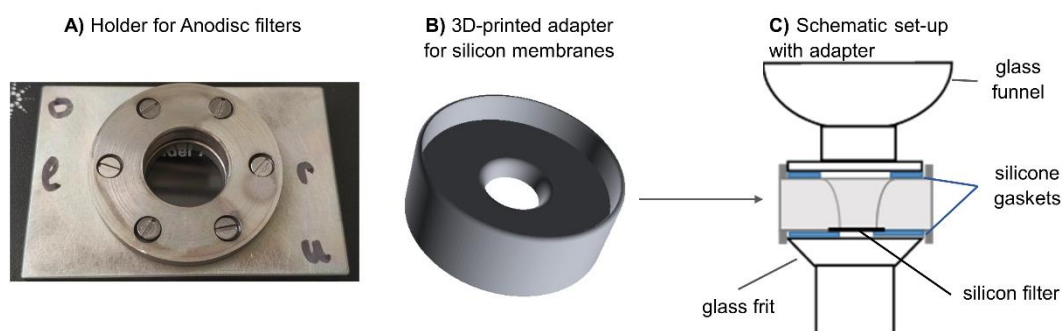


Figure 6. Tools for analysis filter handling. A. Holder for Anodisc membranes and PC membranes (Beer 2019). B. 3D-model of the adapter. C. Schematic filtration set-up, adapted from Lerch (2020).

For samples where even after multi-step matrix digestion too many solids were left to yield a particle monolayer on the Anodisc membrane, silicon filters with pore sizes of  $5\text{-}10 \mu\text{m}$  (SmartMembranes GmbH, Germany) were used. Moreover, they are transparent for a wider range of IR light than Anodisc membranes ( $4,000\text{-}600 \text{ cm}^{-1}$  vs.  $3,800\text{-}1,250 \text{ cm}^{-1}$  (Käppler, Windrich *et al.* 2015)). The silicon filters required some modifications of the filtration set-up because they are square-shaped and relatively thick ( $\sim 300 \mu\text{m}$ ). Following the descriptions from Käppler, Windrich *et al.* (2015), a filter adapter was designed (Autodesk® Inventor, Autodesk Inc., CA, USA) and 3D-printed (Rapidobject GmbH, Germany) as shown in Figure 6

B. Different materials were tested and 'Clear CL03', a photopolymer resin, was found to be ideal. Its walls are smooth, minimizing sticking of particles to it. The material is clear, making it possible to check for a proper fit of the filter. To avoid sample loss, a silicone gasket was placed on the upper and lower end of the adapter, as illustrated in Figure 6 C.

#### 1.4. Fourier-transform infrared imaging for the analysis of microplastics

Infrared (IR) spectroscopy is a vibrational spectroscopy technique that allows to determine the chemical composition of a solid, liquid, or gaseous sample through its interaction with electromagnetic radiation in the infrared range (wavelength  $\lambda = 780 \text{ nm}$  to  $1 \text{ mm}$ ). Depending on the sample's composition, a part of the light is absorbed before reaching a detector. The detector is coupled to a computer that outputs the corresponding IR spectrum. In spectroscopy, 'wavenumbers' are used rather than wavelengths (wavenumber =  $\lambda^{-1}$ ), corresponding to the number of waves passing through  $1 \text{ cm}$ . The wavenumber is directly proportional to the light energy, which eases the interpretation of spectra. For the identification of plastics and other polymers, the mid IR (MIR) range ( $4,000 - 400 \text{ cm}^{-1}$ ) is suitable (Löder, Kuczera *et al.* 2015). As an example, Figure 7 shows the FTIR spectrum of PS. The bands of the spectrum reflect molecular vibrations or rotations induced by the absorbed light energy. In general, absorption happens when a photon that hits an atom lifts its electrons into a higher energy level. Most of the time, electrons are uplifted one energy level. However, at a lower probability, one or more levels can be skipped (overtone vibration). Changing electron energy levels disturbs the equilibrium of interactions between atoms of a molecule (steric effects) that are responsible for their spatial arrangement. Consequently, the atoms start to vibrate in relation to their equilibrium state, as shown on the right side of Figure 7. Rotations are possible as well, but take place mostly in the far IR region ( $\lambda \geq 50 \mu\text{m}$ ). Because the energy levels of electrons are quantized, only very specific wavelengths, i.e. photons containing exactly the right amount of energy, can induce vibration or rotation of a molecule, depending on the strength of interactions between its atoms.

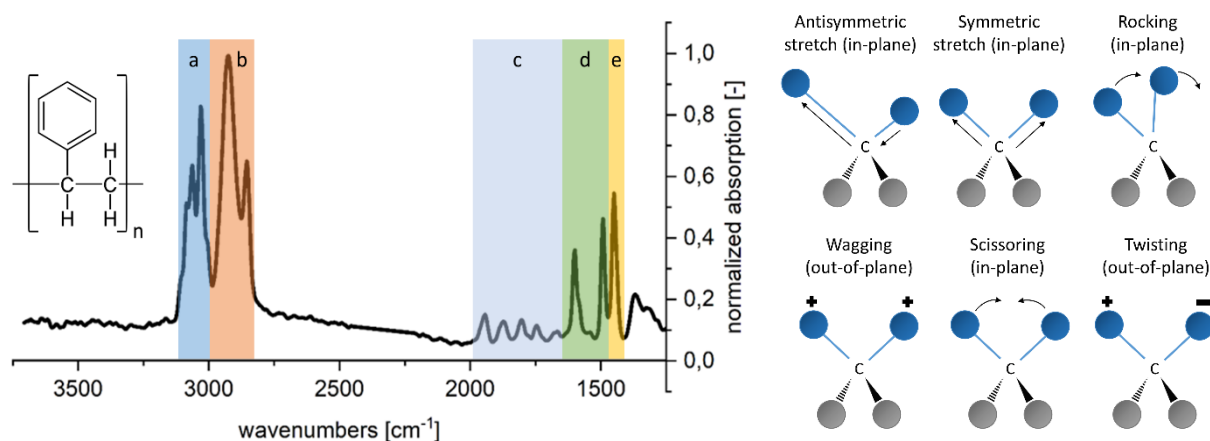


Figure 7. left: Absorbance Infrared spectrum and molecular structure of polystyrene; characteristic bands: a,  $2,800 - 3,060 \text{ cm}^{-1}$ , aromatic C-H stretch; b,  $2,800 - 3,000 \text{ cm}^{-1}$ , aliphatic C-H stretch; c,  $1,650 - 2,000 \text{ cm}^{-1}$ , aromatic C-H bend (overtone); d,  $1,450 - 2,000 \text{ cm}^{-1}$ , aromatic ring stretch; e,  $1,450 \text{ cm}^{-1}$ , alkane  $\text{CH}_2$  bend (Jung, Horgen *et al.* 2018; Al-Kadhemy, Rasheed *et al.* 2016). Right: Modes of molecular vibration; '+' and '-' signs indicate forward and backward movement, respectively (adapted from Günzler and Gremlich (2003a)).

Caused by the electrons' movement, the molecule's charge distribution, or its dipole moment, shifts and becomes asymmetric (Günzler and Gremlich 2003a). The frequency of the molecular vibration equals the light frequency that induced the vibration (Stuart 2004). *Vice versa*, no absorption of light energy takes place in molecules, whose dipole moments would remain symmetric upon irradiation. Consequently, IR spectra only exhibit bands representing vibrations of the functional groups of polymers, but not their symmetrical C-C backbone (Günzler and Gremlich 2003a). Based on the characteristic bands of its spectrum, a sample's

chemical composition can be deduced. The range from 1,500 to 600  $\text{cm}^{-1}$  typically shows a more complex band pattern than the range  $> 1,500 \text{ cm}^{-1}$ , as bands here originate from the coupled vibrations across the molecule, the skeletal vibrations. This so-called fingerprint region is highly specific for a substance, but also more complex to interpret (Stuart 2004).

Using early spectrometers, only one wavelength could be emitted and recorded at once. Interferometers and computers capable of resolving the interferograms into wavenumber-resolved spectra via Fourier transform were developed in the 1960s and 1980s. With these inventions, it became possible to irradiate a sample with light of a range of wavenumbers at once, considerably speeding up the measurements (Günzler and Gremlich 2003c).

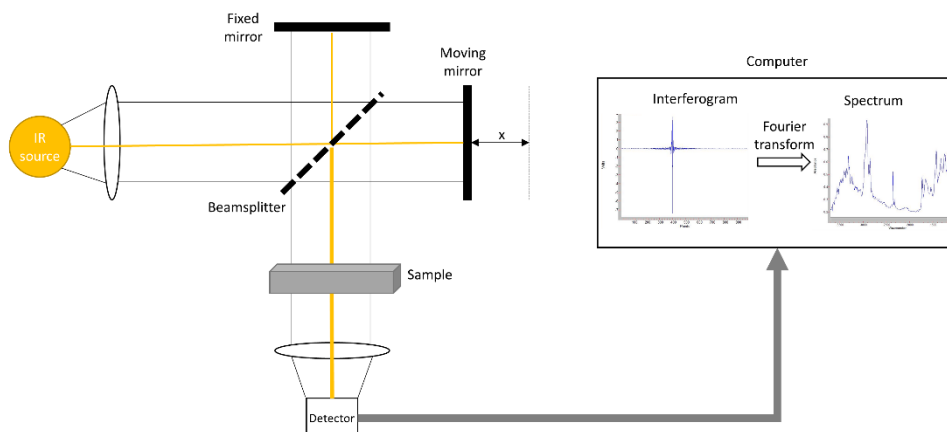


Figure 8. Simplified Michelson interferometer and signal processing, adapted from Günzler and Gremlich (2003b). One mirror constantly moves over a distance  $x$ .

Modern spectrometers usually employ a Michelson-interferometer, schematically shown in Figure 8. In brief, the IR beam hits a beamsplitter, where half of it is reflected to a fixed mirror and the other half passes to a mirror that constantly moves backwards and forwards over the distance  $x$ . After being reflected again, both beams are recombined at the beamsplitter and proceed towards the sample. For  $\lambda = 2x$ , constructive interference occurs, while all other wavelengths experience destructive interference, which enhances the signal-to-noise ratio. The interferogram output by the detector is consequently the intensity of the IR radiance as a function of the moving mirror's position. It is mathematically resolved to wavenumbers *via* FT. The FTIR spectrum is then corrected for the background to yield the sample spectrum. Figure 8 shows a transmission FTIR experiment. Reflection and Attenuated Total Reflection (ATR) experiments are possible, as well. For ATR-FTIR experiments, the sample is pressed onto an optically dense crystal, usually diamond or Germanium. The IR beam is reflected at the interface between the crystal and the sample, thereby penetrating the sample slightly (evanescent wave). This is possible only when the critical angle of incidence, which depends on the refractive indices of the sample and the crystal, is exceeded. The depth of penetration increases with increasing the angle of incidence and with decreasing wavenumbers. The latter causes ATR spectra to typically exhibit lower absorbance values in the higher wavenumber range (e.g. the C-H stretch region in 2,800-3,000  $\text{cm}^{-1}$ ) than transmission or reflection IR spectra (Günzler and Gremlich 2003d). ATR-FTIR experiments can only be conducted for samples big enough to be placed on the crystal one-by-one, restricting the technique to MP particles  $\geq 500 \mu\text{m}$  (Käppler, Windrich *et al.* 2015).

For the analysis of small sample compartments or particles  $< 500 \mu\text{m}$ , FTIR spectrometers can be coupled to a microscope. The procedure is then called FTIR microspectroscopy or  $\mu\text{FTIR}$ . For larger sample areas or large numbers of particles, manual selecting, focusing and measuring is cumbersome and bears the risk of overlooking particles. Usage of Focal Plane

Array (FPA) detectors, however, enables to record spatially resolved IR spectra in the detector's complete field of view (also called tile), creating an artificial IR image of the sample, where each pixel contains one IR spectrum (see Figure 9) (Löder, Kuczera *et al.* 2015). This is termed 'FTIR imaging' and currently is one of the most-used techniques for MP analysis (Cowger, Gray *et al.* 2020). Each pixel corresponds to a projected area on the sample, the size of which depends on the objective's magnification.

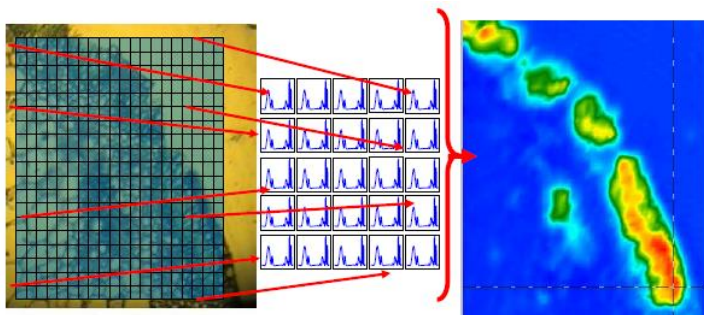


Figure 9. FTIR imaging with a focal plane array (FPA) detector. Image Source: Poster Cary 620 imaging system, Agilent Technologies, Inc.

FPA detectors can comprise up to  $256 \times 256$  mercury cadmium telluride (MCT) detector elements, recording up to 65,536 IR spectra simultaneously. Depending on the sample area to be measured, several tiles can be stitched together. This way, a typical MP sample with approximately  $10 \times 10 \text{ mm}^2$  can be measured within 3 to 4 hours, depending on the FPA detector's size and the objective chosen (Schymanski, Oßmann *et al.* 2021). The resulting IR image can then be analyzed, for example, for MP particles. The here-used method for data analysis is described in section 1.5. Particle sizes can be determined by grouping of neighboring pixels that were assigned to the same substance. Moreover, particle shapes can be determined, which are relevant for (eco-)toxicity of the particles (Gray and Weinstein 2017).

The spatial resolution in FTIR imaging, i.e. the minimum distance between two points to be resolved,  $\Delta x$ , is restricted by the diffraction limit  $n$  of the surrounding medium (i.e. air) and the objective's numerical aperture (NA) as can be deduced from Rayleigh's criterion (Lasch and Naumann 2006):

$$\Delta x = 0.61 \cdot \frac{\lambda}{n \cdot NA} \quad (4)$$

For MIR light, the theoretical maximum spatial resolution achievable is therefore approximately  $2.5 \mu\text{m}$  in air with  $NA = 0.62$  at a wavenumber of  $4,000 \text{ cm}^{-1}$ . In practice, MP particles above sizes between 10 and  $20 \mu\text{m}$  can be analyzed (Xu, Thomas *et al.* 2019), because the image contrast decreases with decreasing distance between two objects, resulting in blurriness (Lasch and Naumann 2006). Moreover, the signal-to-noise ratio of small particles is often poor because of scattering effects at the particle surface (Renner, Schmidt *et al.* 2017).

With FTIR spectroscopy, plastic additives such as plasticizers, flame retardants, or colorants present in small concentrations compared to the bulk plastic are not analyzable. This is, in turn, possible with RM. Additionally, RM can analyze MP particles down to a size of approximately  $300 \text{ nm}$  under ideal conditions. Yet, FTIR imaging provides a powerful balance between spatial resolution and analysis speed, detecting MP particles down to sizes of 10 to  $20 \mu\text{m}$ . Plastic types can be determined by inspecting the characteristic IR bands in the range  $3,800$  to  $1,250 \text{ cm}^{-1}$ . The use of FPA detectors enables to analyze a whole sample area, minimizing the risk of overlooking particles (Schymanski, Oßmann *et al.* 2021).

For this thesis, IR experiments were performed using a Cary 670 FTIR spectrometer (Agilent Technologies, Inc., CA, USA). For ATR-measurements, an ATR unit with a Germanium crystal was used (MIRacle™, PIKE Technologies, WI, USA). For imaging experiments, a Cary 620 FTIR microscope was coupled to the spectrometer. The microscope was equipped with a 15x

objective, corresponding to a projected pixel size of 5.5  $\mu\text{m}$ . Moreover, it comprised a 128  $\times$  128 pixels MCT FPA detector that was cooled to 79 K using liquid nitrogen for the analyses. An automated stage enabled mosaicking of sample areas larger than the FPA's detector field of view ( $\sim 700 \times 700 \mu\text{m}$ ). Typically, a sample image comprised 12  $\times$  12 tiles. Samples on silicon or gold-coated PC filters were scanned in the range from 3700 to 810  $\text{cm}^{-1}$ . For Anodisc membranes, the range was restricted to 3700 to 1250  $\text{cm}^{-1}$  due to the self-absorption of the material (Käppler, Windrich *et al.* 2015). The spectral resolution was 8  $\text{cm}^{-1}$  (Löder, Kuczera *et al.* 2015) and 30 co-added scans were recorded per sample. Prior to each sample scan, 120 co-added background scans were recorded on a clean spot of the filter to maximize the signal-to-noise ratio.

### **1.5. Random Decision Forest Classifiers for machine-learning assisted microplastic identification in FTIR images**

FTIR imaging produces large amounts of data in which MP particles and fibers can be identified. To illustrate this, measuring a 10 mm x 10 mm sample filter results in 3.3 millions of spectra with the instrumental set-up described before. Clearly, computer-assisted, automatic data analysis routines (DARs) are necessary to cope with this amount of data. However, data volume is only one out of several challenges: transmission  $\mu\text{FTIR}$  spectra of microparticles typically suffer from bad quality, reflected for example in a low signal-to-noise ratio. Typical causes are light scattering, mixed spectra resulting from overlaying MP particles and matrix residues or aging of particles (Renner, Schmidt *et al.* 2017). In addition, IR spectra of some polymers look alike or may be confused with natural polymers, when they possess the same IR-active functional groups. The most prominent example for this are PA and protein spectra, that are hard to distinguish (Schymanski, Oßmann *et al.* 2021).

Consequently, a DAR must not only be fast, but also needs to be robust enough to cope with the above-listed challenges. Database matching, as well as supervised and unsupervised machine learning methods have been proposed for this task. A detailed discussion is given in Weisser, Pohl, Heinzinger *et al.* (2022), which is summarized in section 3.2. Like the other steps of the MP analysis pipeline, the DAR should be evaluated thoroughly, as is described in sections 1.6.4 and 3.3.

As has been proposed by Hufnagl, Steiner *et al.* (2019), Random Decision Forest (RDF) classifiers pose a swift and robust option for MP identification in hyperspectral images. The method belongs to the family of supervised machine learning (ML) and was employed for data analysis in this thesis. In supervised ML, the algorithm is provided with a set of labelled training data, that is, for example, spectra of MP particles, which were assigned to their classes or polymer types by a human expert. If pictured like a school lesson, in which the algorithm is the student, it 'learns' how to distinguish the classes based on the teacher's exercises and examples, the training data. To distinguish the classes, a set of features, or spectral descriptors, is identified either by the model itself or, as is the case for RDF classifiers, is provided by the user. An example for a spectral feature is the presence of a band at a certain position (i.e. most plastic IR spectra possess C-H stretch bands between 2,980 and 2,780  $\text{cm}^{-1}$ ), or the ratio of two bands' heights. Using the training data and features, decision trees are 'grown', in which the 'root and branch' nodes represent the features and the 'leaf' nodes represent the classes or polymer types (see Figure 10). Random Decision Forests are an ensemble of decision trees that cast a majority vote on the classification of a sample. In contrast to single decision trees, this leads to a strongly enhanced classification performance (Back, Vargas Junior *et al.* 2022). The reason for this is that each decision tree is grown

independently on a unique subset of training data and features, gained through ‘bagging’ (bootstrap aggregating) (Breiman 2001) and the ‘random subspace method’ (Tin Kam 1998), respectively, as schematically shown in Figure 10. This way, a common problem in ML, over-fitting, is minimized (Hufnagl, Steiner *et al.* 2019). Over-fitting occurs when a model has learned the training data ‘by heart’, but is not able to generalize its knowledge to previously unknown

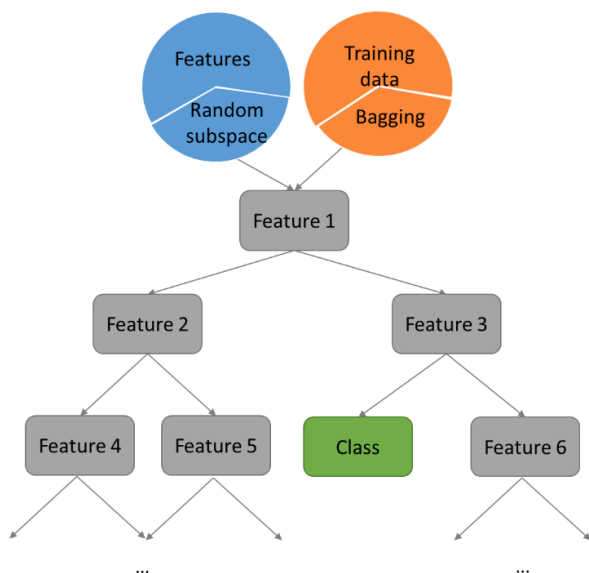


Figure 10. ‘Growing’ a decision tree with a subset of features gained by the random subspace method and a subset of training data, gained through bootstrap aggregating (‘bagging’); grey boxes represent root and branch nodes, the green box represents a leaf node.

data (Ertel 2017). This leads to another important factor for setting up ML models: the training data need to reflect real samples as closely as possible. This means that a), the training spectra need to be acquired in the same way as the samples, i.e. a model that has been trained using ATR-FTIR spectra cannot be expected to work well on transmission  $\mu$ FTIR spectra; b), the factors impairing spectral quality as listed before need to be represented in the training data, meaning they should reflect a certain diversity of spectral qualities (Hufnagl and Stibi 2019; Weisser, Pohl, Ivleva *et al.* 2022); c), all classes to be modelled should be included in the training data in balanced ratios as under-representation of a class can lead to poor performance in classifying it (Japkowicz and Stephen 2002).

A similar advice can be given for the design of the spectral features: while they can be tailored very specifically for certain classes, such as the C-H stretch band pattern of PS, it is this specificity that can lead to poor performance when spectra are distorted or their quality is impaired in another way (e.g. baseline drifts). Providing more general features instead, such as band heights, or band height ratios across the spectral range can be more suitable.

In the family of supervised ML, RDF classifiers are relatively easy to interpret. Other models such as Artificial Neural Networks (ANNs) or Support Vector Machine (SVM) remain a ‘black box’ to the user to a much greater extent. For any ML model, however, the choice of training data is key for its success. Importantly, the fact that human operators are in charge of labelling the training data makes it evident that human bias of the model cannot be fully excluded (Bender, Gebru *et al.* 2021; Weisser, Pohl, Ivleva *et al.* 2022). The necessity for feature input poses another source of bias; however, tools are available to automatize feature design (EPINA ImageLab documentation).

For this work, RDF models were set up using EPINA ImageLab (Epina Softwareentwicklungs- und Vertriebs-GmbH, Austria). The software enables to combine training data sourced from various samples into one set and allows manual and automatized feature design. Further, the number of trees can be optimized using the *tree scan* function. The number of trees here was set between 40 and 60, depending on the model. The software further provides some basic model evaluation by splitting a proportion  $R$  off the training data set to serve as test data. This way, confusion matrices were created showing true and false assignments for each class. At this point, falsely labelled training spectra could be identified by the operator and kicked out easily. Further, the *variable importance* illustrated which features were most valuable for the model, allowing to narrow down the feature set, thereby streamlining it without impairing the model performance. Aiming for a compromise between a high amount of training data and a

not too small test set, R was set to 0.67 and the model optimized using the described functionalities. To assess the model further, Monte Carlo cross evaluation (see 1.6.4) was conducted, using a script kindly provided by Benedikt Hufnagl, Technical University of Vienna. Measures for quality assurance and quality control of the DAR are further given and discussed in section 1.6.4.

## 1.6. Quality assurance and quality control in microplastics research

Employing holistic quality assurance (QA) and quality control (QC) measures is a prerequisite on the way to harmonized and standardized MP analysis pipelines. However, they both pose major challenges to the field: First, MP particles are a collective of analytes that possess a broad variety of features and are heterogeneously distributed. Second, MP is ubiquitous, implying the risk of sample contamination. Third, particles may get lost during sample preparation, or, fourth, be overlooked during instrumental analysis. Lastly, an insufficient DAR can cause erroneous results. This section describes measures for QA and QC that are substantial for method harmonization along the whole MP analysis pipeline (Koelmans, Mohamed Nor *et al.* 2019; Schymanski, Oßmann *et al.* 2021; Primpke, Christiansen *et al.* 2020; Lusher, Munno *et al.* 2020), as summarized in Figure 11. Note that inter-laboratory comparison tests, the 'gold standard' of method standardization are not discussed further here. There is still a substantial lack of realistic MP reference particles < 500 µm. Furthermore, preparing homogeneous samples for the participating labs remains a major challenge (Belz, Bianchi *et al.* 2021; Eitzen, Paul *et al.* 2019), lowering the expressiveness of these tests.

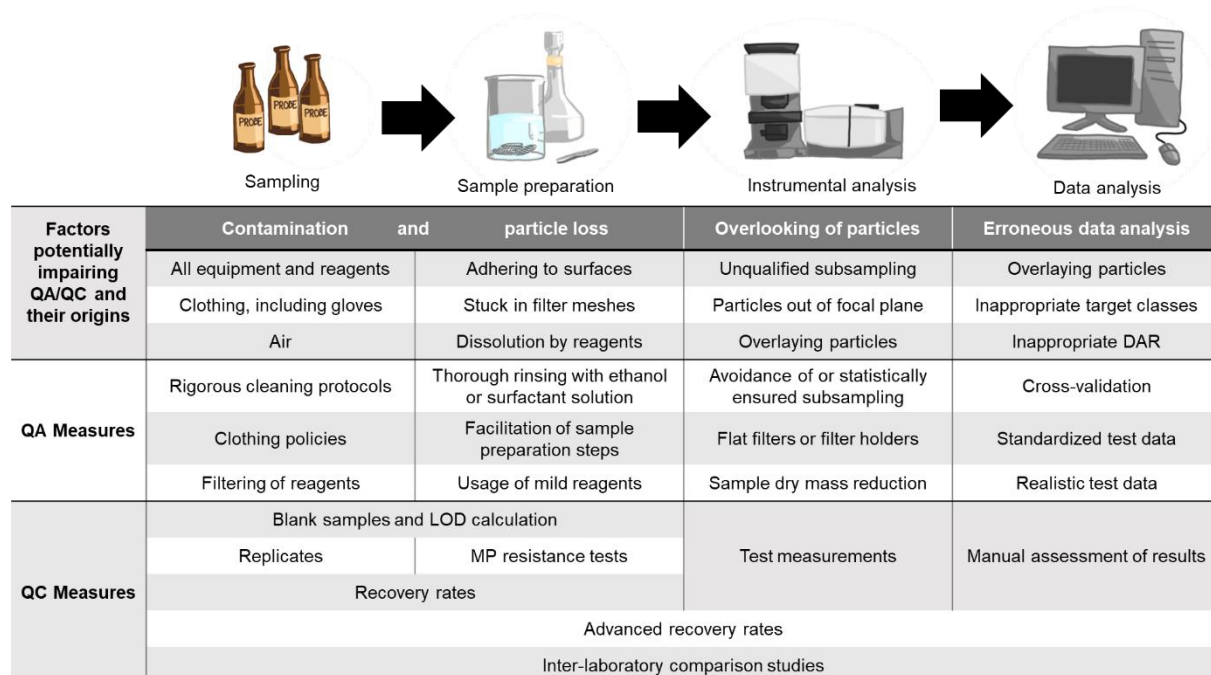


Figure 11. Summary of factors known to influence the quality of MP analysis and measures to assure analysis quality (QA) and to control it (QC). LOD = Limit Of Detection; DAR = Data Analysis Routine.

### 1.6.1. Contamination prevention and assessment

To prevent sample contamination during sampling and sample preparation as part of the QA measures, the rules listed below were followed during the experimental part of this thesis (see also Schymanski, Oßmann *et al.* (2021); (2018); Braun (2021)):

- Avoidance of plastic materials, except for natural rubber and Viton® for tubes and gaskets
- Working in a HEPA H14 clean air bench (V1300, Alpina Polska Sp. Z o.o, Konin, Poland), whenever possible

- Covering samples with watch glasses, glass petri dishes or aluminum foil when not in use
- Wearing purple cotton laboratory coats and green PP hairnets
- Usage of gloves only when necessary for safety reasons
- Strict cleaning protocols including manual scrubbing and ultrasonic cleaning (20 minutes, 45 kHz) for all equipment
- Filtering of all reagents, including demineralized water, through glass microfiber or mixed cellulose fiber ester membranes with 1.2 µm pores
- Regular wiping down all surfaces in the laboratory with cotton cloth
- Flushing the funnel used for filtration with EtOH until no particles came off anymore (checked under stereomicroscope)

As contamination with MP can never be fully avoided, blank samples were prepared in parallel with each set of samples. Blank samples were treated exactly as samples were treated, starting with cleaning of all equipment, sampling, sample preparation and the final analysis. The limit of detection (LOD) for each type of sample was calculated from the corresponding blank values as follows (Schymanski, Oßmann *et al.* 2021; Weisser, Beer *et al.* 2021):

$$\text{LOD} = \text{mean}_{\text{blanks}} + 3 \times \text{standard deviation}_{\text{blanks}} \quad (5)$$

Blank values are expressed as absolute numbers of MP particles per sample rather than as concentrations, because they do not comprise a sample whose volume or mass they can be related to. If the results needed to be extrapolated (e.g. from 1 g to 1 kg of sample), the blank values were also extrapolated. If a sample's MP concentration was lower than or equal to the LOD, it was considered free from MP. Further, a series of air blanks was conducted to assess airborne MP contamination. For this purpose, wetted Anodisc membranes were placed into the laminar flow bench during sample preparation.

### 1.6.2. Particle loss assessment

While on one hand, reducing the risk of contaminating samples is vital for MP analysis, on the other hand, there is also a high risk for losing particles during sample preparation. Potential reasons for particle loss are adhesion to parts of the equipment (Dimante-Deimantovica, Suhareva *et al.* 2022; Eitzen, Paul *et al.* 2019), getting stuck in filter pores and sieve meshes (Dimante-Deimantovica, Suhareva *et al.* 2022), as well as dissolution of particles by chemical reagents (Hurley, Lusher *et al.* 2018). The latter was tested by exposing reference MP particles to a variety of chemical treatments and determine their sizes before and after the treatment (see Al-Azzawi, Kefer *et al.* (2020)). In addition, chemical alterations of the particles were examined by reflectance µFTIR. To do so, the treated particles were washed with filtered demineralized water and deposited on gold-coated PC membranes. µFTIR in reflectance mode, in contrast to transmission mode, gathers information about the particle surface rather than the bulk, allowing to search for modifications in the polymer spectra such as newly formed bands in the region around 1,700 cm<sup>-1</sup> that hint at the formation of C=O bands (von der Esch, Lanzinger *et al.* 2020).

To account for particle losses not caused by chemical reagents but during sample handling, recovery rates were determined for each sample preparation step using pink PS particles. The particles were cryo-milled (Simone Kefer, Chair of Brewery and Beverage Technology, TUM) and treated as reported in von der Esch, Lanzinger *et al.* (2020) to make their surfaces more hydrophilic, thereby easing their handleability and suspensibility. One hundred particles with sizes about 63-125 µm were counted using a single-haired brush under a stereomicroscope and spiked into, for example, a bottle. This procedure was found to yield more reproducible results than preparing a particle suspension for spiking. Then, sample preparation was

conducted as usual, e.g. the bottle was flushed with SDS and ethanol (EtOH). All liquids were filtered through a PC membrane filter (diameter 25 mm) or a silicon filter, depending on which filter should be used for the respective sample type, and the reference particles counted again. The recovery rate (RR) is expressed as the percentage of recovered particles. RRs were assessed in triplicates, and are given alongside the MP findings to illustrate the level of potential underestimation of MP counts due to particle losses.

### 1.6.3. Sample analyzability

In the beginning, dry mass reduction was chosen to evaluate the success of MP isolation from a sample matrix. However, FTIR analysis of some samples was impaired by matrix residues despite dry mass reduction > 90%. Therefore, sample analyzability was tested by spiking the food or beverage in question with an arbitrary number of cryo-milled PS reference particles < 200  $\mu\text{m}$ . After the digestion, the sample underwent FTIR imaging and was checked for detectability of the spiked-in particles. Only if the particle spectra were not impaired by matrix spectra, the digestion protocol was considered suitable.

### 1.6.4. Data analysis routine performance evaluation

An often-neglected aspect in QA/QC of the MP analysis pipeline is the very last step, the evaluation of spectroscopic data. While the often-insufficient reporting transparency has been outlined in section 1.2, the basics of data analysis routine (DAR) evaluation and its current state in the literature are summarized in the following.

A DAR's purpose is to assign the sample spectra to the correct classes, i.e. substances, automatically. This process is also called 'prediction' or 'classification'. Even though these *termini* stem from the ML context, they are used here for both, ML and database matching. Regardless of the type of DAR, a test data set should be prepared and used to assess the DAR's performance (Skansi 2018). The ground truth of the test data is defined by manual assignment of the spectra, which is considered the 'gold standard' (Renner, Nellessen *et al.* 2019). This assessment should comprise true positive, false positive, false negative, and true negative results (TP, FP, FN, and TN, respectively). Importantly, the test data must be separated from the training data or database, respectively, because tests on (parts of) the training data will result in over-optimistic performance evaluation. It is advisable to determine the ground truth in advance, rather than checking the DAR's assignments after classification. This contributes to minimizing human bias during DAR evaluation. Confusion matrices are a simple method of summarizing the results while giving insight into the performance of each class as shown in Figure 12 (ISO/DIS 24187, Hufnagl *et al.* 2019; Ballabio, Grisoni, and Todeschini 2018). To evaluate ML-based DARs, bias can be reduced further through cross-validation (CV), where test data are subsampled from a data set repeatedly, while the remaining data serve as training data. This procedure further reduces the risk of over-fitting, especially in cases where training data is scarce. A variant of CV is Monte Carlo CV (MCCV),

|                 |         | Predicted Class |         |         | Actual total |
|-----------------|---------|-----------------|---------|---------|--------------|
|                 |         | Class 1         | Class 2 | Class 3 |              |
| Actual Class    | Class 1 | 80              | 15      | 5       | 100          |
|                 | Class 2 | 0               | 95      | 5       | 100          |
|                 | Class 3 | 10              | 0       | 90      | 100          |
| Predicted total |         | 90              | 100     | 100     |              |

Figure 12. Example of a 3-class confusion matrix; grey boxes highlight true positive (Reprint from Weisser, Pohl, Heinzinger *et al.* (2022) with permission from the publisher).

where the test data are split off iteratively from the whole, original dataset (Xu and Liang 2001). Importantly, training, test, and evaluation data should reflect realistic sample data as much as possible (Back, Vargas Junior *et al.* 2022).

If this advice for bias minimization is followed, the confusion matrix can serve as the basis for QA of the DAR. First, it reveals class confusions. Second, based on the confusion matrix, class-specific and global performance metrics can be calculated as in formulae 6-11 for each class  $g = \{1, 2, \dots, G\}$ , where  $G$  is the total number of classes (adapted from Ballabio, Grisoni *et al.* (2018)). All metrics can take values between 0 and 1, where 0 represents the poorest possible performance and 1 would be a perfect classification result.

|                      |              |                                   |     |
|----------------------|--------------|-----------------------------------|-----|
| Single-class metrics | Sensitivity: | $Sn_g = \frac{TP_g}{TP_g + FN_g}$ | (6) |
|----------------------|--------------|-----------------------------------|-----|

|              |                                   |     |
|--------------|-----------------------------------|-----|
| Specificity: | $Sp_g = \frac{TN_g}{TN_g + FP_g}$ | (7) |
|--------------|-----------------------------------|-----|

|            |                                   |     |
|------------|-----------------------------------|-----|
| Precision: | $Pr_g = \frac{TP_g}{TP_g + FP_g}$ | (8) |
|------------|-----------------------------------|-----|

|                |           |   |     |
|----------------|-----------|---|-----|
| Global metrics | Accuracy: | $Acc = \frac{\sum_{g=1}^G (TP_g + TN_g)}{\sum_{g=1}^G (TP_g + TN_g + FP_g + FN_g)}$ | (9) |
|----------------|-----------|---|-----|

|   |                                     |      |
|---|-------------------------------------|------|
| Average sensitivity or<br>Non-Error-Rate: | $NER = \frac{\sum_{g=1}^G Sn_g}{G}$ | (10) |
|---|-------------------------------------|------|

|                   |                                    |      |
|-------------------|------------------------------------|------|
| Average precision | $Pr = \frac{\sum_{g=1}^G Pr_g}{G}$ | (11) |
|-------------------|------------------------------------|------|

Accordingly, sensitivity ( $Sn_g$ ) represents the ability of a model to correctly identify samples belonging to the  $g$ th class; specificity ( $Sp_g$ ) expresses the ability to correctly reject samples belonging to others than the correct class  $g$ ; precision ( $Pr_g$ ) reflects the avoidance of FP predictions for the  $g$ th class. Accuracy (Acc) corresponds to the share of correct classifications over all classifications. Together with Average Precision (Pr) and average  $Sn_g$ , also called Non-Error-Rate (NER), a model's performance can be assessed on a global level. The global metrics should be used with care if the number of test data points is imbalanced across the classes, as this causes bias in favor of the highly represented classes (Ballabio, Grisoni *et al.* 2018).

With these evaluation tools at hand, DARs can be assessed concisely, but they are still scarcely used in the context of MP research. In addition, there is some confusion about them, as they are often named arbitrarily and are not always clearly defined in the literature. For example, Morgado, Palma *et al.* (2020) used 'TP' as abbreviation for 'true positive result rate', calculated equal to Acc. Similarly, Primpke, Lorenz *et al.* (2017) calculated a 'TP rate' to illustrate their results. In turn, Renner, Sauerbier *et al.* (2019) used 'TP rates', which supposedly are equal to  $Sn_g$ , to evaluate their DAR. Kedzierski, Falcou-Préfol *et al.* (2019) evaluated their DAR based on the 'difference' between the DAR's and a human expert's results, which can be assumed to reflect 1-Acc.

Another issue is that DARs are usually evaluated on sets of individual spectra, but not on whole hyperspectral images. Such evaluations, however, do not cover the full complexity of a DAR as described and shown in section 3.3. If FTIR images were used for DAR evaluation, this did not go beyond 'visual inspection' (Hufnagl, Steiner *et al.* 2019) or qualitative comparison of particle false color images (Wander, Vianello *et al.* 2020).

## 2. Aims of the project

This doctorate project was started with the intend of gaining clarity about the main entry paths of MP into beverages and plant-based foods. It quickly became clear that this was only feasible with a high-throughput analysis pipeline; however, no suitable standard methods were established at that time. Consequently, the first goal was to test and optimize sample-matrix dependent methods for sampling and sample preparation. Second, for the instrumental analysis, a good compromise between analysis speed and exactness was required, leading to the implementation of FTIR imaging at the chair. The high amounts of data to be interpreted, however, posed another, third challenge to be solved and led to establishing a ML-based method.

In the second half of the project, efforts were made to complement the measures of QA/QC that meanwhile had been established for sampling, sample preparation, and instrumental analysis for the last part of the pipeline, the data analysis. Especially, the validity of evaluating a data analysis routine on single, isolated spectra was questioned.

Moreover, a strategy for the estimation of typical error types occurring during MP recognition in FTIR images, such as over-segmentation and overlooking of particles, was elaborated. In this context, fully evaluated datasets were published, pushing forward the comparability and harmonization of automated MP recognition techniques.

Lastly, MP concentrations in beverages and food were to be analyzed. The most important sustenance, drinking water, was analyzed in detail for MP entry paths by means of a stepwise sampling campaign along the process of mineral water bottling. Similarly, entries of MP during the production of a variety of foods, such as bread, fruit purees, and tea were assessed.

Having the goal of a fast and versatile MP analysis pipeline in mind, all methods and workflows were chosen and adapted to be quick and cost-efficient, as illustrated in Figure 13. This included a robust QA/QC system for all steps of the analysis pipeline, thereby contributing to the ongoing harmonization of MP analysis.

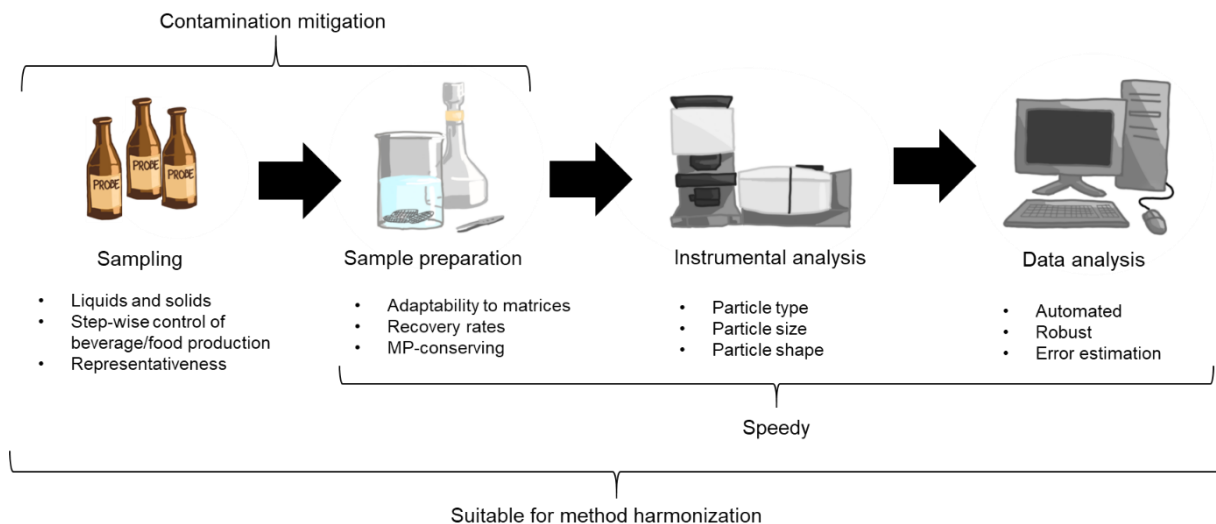


Figure 13. Summary of this thesis' aims. Illustrations created by Teresa Pohl with kind permission to use here.

### 3. Results

This section summarizes the experimental results for MP-specific sample preparation and the success of QA/QC measures taken (section 3.1). Next, proposed methods for MP recognition in hyperspectral images are summarized (section 3.2), and a novel method for their evaluation is presented (section 3.3). Lastly, entry paths for MP into bottled mineral water and a selection of other beverages and foods are shown (sections 3.4 and 3.5). Most of the results presented here have already been published elsewhere. Whenever this is the case, this is indicated at the beginning of the respective subsection. Some results were gained during students' theses under Jana Weißer's supervision. These are cited accordingly.

A discussion of all results presented here can be found in section 4.

#### 3.1. Sample preparation of beverages and plant-based food products for microplastic analysis

As described in section 1.3.2, chemical and enzymatic methods were tested for the isolation of MP particles from their surrounding food matrix to avoid interference during the spectroscopic analysis. Their effectiveness is presented in the following, as well as their impacts on MP particles.

##### 3.1.1. Sample matrix-dependent degradation methods and analysis filters

Food matrices were to be degraded to yield analyzable samples. The first measure to evaluate the goodness of a degradation method was dry mass reduction. Secondly, sample analyzability by FTIR imaging was assessed, see 1.6.3.

##### Improved Fenton reaction by combination with ascorbic acid

The effectiveness of the adapted Fenton protocol for the degradation of food was tested and evaluated based on the decrease of dry mass of the 'strawberry' and 'pear' purees (as described in the experimental part in section 1.3.2).

In general, higher dry mass reduction was achieved for the strawberry puree than for the pear puree, as can be seen in Figure 14. For both, however, it was observed that the addition of ascorbic acid (AAH) increased the degradation. The pear puree reached  $88.62 \pm 0.24\%$  dry mass reduction without AAH and  $92.01 \pm 0.36\%$  with AAH. The degradation of strawberry puree increased from  $91.61 \pm 0.41\%$  to  $97.24 \pm 0.31\%$  when AAH was added. Despite these high degradation rates, residues of the matrices were still present after the Fenton + AAH treatment of all foods and beverages tested, except for water and a Pilsner style, filtered beer. This showed that more specific treatments were necessary and consequently, technical grade enzymes were tested for the model foods.

##### Enzymatic degradation

First, a suitable reaction system regarding the buffer type, pH, and temperature had to be established for each enzyme employed. In contrast to other reports (Löder, Imhof *et al.* 2017), buffer concentrations of  $> 0.1$  M were found to flocculate all enzymes tested within one hour. Instead, a sodium hydroxide-citric acid buffer with 0.1 M was found suitable for all enzymes tested. When pH and temperature were set to the enzyme optima as recommended by the manufacturers and reported by Löder, Imhof *et al.* (2017), the enzymes denatured. When choosing milder conditions, i.e. a pH of 6 and a temperature of 40-50°C, a stability of at least 24 h for all enzymes was reached, except for *Xylanase 2x*, for which a stabilization longer than 3.5 h could not be achieved.

### 3 - Results

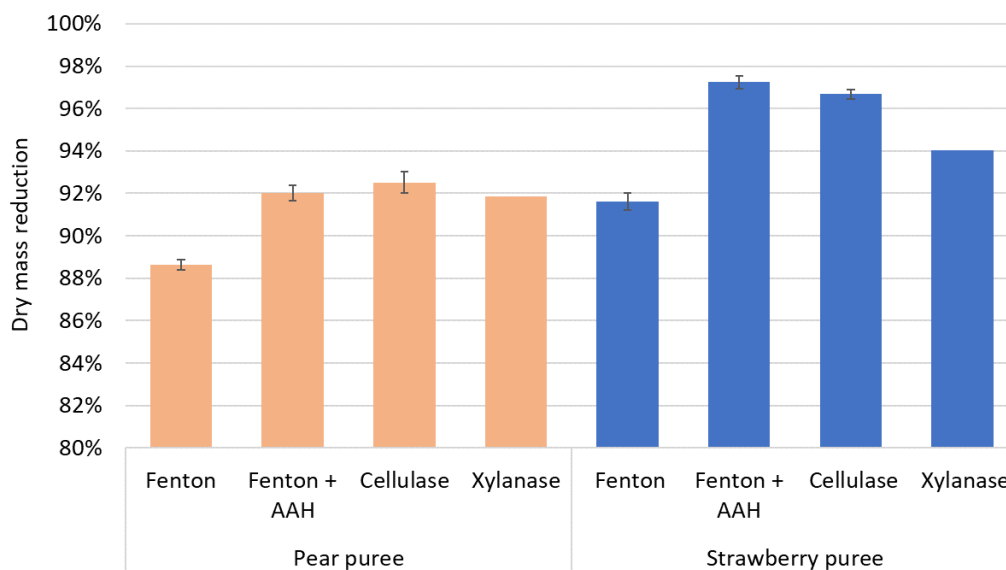


Figure 14. Dry mass reduction for pear and strawberry fruit purees for Fenton treatment with and without addition of ascorbic acid (AAH), cellulase and xylanase.

Adding  $\text{Ca}^{2+}$  did not bring any advantage after optimization of the other reaction conditions and was therefore not considered further (Dunkel 2018). The optimized conditions are summarized in Table 2. To keep the processes as simple as possible, it was decided to use *Amylase FL* rather than *Amylase Thermo*, so all enzymes could be incubated at  $40^\circ\text{C}$ , allowing the parallelization of experiments in one single water bath. Another advantage of using one buffer for all enzymes is that it allows to further facilitate workflows in the laboratory.

Having the most suitable reaction conditions identified, the degradation of pear and strawberry purees by cellulase and xylanase were tested. While experiments with xylanase had to be terminated after the first run because the filters clogged, the samples treated with cellulase reached dry mass reductions similar to the Fenton + AAH treatment. Again, higher degradation rates were yielded for the strawberry sample. A slightly higher degradation rate ( $+0.56\% \pm 0.08\%$ ) was achieved with Fenton + AAH than with cellulase for the strawberry puree. For the pear samples, the opposite was the case ( $+0.51\% \pm 0.13\%$ ).

Table 2. Reaction conditions for enzymatic degradation of food matrices, optimized for long enzyme stability. Results from Dunkel (2018) under Jana Weißer's supervision.

| Technical grade enzyme | Buffer concentration | Buffer pH | Temperature        | Stable for |
|------------------------|----------------------|-----------|--------------------|------------|
| Cellulase TXL          | 0.1 M                | 6.0       | $40^\circ\text{C}$ | > 24 h     |
| Amylase FL             |                      |           |                    |            |
| Pektinase L-40         |                      |           |                    |            |
| Amylase Thermo         |                      |           | $50^\circ\text{C}$ |            |
| Xylanase 2x            |                      |           | $40^\circ\text{C}$ |            |

In the course of this thesis, it became clear that a high dry mass reduction does not guarantee a sample to be analyzable with FTIR imaging (section 4.2). By assessing the analyzability with  $\mu\text{FTIR}$  instead, it was found that apple puree was degraded best with cellulase. Pectinase, in turn, did not give any advantage compared with cellulase (Eberl 2020).

### 3 - Results

For rye and wheat flours and the bread dough (made from a mixture of both flour types), a combination of cellulase and amylase was necessary (Hubin 2020). Wheat beer and cloudy lemonade were most successfully degraded with xylanase (Lerch 2020), and peppermint tea required a combination of xylanase and cellulase (Müller 2020). It is important to note, however, that all final matrix degradation protocols included Fenton + AAH for both the first and last step of the protocol, with one or more enzymatic treatment steps in between as is summarized in Figure 15. Further, a filtration through stainless steel sieves was necessary after each treatment step (not shown in Figure 15) to remove any reagents from the previous step that may impair the next step, especially when an enzymatic treatment followed a chemical treatment.

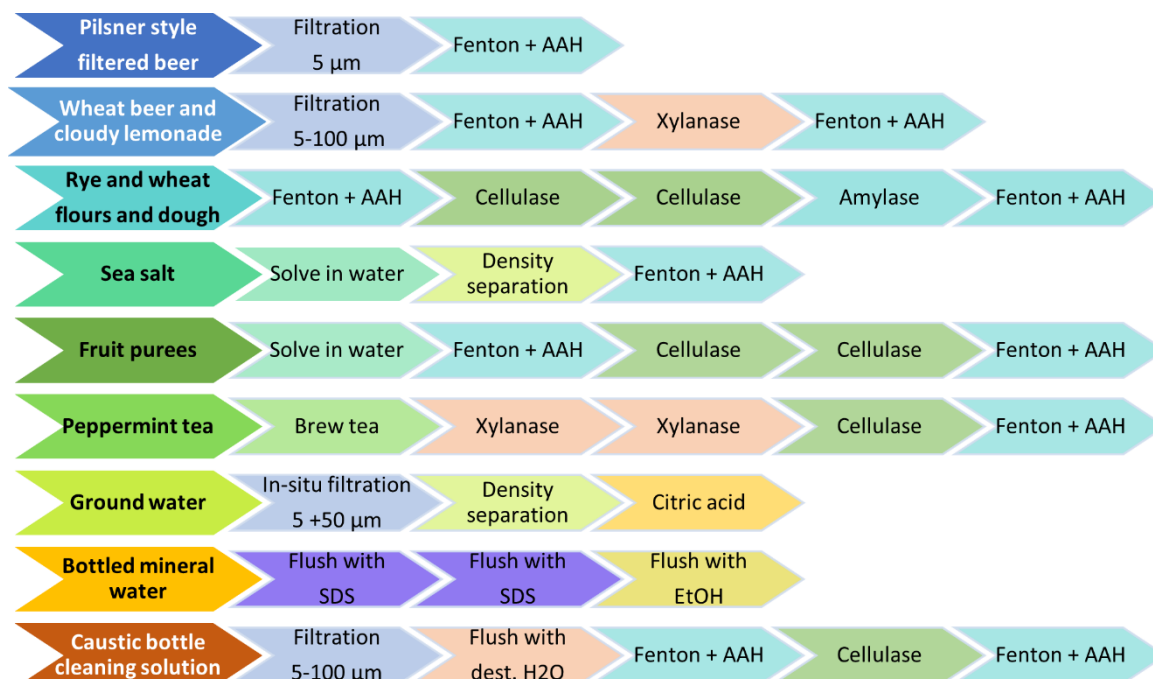


Figure 15. Summary of final sample matrix-dependent degradation protocols; not shown are filtrations between the treatment steps and the final filtration through the analysis filter. Results gained under Jana Weisser's supervision by Eberl (2020), Hubin (2020), Lerch (2020), and Müller (2020). AAH = Ascorbic Acid; SDS = Sodium Dodecyl Sulfate.

### Analysis filters

When Anodisc membranes or PC membranes were used, FTIR imaging suffered from the filters' unevenness causing only parts of it to be in the microscope's focal plane. To compensate for this, the filters were placed into a custom-made filter holder (see Figure 6 A). Flatness with and without the holder was assessed by Elisabeth von der Esch (Institute of Hydrochemistry and Chair of Analytical Chemistry and Water Chemistry, TUM), resulting in a height difference (lowest versus highest spot) of 360  $\mu\text{m}$  without and 132  $\mu\text{m}$  with the holder.



Figure 16. Pink polystyrene particles accumulated at the rim of and adhered to a silicon filter adapter. A piece of a broken membrane at the right. Photo: Lerch (2020).

The silicon filters, in turn, were innately very flat and even. No instrumental assessment of their flatness was undertaken as their flatness was evident when focusing the microscope and moving the stage. Occasionally, the silicon filters broke during handling, when not placed correctly into the adapter. Moreover, particle loss was observed because particles were stuck

between the filter and the adapter as can be seen in Figure 16. Both issues, breaking of the filters and particle loss, were significantly reduced after introducing the usage of silicone gaskets during filtration (see Figure 6 C).

#### **3.1.2. Quality assurance and quality control during sampling and sample preparation**

A broad variety of measures was taken to avoid MP contamination during sampling and sample preparation, see 1.6.1. The success of these measures was controlled by preparing blank samples along with each set of samples, using the same reagents and pieces of equipment.

The air blank samples were nearly free of MP (3 MP particles in 10 air blanks in total), however, the procedural blanks were not; Table 3 summarizes the results from blank samples corresponding to eight different sample types, or sample preparation procedures, respectively, including the reagents utilized and the most abundant plastic types in the blanks. The LOD was calculated according to formula 5.

All MP concentrations were rounded to integers. Most mean blanks ranged between 5 and 19 MP, with outliers for the fruit puree assessment ( $73 \text{ MP} \pm 7 \text{ MP}$ ) and the flour and dough samples with  $295 \text{ MP} \pm 134 \text{ MP}$ . The most abundant plastic types in the blank samples were PS, PE, and polytetrafluoroethylene (PTFE). During sample preparation, especially the usage of chemical reagents may damage MP particles. For instance, potassium hydroxide (KOH) reportedly is an effective sample matrix degrader (Süssmann, Krause *et al.* 2021). However, KOH it can induce the formation of carbonyl groups on MP particle surfaces, thereby altering their IR spectra. While this mechanism can be beneficial for the production of suspensible, realistic reference particles (von der Esch, Lanzinger *et al.* 2020), it can hamper MP recognition (De Frond, Rubinovitz *et al.* 2021; Munno, De Frond *et al.* 2020). In the worst case, it can even lead to the complete dissolution of MP particles, as was experienced during the contribution to the work of Al-Azzawi, Kefer *et al.* (2020). In this study, changes of reflectance  $\mu\text{FTIR}$  spectra of PS, PE, PET, PP, polyamide (PA), polylactic acid (PLA), and PVC, induced by KOH (10%), Fenton (30%  $\text{H}_2\text{O}_2$  + 20 g/L  $\text{FeSO}_4$ ), and  $\text{H}_2\text{O}_2$  (30%) treatments were investigated. Results showed that the combination of KOH with PLA and PET led to dissolution of the particles, while for all other combinations, the particles remained stable. Interestingly, no significant changes of the IR spectra of KOH-treated PLA and PET particles were observed. Only the spectra of PVC treated with one of the three protocols showed a newly introduced band at  $3,650 \text{ cm}^{-1}$ , hinting at the formation of OH groups. Further, the study showed that the reaction temperature plays a role, as well; it should be kept below  $60^\circ\text{C}$  to avoid melting and swelling of the particles (Al-Azzawi, Kefer *et al.* 2020).

### 3 - Results

Table 3. Blank and limit of detection (LOD) values for different sample types examined, including plastic types most abundant in blank samples; n = number of replicates, EtOH = Ethanol; SDS = Sodium Dodecyl Sulfate; PEST = Polyester, PS = Polystyrene; PE = Polyethylene; PP = Polypropylene; PA = Polyamide; PTFE = Polytetrafluoroethylene; PVC = Polyvinyl Chloride; all experiments were conducted by Jana Weißer or under her supervision. \*estimation from only one blank sample, see 3.5.

| Sample type                    | Reference                          | Chemicals and solvents employed       | Blank mean $\pm$ standard deviation [no. of MP per sample] | Most abundant plastic types | LOD |
|--------------------------------|------------------------------------|---------------------------------------|--|-----------------------------|-----|
| Raw ground water (n=4)         | Weisser, Beer <i>et al.</i> (2021) | EtOH, ZnCl <sub>2</sub> , citric acid | 12 $\pm$ 8   | PS, PE                      | 36  |
| Deferrized ground water (n=4)  |                                    | EtOH, citric acid                     | 5 $\pm$ 5  | PE, PEST                    | 20  |
| Bottles (n=4)                  |                                    | SDS, EtOH                             | 13 $\pm$ 9   | PS, PE, PP                  | 47  |
| Caustic washing solution (n=3) |                                    | Fenton, buffer, EtOH                  | 11 $\pm$ 2   | PS, PE                      | 18  |
| Fruit puree (n=2)              | Eberl (2020)                       | Fenton, buffer, EtOH                  | 73 $\pm$ 7   | PTFE, PE, PP                | 64  |
| Tea (n=2)                      | Müller (2020)                      | Fenton, buffer, EtOH                  | 15 $\pm$ 3   | PTFE, PA                    | 24  |
| Flour/dough (n=2)              | Hubin (2020)                       | Fenton, buffer, EtOH                  | 295 $\pm$ 134  | PE, PP                      | 697 |
| Sea salt (n=1)                 |                                    | ZnCl <sub>2</sub> , Fenton, EtOH      | 19   | PVC, PS, PE                 | 33* |

Additionally, the above-mentioned reference particles were tested for their persistence against the protocols used in this thesis: Fenton reaction with AAH, enzymatic treatment in sodium hydroxide-citric acid buffer, citric acid, and density separation in ZnCl<sub>2</sub> (details in section 1.3.2). While the first two did not cause any adverse effects on the particles, ZnCl<sub>2</sub> lead to strong aggregation of PA particles, while their IR spectra remained unchanged.

To assess potential losses of particles during sample preparation, recovery rates (RRs) were determined in triplicates by spiking a sample with a known number of pink PS particles.

Table 4 shows the RRs determined, where using a PC membrane as the final filter mimicked the usage of Anodisc membranes. The highest RR was achieved for flushing water bottles with 86  $\pm$  8% of PS particles recovered (Weisser, Beer *et al.* 2021). The filtering through stainless steel sieves and suspending particles from them yielded a slightly lower RR of 83%  $\pm$  11% (Müller 2020). From density separation, 63%  $\pm$  8% of particles were recovered when filtering through a PC membrane lastly (Weisser, Beer *et al.* 2021). In contrast, only 54%  $\pm$  16% recovery was achieved for density separation when the final filter was a silicon filter (Hubin 2020).

The lowest RR, 58%  $\pm$  6%, was found for the process of extracting particles from the stainless steel cartridge filters used for in-situ filtration of ground water (Weisser, Beer *et al.* 2021).

### 3 - Results

Table 4. Recovery rates for different procedures of sample preparation, determined using polystyrene (PS) particles with a diameter of 63-125 µm. PC = Polycarbonate. Results gained by Jana Weißer or under her supervision.

| <b>Process</b>                                | <b>Extraction from stainless steel cartridge filters</b> | <b>Bottle flushing</b>             | <b>Density separation</b>          |                | <b>Filtration through stainless steel sieves and re-suspending</b> |
|---|--|------------------------------------|------------------------------------|----------------|--|
| <b>Reference</b>                              | Weisser, Beer <i>et al.</i> (2021)                       | Weisser, Beer <i>et al.</i> (2021) | Weisser, Beer <i>et al.</i> (2021) | Hubin (2020)   | Müller (2020)  |
| <b>Final filter</b>                           | PC membrane  | PC membrane                        | PC membrane                        | Silicon filter | PC membrane  |
| <b>Mean recovery ± standard deviation [%]</b> | 58 ± 6   | 86 ± 8                             | 63 ± 8                             | 54 ± 16        | 83 ± 11  |

### 3.2. The identification of microplastics based on vibrational spectroscopy data – A critical review of data analysis routines

This chapter refers to the publication ‘The identification of microplastics based on vibrational spectroscopy data - A critical review of data analysis routines’, authored by **Weisser J**, Pohl T, Heinzinger M, Ivleva NP, T Hofmann, and Glas K. The article was published in 2022 in Trends in Analytical Chemistry, Vol. 148, Pages 116535, DOI 10.1016/j.trac.2022.116535.

Jana Weißer (Weisser) led the conceptualization of the review article and conducted the literature research. Teresa Pohl and Michael Heinzinger contributed through literature research, writing parts of the article and reviewing it. Michael Heinzinger prepared a figure for the article. The work was supervised and reviewed by Karl Glas, Natalia P. Ivleva, and Thomas Hofmann.

A full copy of the article can be found in the appendix. In accordance with the publisher Elsevier, inclusion of the full article in the author’s dissertation is permitted as part of the author’s rights granted upon acceptance of the article.

Despite large progress in the harmonization of MP analysis including scientific publications (Al-Azzawi, Kefer *et al.* 2020; Schymanski, Oßmann *et al.* 2021; Primpke, Christiansen *et al.* 2020; Braun 2021; Pérez-Guevara, Roy *et al.* 2022) as well as national and international standards (DIN/TS 10068, ISO/DIS 24187, ISO/DIS 4484, ISO/NP 5667-27 (draft stage), ISO/NP 16094 (draft stage), ISO/TR 21960), data analysis for the spectroscopic methods has seldom been discussed. While insufficient reporting of details is an issue (see section 1.2), the methods that are reported often have severe weaknesses. For instance, to the best of our knowledge, no assessment of overlooked particles has been reported, so far.

Database matching is the most commonly used DAR, however, its performance strongly depends on the database and spectra similarity metric chosen. This becomes clear when looking at Table 5, where analysis results for the sample RefEnv1 (Primpke, Wirth *et al.* 2018) were summarized, showing that the database used and the spectral range of the FTIR measurement can have massive impact on the results.

Table 5. Analysis results for sample RefEnv1 using different databases and spectral ranges (Reprint from Weisser, Pohl, Heinzinger *et al.* (2022) with permission from the publisher). MP = Microplastic.

| Reference                            | Spectral range test FTIR image [cm <sup>-1</sup> ] | Database                            | Total particles identified | MP identified | Certain assignments | Mis-assignments |
|--------------------------------------|--|-------------------------------------|----------------------------|---------------|---------------------|-----------------|
| Primpke, Lorenz <i>et al.</i> (2017) | 3,200 – 1,250                                      | Löder, Kuczera <i>et al.</i> (2015) | 1,097                      | 733           | 82.1%               | 3.1%            |
| Primpke, Wirth <i>et al.</i> (2018)  | 3,200 – 1,250                                      | Primpke, Wirth <i>et al.</i> (2018) | 1,221                      | 195           | 82.8%               | 1.6%            |
| Primpke, Wirth <i>et al.</i> (2018)  | 3,600 – 1,250                                      | Löder, Kuczera <i>et al.</i> (2015) | 701                        | 281           | Not reported        | Not reported    |

Several studies (Primpke, Wirth *et al.* 2018; Munno, De Frond *et al.* 2020; De Frond, Rubinovitz *et al.* 2021) have shown that in general, databases tailored specifically for MP research are more suitable than commercial databases. The reason for this is that the latter do not comprise spectra of aged plastics and usually lack spectra of typical matrix residues that can be

confused with MP spectra (PA and proteins, for instance). Looking at different similarity metrics proposed, Pearson correlation seems to be best suited, especially when a weighted combination of correlations of raw and derivative spectra is employed (Morgado, Palma *et al.* 2020; Pimpke, Cross *et al.* 2020). Adequate thresholds should be chosen separately for each database entry (Morgado, Palma *et al.* 2020; Weisser, Pohl, Ivleva *et al.* 2022). When applied correctly, database matching was shown to yield TP rates between 82% (Löder, Kuczera *et al.* 2015) and 99% (Renner, Sauerbier *et al.* 2019).

Unsupervised ML techniques like Principal Component Analysis (PCA) have been proposed for both data exploration and spectra classification (Hufnagl, Steiner *et al.* 2019; Wander, Vianello *et al.* 2020). It was shown that PCA is capable of separating potential MP spectra from a sample's background, which reduces the amount of data to be classified in subsequent steps (Wander, Vianello *et al.* 2020). Further, the dimensionality reduction inherent to most explorative methods reduces the computation time of subsequent analyses. However, a sharp differentiation of all substances present in a sample could not be achieved in real-world samples (Wander, Vianello *et al.* 2020), but only in idealized reference data sets (Xu, Hassellöv *et al.* 2020).

Classification, in turn, can be achieved by applying supervised ML models like Support Vector Machine (SVM), Artificial Neural Networks (ANN) or RDF classifiers (Back, Vargas Junior *et al.* 2022). RDF models, for instance, were found to work at a similar accuracy as database matching (95.45% (Weisser, Beer *et al.* 2021) to 97.66 % (Hufnagl, Stibi *et al.* 2022)), whilst classifying a sample within minutes compared to the often hours-long database matching (Hufnagl, Stibi *et al.* 2022). Adding new substance classes to a ML model, however, can require another training phase, whereas new references can easily be appended to existing databases.

As any other analysis method, DARs should be thoroughly evaluated. Most studies report some sort of evaluation of their DAR, yet, there is no commonly agreed best practice for doing so. As such, comparability of the DARs is limited, with the exception of the work by Back, Vargas Junior *et al.* (2022) which compared the performance of seven ML techniques via MCCV. For the first time, this work holistically compared different DARs using always the same test and training data sets of ATR-FTIR spectra. SVM was found to be the algorithm providing the best cost-benefit ratio, taking into account the effort for training the model. A DAR comparison based on  $\mu$ FTIR or Raman spectra of MP particles < 100  $\mu$ m, however, would reflect MP analysis at a more realistic stage, as ATR-FTIR spectra are typically less noise-prone than transmission or reflection FTIR spectra (Comnea-Stancu, Wieland *et al.* 2017; Cowger, Gray *et al.* 2020).

### 3.3. Know what you don't know: assessment of overlooked microplastic particles in FTIR images

This chapter refers to the publication 'Know what you don't know: assessment of overlooked microplastic particles in FTIR images, authored by **Weisser J**, Pohl T, Ivleva NP, Hofmann T, and Glas K. The article was published in 2022 in *microplastics* Vol. 1, Issue 3, Pages 359-376.

Jana Weißer (Weisser) led the conceptualization of the study and developed the methodology. Teresa Pohl contributed to both. Teresa Pohl wrote the code based on a concept developed by Jana Weißer. Jana Weißer validated the code and adapted it to bring it into its final stage. Formal analysis and investigations were conducted by Jana Weißer, as well as the preparation of the manuscript. All authors revised the manuscript. The work was under supervision by Karl Glas, Natalia P. Ivleva, and Thomas Hofmann.

A full copy of the article can be found in the appendix. The article has been published under an open access Creative Commons CC BY license. Therefore, any part of the article may be reused without permission provided that the original article is clearly cited.

As has been outlined in the previous section, there remains a gap in the harmonization of MP analysis at the last step of the pipeline, the data analysis. To enhance comparability of DARs, a ground truth **Reference Image of MicroPlastics, RefIMP**, was created and published. RefIMP reflects state-of-the-art FTIR imaging-based MP analysis, containing the most important plastic types and sample matrix residues in size ranges from 11  $\mu\text{m}$  to 666  $\mu\text{m}$  and 11  $\mu\text{m}$  to 1,890  $\mu\text{m}$ , respectively, see Figure 17. The performance of any DAR in classifying RefIMP can be automatically evaluated using the MatLab®-script MPVal, provided alongside with it. MPVal compares the list of particles found by a DAR to the ground truth, counting TP and FP results.

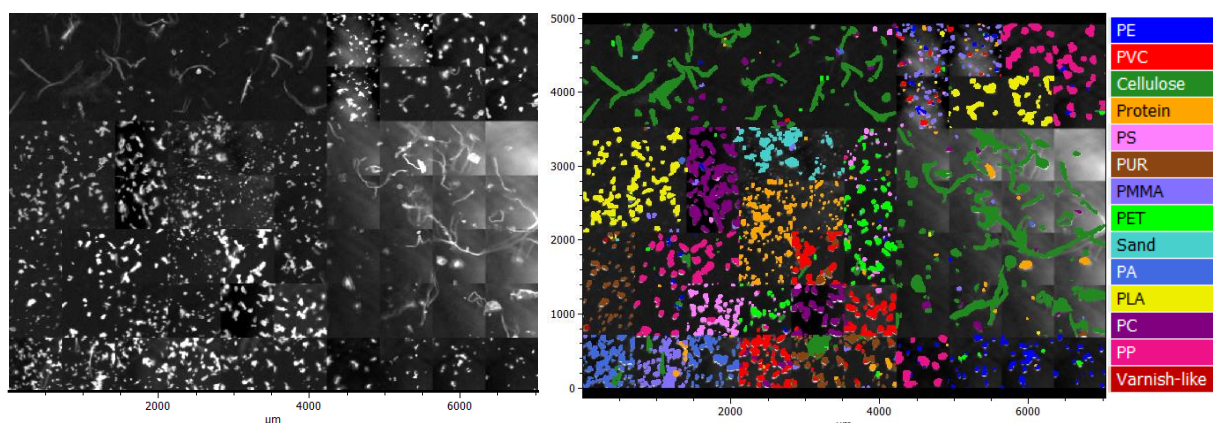


Figure 17. Left: Fourier-transform Infrared image RefIMP, intensity filtered at  $2,920\text{ cm}^{-1}$ ; right: color-coded particles; reprinted from Weisser, Pohl, Ivleva *et al.* (2022) under CC-BY license. PE = Polyethylene; PVC = Polyvinyl Chloride; PS = Polystyrene; PUR = Polyurethane; PMMA = Polymethyl Methacrylate; PET = Polyethylene Terephthalate; PA = Polyamide; PLA = Polylactic Acid; PC = Polycarbonate; PP = Polypropylene.

Special attention was given to typical error types such as undetected and over-segmented particles, as well as the occurrence of 'ghost particles', i.e. particles detected in places where there is no particle, representing a special case of FP results. For such cases, the calculation of the evaluation metrics Acc, Sn, and Sp (see section 1.6.4) had to be adapted, as they originally base on the assumption that the number of samples, or particles, stays constant (Ballabio, Grisoni *et al.* 2018). The heatmaps (see Figure 27) created using MPVal give detailed and concise insight into correct predictions and into all error types.

Testing the following three hypotheses illustrated the application of RefIMP and MPVal, demonstrating that

- I. using masks that filter out potential MP particles from the sample background bears the risk of overlooking MP;
- II. RDF models benefit from diverse training data, which becomes evident only when evaluating their performance on an FTIR image, but not on single spectra;
- III. tuning of the model's hyperparameters cannot be done meaningfully on the level of isolated spectra, but only in combination with a reference image.

In general, it can be said that when optimizing a model, a balance needs to be found between minimizing errors (overlooking of particles and false type assignments, for instance) and minimizing the time necessary for manual corrections of the model's results (mostly ghost particles). Further, the study provided detailed insight into the behavior of RDF models: training data diversity, i.e., the inclusion of high- and low-quality spectra, was shown to substantially increase the number of TP results, while lowering the number of overlooked and ghost particles. Interestingly, a diversity of 25% (the remaining 75% were duplicates of high-quality spectra), already enhanced the model's accuracy from  $0.614 \pm 0.007$  to  $0.855 \pm 0.005$ , compared to 0% diversity.

Moreover, it was found that using MCCV, the performance was severely over-estimated compared with the results derived from using MPVal and RefIMP, highlighting one more time the necessity for a reference image.

All factors covered by the example hypothesis tests (background masks, training data diversity, and model hyperparameters) played a role for the overlooking of particles. The lowest rate of overlooked particles reached was 7.99%. The same model correctly assigned 86.97% of particles while 5.04% were assigned to wrong types.

### 3.4. From the Well to the Bottle: Identifying Sources of Microplastics in Mineral Water

This chapter refers to the publication 'From the Well to the Bottle: Identifying Sources of Microplastics in Mineral Water', authored by **Weisser J**, Beer I, Hufnagl B, Hofmann T, Lohninger H, Ivleva NP, and Glas K. The article was published in 2021 in *Water* Vol. 13, Issue 6, Pages 841.

Jana Weißer (Weisser) led the conceptualization of the study and conducted most of the experiments. Irina Beer contributed to both. Software design and validation were conducted by Jana Weißer, Benedikt Hufnagl and Hans Lohninger. Jana Weißer was in charge of writing and revising the manuscript, with contributions from all authors. The work was supervised by Karl Glas, Natalia P. Ivleva, Hans Lohninger, and Thomas Hofmann.

A full copy of the article can be found in the appendix. The article has been published under an open access Creative Commons CC BY license. Therefore, any part of the article may be reprinted without permission provided that the original article is clearly cited.

To investigate the potential MP entry paths into bottled water, samples were taken along the process of bottling and bottle cleaning at four water-bottling companies in Germany as shown in Figure 18. The investigation focused on glass bottles with aluminum screw caps.

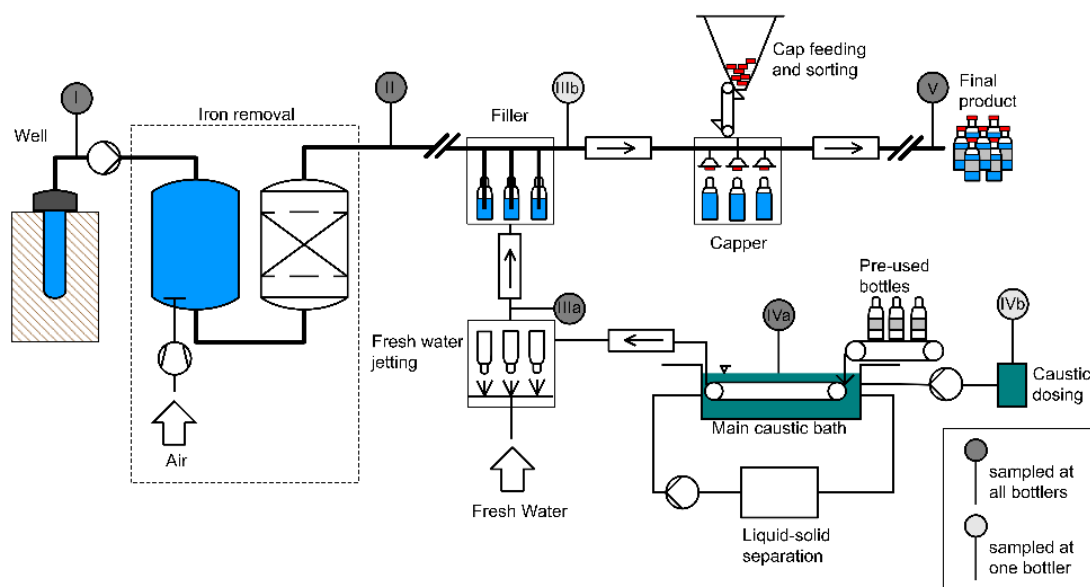


Figure 18. Illustration of the process of mineral water bottling including bottle cleaning. Roman numerals indicate sampling points. (Reprinted from Weisser, Beer *et al.* (2021) under CC-BY license).

Inorganic substances were removed from the *in-situ* filtered groundwater and deferrized water samples using density separation and citric acid. Cleaned bottles, filled bottles, and filled and capped bottles were emptied (where applicable) and particles flushed out. Caustic cleaning soda samples underwent chemical and enzymatic digestion (see section 1.3.2). All samples were finally filtered through Anodisc membrane filters and underwent  $\mu$ FTIR imaging (see chapter 1.4). The  $\mu$ FTIR images were evaluated for MP particles  $\geq 11 \mu\text{m}$  using an RDF model (see chapter 1.5), with 95.45% accuracy (based on MCCV). During all analysis steps, special attention was given to quality assurance and quality control as is described in section 1.6.

### 3 - Results

Expectedly, ground- and deferrized water contained very low numbers of MP  $\geq 11 \mu\text{m}$  ( $97 \text{ MP m}^{-3} \pm 53 \text{ MP m}^{-3}$  and  $49 \text{ MP m}^{-3} \pm 3 \text{ MP m}^{-3}$ , respectively), while the bottle cleaning soda reached  $1,826 \text{ MP L}^{-1} \pm 1,199 \text{ MP L}^{-1}$ . Cleaned bottles, however, were all below LOD, leading to rejection of the hypothesis that the bottle cleaning process was the main MP entry path. In the filled and capped bottles, however, a sharp rise in MP concentrations was observed with  $317 \text{ MP L}^{-1} \pm 257 \text{ MP L}^{-1}$  (LOD 40 MP) as shown in Figure 19. The analysis of three filled, but uncapped bottles resulted in values  $< \text{LOD}$ , hinting at the capping process to be the main source for MP, as well. This hypothesis was supported by the fact that between 57% to 96% of the MP particles were classified as PE and could be traced back to the PE-similar cap sealing material.

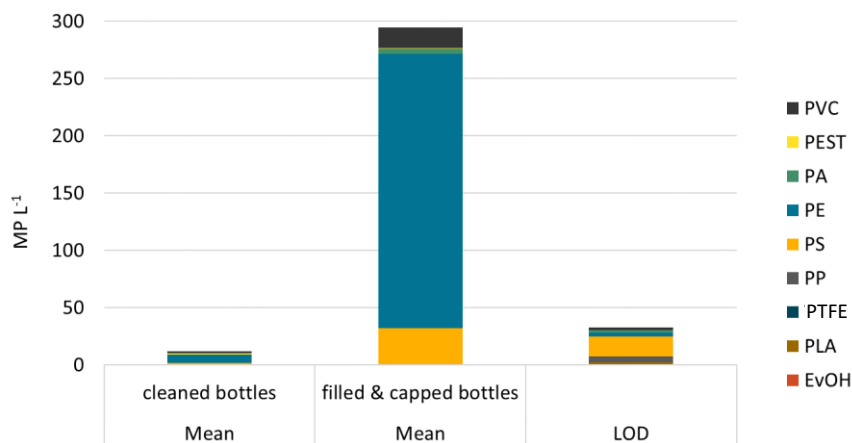


Figure 19. MP concentrations detected from groundwater well to filled and capped water bottles and corresponding limit of detection (LOD). PP = Polypropylene, PS = Polystyrene, PE = Polyethylene, PA = Polyamide, PEST = Polyester, EvOH = Ethylene Vinyl Alcohol, PVC = Polyvinyl Chloride, PLA = Polylactic Acid, PTFE = Polytetrafluoroethylene.

The generation of MP through bottle cap twisting (opening and closing) is known from the literature (Winkler, Santo *et al.* 2019); therefore, it can be concluded that the MP particles found mostly stemmed from abrasion from the bottle cap sealing. According to the results presented, this poses the most important point of entry for MP particles  $\geq 11 \mu\text{m}$  into bottled mineral water.

### 3.5. Entry paths for microplastics during the production and preparation of selected foods

Having the goal in mind to minimize MP entry into beverages and food, the identification of the entry paths clearly is essential. Model foods were chosen for these investigations based on their relevance regarding consumed amounts and consumer sensitivity. As such, bread was chosen because it is a staple food in the western world. Apple puree intended for infant feeding represents an example for sensitive foods. After reports on extraordinary high findings of MP and NP in tea and potential high intake rates associated therewith (Hernandez, Xu *et al.* 2019; Xu, Lin *et al.* 2021; Afrin, Rahman *et al.* 2022), tea filled in paper- and plastic-based filter bags was included, as well. All findings are summarized in the following and will be discussed in relation to the corresponding LODs and RRs in section 4.4. Raw data for the bread, flour and salt samples taken at a bakery stemmed from Hubin (2020) and raw data for homemade and industrial apple puree were acquired by Eberl (2020). Tea samples were examined by Müller (2020). MP types were determined through FTIR imaging and matrix-specific RDF models. At all time, the QA/QC measures as described in section 1.6 were followed. The above-mentioned works were conducted under Jana Weißer's supervision and data were re-prepared for presentation here by her.

#### Bread production

At a Munich bakery, samples were taken from rye flour, bread dough, and sea salt from the French Atlantic coast. Triplicate samples of flour and dough were prepared as summarized in Figure 15 and analyzed using FTIR imaging and an RDF model. Determined MP concentrations are shown in Figure 20. Accordingly,  $335 \text{ MP g}^{-1}_{\text{DW}} \pm 93 \text{ MP g}^{-1}_{\text{DW}}$  (MP per g dry weight, DW) were determined in the rye flour samples and  $1,091 \text{ MP g}^{-1}_{\text{DW}} \pm 179 \text{ MP g}^{-1}_{\text{DW}}$  in the dough samples. The LOD for both flour and dough samples amounted 408 MP.

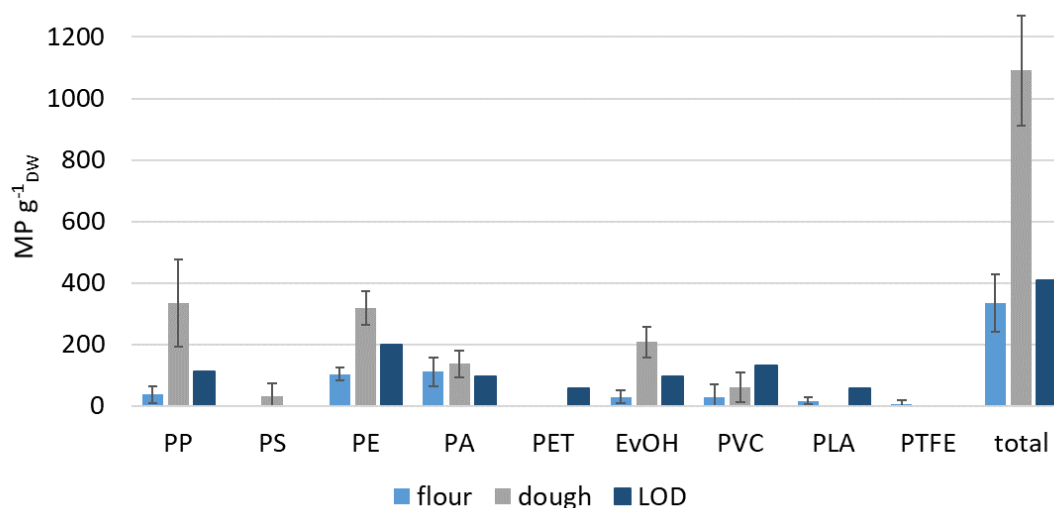


Figure 20. MP findings in rye flour and dough with corresponding LODs (limits of detection). PP = Polypropylene, PS = Polystyrene, PE = Polyethylene, PA = Polyamide, PEST = Polyester, EvOH = Ethylene Vinyl Alcohol, PVC = Polyvinyl Chloride, PLA = Polylactic Acid, PTFE = Polytetrafluoroethylene.

Most MP particles in the dough were identified as PE, PP, and ethylene vinyl alcohol (EvOH) ( $318 \text{ MP g}^{-1}_{\text{DW}} \pm 54 \text{ MP g}^{-1}_{\text{DW}}$ ,  $336 \text{ MP g}^{-1}_{\text{DW}} \pm 141 \text{ MP g}^{-1}_{\text{DW}}$ , and  $208 \text{ MP g}^{-1}_{\text{DW}} \pm 49 \text{ MP g}^{-1}_{\text{DW}}$ , respectively). Most particles (~77%) were between 11  $\mu\text{m}$  and 20  $\mu\text{m}$  small. As is typical for MP, particle numbers decreased with increasing sizes, as Figure 21 illustrates. Size distributions were similar in the blank samples, while in the flour samples, only ~19% of MP fell into the smallest size category and ~38% were sized 20  $\mu\text{m}$  to 50  $\mu\text{m}$ . The size categories 50  $\mu\text{m}$  to 100  $\mu\text{m}$  and 100  $\mu\text{m}$  to 500  $\mu\text{m}$  accounted for 17% and 22%, respectively.

### 3 - Results

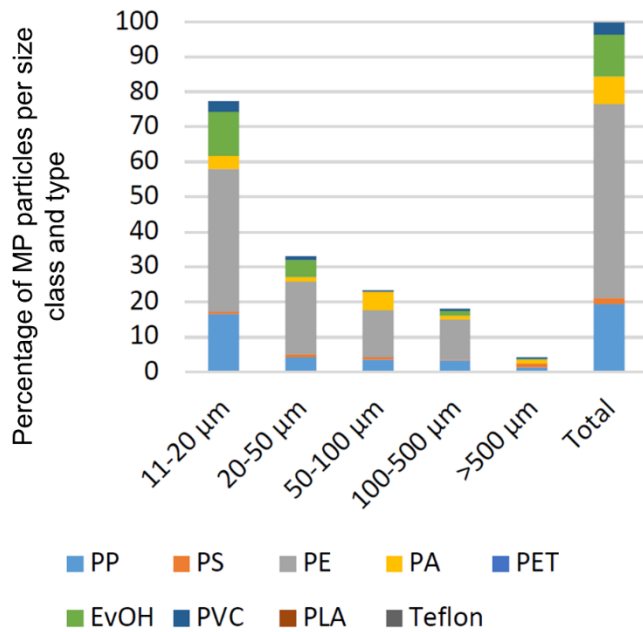


Figure 21. Size distributions in percent of MP particles in bread dough. PP = Polypropylene, PS = Polystyrene, PE = Polyethylene, PA = Polyamide, PEST = Polyester, EvOH = Ethylene Vinyl Alcohol, PVC = Polyvinyl Chloride, PLA = Polylactic Acid, PTFE = Polytetrafluoroethylene.

The sea salt sampled contained  $270 \text{ MP kg}^{-1} \pm 10 \text{ MP kg}^{-1}$ . Because only one blank value (resulting in 19 MP) was employed due to time restrictions, the LOD was conservatively assumed as this blank  $\times 1.75$ , corresponding to 33 MP. The most abundant polymer types were PE, PP, and PVC as shown in Figure 22.

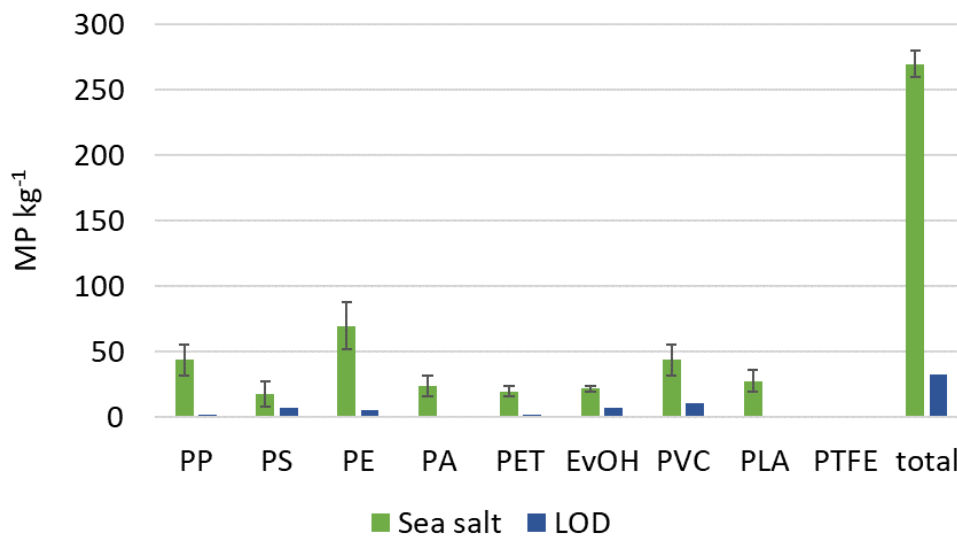


Figure 22. MP findings in sea salt with corresponding LOD. PP = Polypropylene, PS = Polystyrene, PE = Polyethylene, PA = Polyamide, PEST = Polyester, EvOH = Ethylene Vinyl Alcohol, PVC = Polyvinyl Chloride, PLA = Polylactic Acid, PTFE = Polytetrafluoroethylene.

#### Apple puree production

An investigation on plastic kitchen equipment as a possible MP source was carried out. For this purpose, apple puree was prepared in a technical scale using stainless steel equipment as is standard in the food industry ('industrial apple puree'). Another batch was prepared in a

### 3 - Results

private kitchen ('homemade apple puree') using a cutting board, a bowl, a sieve, and a funnel made of PP, a PVC sieve, a PA cooking spoon, and a PTFE spatula.

Figure 23 shows the results from triplicate analyses after sample preparation as summarized in Figure 15. In the 'industrial' apple puree,  $56 \text{ MP g}^{-1}_{\text{DW}} \pm 27 \text{ MP g}^{-1}_{\text{DW}}$  were detected and  $82 \text{ MP g}^{-1}_{\text{DW}} \pm 33 \text{ MP g}^{-1}_{\text{DW}}$  in the 'homemade' apple puree. Both batches contained mostly PE and PTFE, and PP, PS, PA, and PET were present in smaller amounts. In the homemade puree, EvOH and a small number of PVC particles were found in addition. The corresponding LOD was 92 MP and comprised mostly PTFE and PE. Particle sizes in both batches ranged from  $60 \mu\text{m}$  to  $2,750 \mu\text{m}$ .

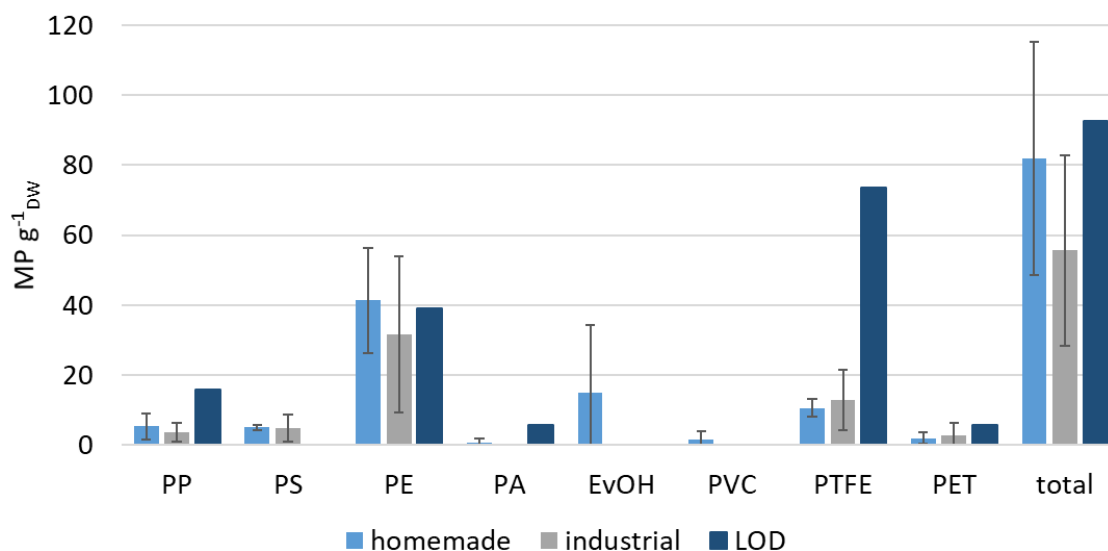


Figure 23. MP findings in apple puree prepared in a private kitchen ('homemade') and at a technical scale ('industrial') with corresponding LODs. PP = Polypropylene, PS = Polystyrene, PE = Polyethylene, PA = Polyamide, PEST = Polyester, EvOH = Ethylene Vinyl Alcohol, PVC = Polyvinyl Chloride, PLA = Polylactic Acid, PTFE = Polytetrafluoroethylene.

#### Tea preparation

Peppermint tea was provided in standard filter bags made mainly from cellulose, and pyramid filter bags made from PLA. Tea was brewed according to the manufacturer's instructions and the solids present in the extract after removing the bag were treated as is summarized in Figure 15. While the blank samples did not contain PLA as shown in Figure 25, the tea prepared from PLA pyramid bags ( $n=3$ ) contained on average  $9 \pm 6$  PLA particles per cup (150 mL), i.e. per tea bag, most of which were fibers ranging from  $100 \mu\text{m}$  to  $500 \mu\text{m}$  in length. The only other polymer detected above LOD in the PLA bags was PET with  $3 \pm 1$  MP per cup.

The particle size distribution is shown in Figure 24. The MP particle numbers do not rise with decreasing particle sizes, but stay almost constant.

No PLA was detected in the tea prepared from standard cellulose-based tea bags. The only plastic type above LOD was PP with  $2 \pm 2$  MP.

### 3 - Results

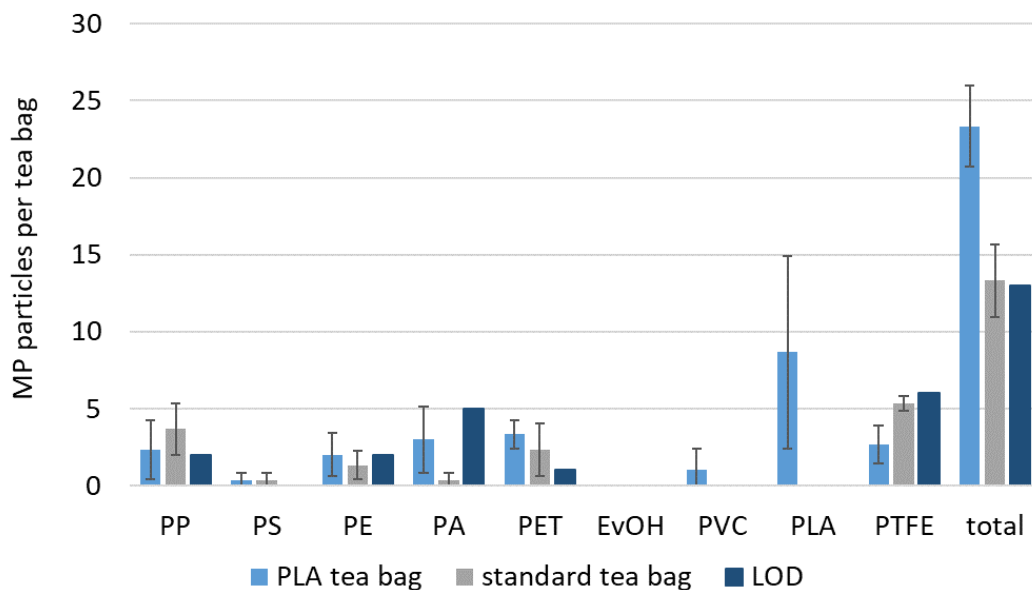


Figure 25. MP findings in tea prepared from standard paper-based and PLA tea bags with corresponding limit of detection (LOD). PP = Polypropylene, PS = Polystyrene, PE = Polyethylene, PA = Polyamide, PEST = Polyester, EvOH = Ethylene Vinyl Alcohol, PVC = Polyvinyl Chloride, PLA = Polylactic Acid, PTFE = Polytetrafluoroethylene.

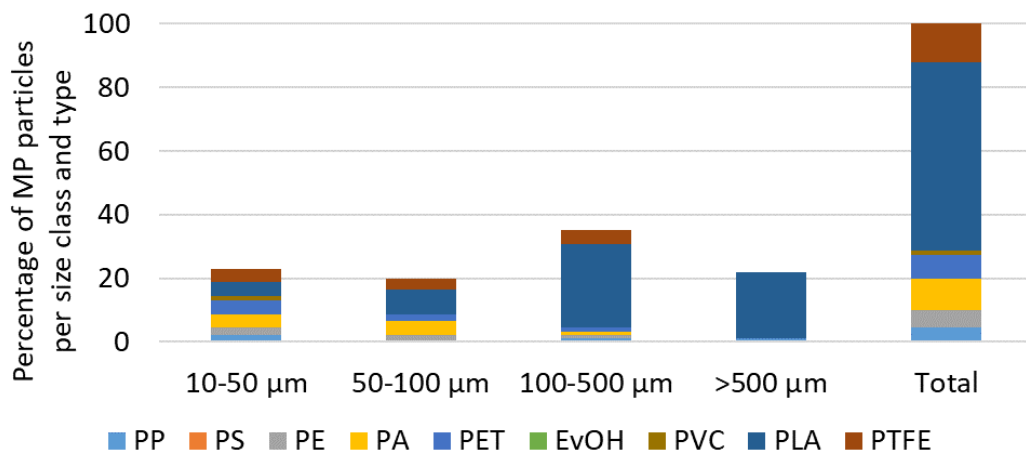


Figure 24. Size distributions in percent of MP particles in tea prepared from PLA tea bags. PP = Polypropylene, PS = Polystyrene, PE = Polyethylene, PA = Polyamide, PEST = Polyester, EvOH = Ethylene Vinyl Alcohol, PVC = Polyvinyl Chloride, PLA = Polylactic Acid, PTFE = Polytetrafluoroethylene.

## 4. Discussion

By the start of this doctorate project, no standard methods for MP analysis were available. Meanwhile, progress has been made for all steps along the MP analysis pipeline. Section 4.1 discusses the experimental results and success of matrix degradation for different food types. These results and QA/QC related results are discussed regarding their meaningfulness for method harmonization in section 4.2. Section 4.3 discusses QA/QC for the evaluation of DARs. Finally, section 4.4 discusses the knowledge gained on MP entry paths into processed food and beverages.

### 4.1. Proceedings in matrix-dependent sample preparation for MP analysis

Preparing a sample for MP analysis typically requires a series of digestion steps. As the results for the digestion of pear and strawberry puree (Figure 14) showed exemplarily, the efficiency of matrix digestion varies depending on the sample composition.

#### Enzymatic matrix degradation

Both strawberry and pear puree were degraded to more than 90% by cellulase. The degradation was higher for the pear puree, which may be attributed to the contents of dietary fibers of the two fruits: strawberries contain less insoluble dietary fibers compared to pears (27 g kg<sup>-1</sup> and 29 g kg<sup>-1</sup>, respectively, Chareoansiri and Kongkachuichai (2009)). Consequently, the pear sample provided more cellulosic structures to be degraded by the cellulase. This result indicates that for foods with high contents of dietary fibers, sample preparation should include at least one cellulase step.

Both flour and bread samples further required amylase in addition to cellulase because of their starch content.

For breaking down the cell walls of the yeast *Saccharomyces cerevisiae* in wheat beer, cellulase was found unsatisfying. Being an endo- $\beta$ -1,4-glucanase, it was incapable of cleaving the  $\beta$ -1,3-glucan bonds, which make up 50% of *S. cerevisiae* cell walls. The yeast cells, however, were well-degradable with *Xylanase 2x*, as this mixture comprises both an endo-1,4- $\beta$ -D-xylanase, and an endo-1,3- $\beta$ -D-xylanase, the latter of which cleaves 1,3- $\beta$ -D-glycosidic linkages in xylans. Moreover, it possesses a mannanase activity that can cleave the mannose structures of mannoproteins, which make up 40% of *S. cerevisiae* cell walls (Lipke and Ovalle 1998). Because of this variety of enzymatic activities, *Xylanase 2x* was superior in the degradation of mixtures of complex high-polymeric matrices like yeast cells.

Interestingly, using *Xylanase 2x* as the first degradation step for fruit puree led to poor filterability of the sample, while for tea leaves, this was not the case. Here, *Xylanase 2x* was found to yield slightly higher dry mass reduction rates for tea leaves than cellulase, however, only 43% degradation were achieved at maximum (Dunkel 2018). Combining two xylanase and one cellulase degradation step with a final Fenton + AAH reaction, ~60% matrix degradation were achieved, yielding analyzable tea samples (Müller 2020).

In contrast to the other enzymes employed, *Xylanase 2x* was stable for only 3.5 h at 40°C in a citric acid-sodium hydroxide buffer (pH 6, 0.1 M). On one hand, this lowered the total time necessary for matrix degradation compared with the other enzymes used. On the other hand, this resulted in less flexibility in planning experiments compared with the other enzymes, which all were stable for at least 24 h under the same conditions. However, the advantages of *Xylanase 2x* for degradation of tea and yeast outweighed this.

In general, prolonging the incubation time for enzymatic degradation to over 24 h did not enhance the result as shown exemplarily in Figure 26 A+B.

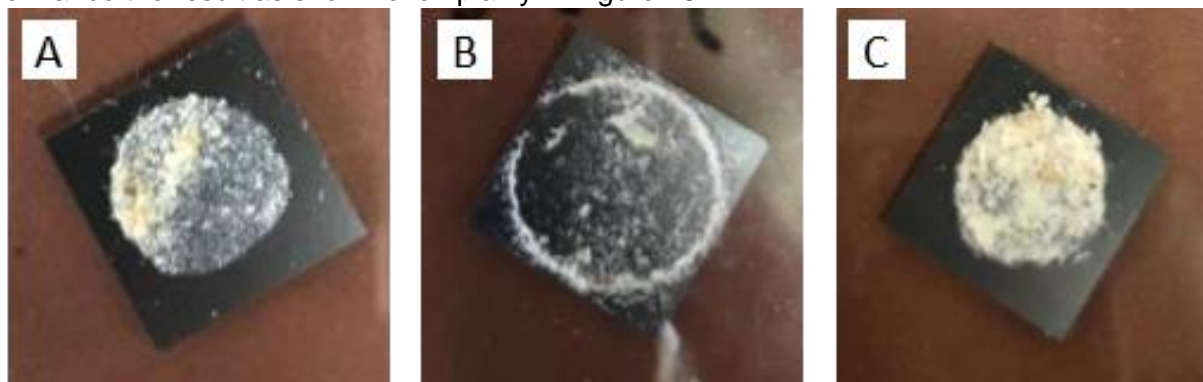


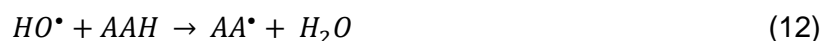
Figure 26. Examples for residues of apple puree on silicon filters after treatment with: A, Fenton + AAH /96 h cellulase/Fenton + AAH; B, Fenton + AAH /24 h cellulase/Fenton + AAH; C, 24 h cellulase/24 h cellulase/Fenton + AAH. Photos by Eberl (2020). AAH = Ascorbic Acid.

These examples show that enzymatic matrix degradation is an important tool for food matrix degradation; yet, suitable enzymes need to be chosen with care according to the target bonds to cleave. Even small-seeming differences in the composition of samples can have large influences on the degradation result, potentially leaving matrix residues that hamper the spectroscopic analysis.

#### Fenton's reagent for matrix degradation

Less specific, but not less relevant than enzymatic sample digestion are approaches based on chemicals, such as Fenton's reagent. When testing Fenton's reaction as described in the literature (Masura, Baker *et al.* 2015), unwanted iron precipitates were formed. As proposed by Al-Azzawi, Kefer *et al.* (2020), concentrated sulfuric acid can be added to re-solve the precipitates without risking MP damages. However, it was shown that the formation of precipitates can be fully avoided through adapting the protocol as has been described in section 3.1.1. Further, adding AAH to the solution lead to strong decrease of the turbidity of the sample (visible upon visual inspection). Therefore, adding AAH was adapted as a standard for degrading sample matrices: most sample preparation procedures were started with a Fenton + AAH treatment to make the sample more accessible for the following enzymatic treatment(s). Further, Fenton + AAH was employed as a final 'clean up' step after enzymatic digestions. Comparing the residues from apple puree samples on a silicon filter with (Figure 26 B) and without (Figure 26 C) an initial Fenton + AAH step, it can be seen that the latter left a lot more matrix residues on the filter. The cleaner the filter, the higher its analyzability. This way, the success of framing the sample preparation with Fenton + AAH becomes evident.

Adding AAH has already been shown to enhance the degradation of organics in industrial and environmental remediation applications of Fenton's reaction before. This is because AAH radicals ( $AA^\bullet$ ) act as reductant for  $Fe^{3+}$  to  $Fe^{2+}$ , see equations 12+13 (Bolobajev, Trapido *et al.* 2015). This i) happens without requiring  $H_2O_2$ , therefore leaving more hydroxyl radicals for reacting with the sample matrix, and ii) further reduces the risk of  $Fe^{3+}$ -based precipitates such as ferric oxyhydroxide (Bolobajev, Trapido *et al.* 2015).



It can be concluded that adding AAH enhanced the effectiveness of organic matrix degradation, yielding sample dry mass reductions between 92 and 97% (values for pear and strawberry purees, respectively). The varying effectiveness of the treatment depending on the type of sample may be attributed to its content of insoluble dietary fibers. Opposed to the effectiveness of cellulase as described before, Fenton + AAH seem to be more efficient for samples with lower contents of insoluble dietary fibers, as the results from strawberry and pear puree indicate.

### **Final filtration**

The filter used for the final filtration step had some additional influence on the sample matrix residues finally present, as the pores of Anodisc membranes were much smaller than the pores of the silicon filters (0.2  $\mu\text{m}$  vs. 5-10  $\mu\text{m}$ , respectively). Thus, using silicon filters instead of Anodisc membranes lead to removal of particles too small to be analyzable with FTIR imaging. In addition, silicon filters are, unlike Anodisc membranes, resistant towards Fenton's reagent, so no additional filtering for removing aggressive chemicals was necessary. Consequently, Anodisc membranes were used mainly for water samples, however, even for water samples, silicon filters can be preferred because of their higher filtration rates and flatness (see section 3.1.1). In turn, the recovery rate may be smaller using silicon filters, due to the more complicated filtration set-up, see section 3.1.2.

### **Success of sample matrix degradation**

When assessing sample degradation based on the sample analyzability in FTIR imaging (see next section), it became clear that enzymatic and chemical degradation steps had to be combined for most beverages and food (compare Löder, Imhof *et al.* (2017)), as summarized in Figure 15. For beverages (cloudy lemonade, Pilsner style beer, and wheat beer), the goal of making one unit of consumption, i.e., 330 to 500 mL, analyzable was fulfilled. However, other foods could only be analyzed in amounts between 150 and 6,500 mg (Eberl 2020; Hubin 2020) to avoid overlaying of remaining particles on the sample filter. Across all sample types, cellulose and similar structures (identified via  $\mu\text{FTIR}$ ) were the most persistent and impairing type of sample matrix residues.

## **4.2. Quality assurance and quality control in sampling and sample preparation**

This section discusses the findings explained in sections 4.1 and 3.1.2 with regard to their significance for QA and QC of MP analysis.

### **Analyzability of digested samples**

Initially, dry mass reduction was used to assess the success of sample preparation. During this thesis, however, it was experienced that this measure was not fully reliable. Even when degradation rates close to 100% were achieved, light-weight, yet voluminous matrix residues were still present that hampered the spectroscopic analysis. This applied to all foods examined except for drinking water, raising doubt on the suitability of dry mass reduction as a QA/QC measure. Instead, the spectra quality of spiked-in particles was used as a criterion for evaluating the success of matrix degradation.

The drawback of this procedure is of course that it relies on the operator's experience in spectra interpretation and remains somewhat subjective, while dry mass reduction is a more concise and scalable variable. In addition, the spiked-in particles may not fully reflect the

complexity of MP particles present in a sample, neither concerning plastic types nor potentially built matrix films on the particles' surfaces.

It is concluded here that even though dry mass reduction is a scalable, objective indicator for the success of a sample preparation procedure, it should be complemented with assessing the sample's analyzability. For this purpose, spiking with reference particles should be employed to make the procedure traceable and to qualify it as a QC method contributing to the ongoing harmonization. Spiking with known amounts of reference particles of all types and sizes targeted in the analysis would even make the process eligible as a QC measure for sample preparation, instrumental analysis, and data analysis combined, as is discussed further in 4.3.

### **Contamination prevention and monitoring**

The measures taken to minimize airborne contamination (e.g. via working under a laminar flow workbench and wearing cotton lab coats) were assessed by preparing 'air blanks' as part of the study Weisser, Beer *et al.* (2021). With a total of 3 MP particles in 10 air blanks, mitigation of airborne contamination can be regarded successful. To make the analyses more time-efficient, only combined sampling and process blanks were employed from there on.

Sampling and process blanks, i.e., blanks mimicking sampling and sample preparation procedures, in turn, were confirmed to be an indispensable QA/QC tool, as they were never free from MP (see Table 3), indicating contamination via the reagents and/or the vessels used. Despite the strict cleaning protocols, it could not be guaranteed that all vessels were completely free of MP, as the particles tend to stick on glass walls (Eitzen, Paul *et al.* 2019). It can, however not be concluded that the cleaning protocol was completely ineffective as two sampling blanks of cartridge filters for volume-reduced sampling of ground water were free of MP. Nevertheless, they comprised high amounts of hemp fibers, stemming from the hemp sealing material used for the cartridge filters. Consequently, even though hemp fibers are non-plastics, PTFE sealing tape should be used instead if PTFE is excluded from the target polymers.

Contaminated glassware or other equipment for sample handling further most likely led to contamination of the filtered reagents stored in glass containers. The most abundant plastic type in the blank samples were PS, PE, and PTFE, the origins of which could not be cleared up ultimately. Possible sources may be the PE bags that the stainless steel filters were delivered in, the plastic box of the cellulose ester membrane filters, the PTFE coating of the forceps used for handling the silicon filters, or other inevitable plastic items in the laboratory. As was found by Witzig, Földi *et al.* (2020), disposable lab gloves can lead to false positive PE results. In the present work, gloves were worn only when inevitable for operator safety and contact between gloves and sample contact surfaces was avoided. Despite meticulous attention, it can not be fully excluded that the PE findings in the blank samples and consequently also a part of the PE findings in the samples derived from the gloves worn.

In other works, very broad ranges of sample blank values have been reported, ranging from 0 MP (Corami, Rosso *et al.* 2020) to 151 MP (Mintenig, Int-Veen *et al.* 2017). Only studies analyzing MP starting from 10  $\mu\text{m}$  were considered here. Regarding the sample preparation protocols, no connection between blank values and the number of sample preparation steps or chemicals applied could be found, neither in the literature nor in this work. In most cases, no efforts were made to trace back the sources of contamination, with the exception of Löder, Imhof *et al.* (2017) who identified PP bottle screw caps as a source of PP contamination.

It can thus be concluded that the blank values reached in this work are within the expectable range. Ideally, experiments should be conducted in a clean room free of any plastic items,

which, in practice, is hardly feasible, not only because some pieces of equipment cannot be replaced by non-plastics, but also due to restricted lab space and pecuniary resources.

### Particle loss assessment

When assessing the stability of reference MP particles against the reagents used for sample preparation, most polymers were stable. The sole exception were PA particles, which aggregated in the  $\text{ZnCl}_2$  solution used for density separation. Consequently, PA numbers in ground water and sea salt samples may have been underestimated, while their sizes may be overestimated in this and other works using  $\text{ZnCl}_2$ .

As is apparent from Table 4, RRs declined with rising complexity of sample preparation procedures, where the flushing of bottles represents the easiest procedure and flushing from cartridge filters represents the most complex one. Not only, the risk of particles getting stuck is higher because of the cartridges' high filtration area, but they are also more prone to splattering while rinsing them. Using a similar filtration device, Lenz and Labrenz (2018) reported an RR of  $98.9\% \pm 0.89\%$ , which is 1.7-fold higher than the recovery achieved here. However, they used cylindrical red PA pieces with 450 mm to 480  $\mu\text{m}$  length to determine the RR. It can be argued that these rather big, regularly shaped particles were easier to recover than the smaller ( $\sim 100\text{-}200 \mu\text{m}$ ), irregularly formed particles used in Weisser, Beer *et al.* (2021). This assumption is supported by the findings of others (Wang, Taylor *et al.* 2018; Weber, Kerpen *et al.* 2020; Hurley, Lusher *et al.* 2018; Way, Hudson *et al.* 2022). Further, different types of plastics may yield varying RRs (Monteiro, Rocha-Santos *et al.* 2022), thus, comparisons are drawn here only to studies using PS particles. Note however, that first, PS properties may differ between manufacturers (Ramsperger, Jasinski *et al.* 2022) and second, the hydrophilization undertaken here may have positively influenced the RRs. It was, however, considered that hydrophilized particles behaved more like 'natural' MP than non-hydrophilized particles (von der Esch, Lanzinger *et al.* 2020).

The third-highest RR was found for the density separation process, which was done in a conical separatory funnel, which is a standard laboratory equipment. Note that in order to clean the particles from the  $\text{ZnCl}_2$  solution, the particles had to be filtered through a stainless steel filter and flushed to remove residues of  $\text{ZnCl}_2$  before filtering them through a PC membrane to determine the RR. The RR reported thus reflects a combination of all these steps. Specialized devices like the Munich Plastic Sediment Separator (MPSS) were shown to yield RRs of 95.5% for particles  $< 310 \mu\text{m}$  of 10 different plastic types (Imhof, Schmid *et al.* 2012). It seems, moreover, that the ratio of sample volume to separatory funnel volume influences particle recovery, with lower ratios being favorable (Dimante-Deimantovica, Suhareva *et al.* 2022).

For the filtration through stainless steel filters, the second-highest RR was determined. Because this procedure was used multiple times in some sample preparation protocols, it can be assumed that the recovery after a series of filtrations is much lower.

According to Dimante-Deimantovica, Suhareva *et al.* (2022), vacuum filtration yields lower recovery than gravity-driven wet-sieving. In their experiments with 100  $\mu\text{m}$  PS beads, this was most likely attributed to the detachable parts of the filtration device. Similar observations were made by Lerch (2020), showing that particles can get trapped in gaps between the parts of the vacuum filtration system.

The adapter for the silicon membranes adds even more gaps that the particles can get into. This is supported by the finding that when assessing the RR for density separation using silicon filters for the last filtration step, only  $54\% \pm 16\%$  of particles were recovered (Hubin 2020), opposed to  $63\% \pm 8\%$  when using the PC membrane in the final filtration (Weisser, Beer *et al.* 2021). Note that a dependency of the recovery rate from the operator cannot be ruled out.

As described before (section 3.1.1), particle loss was observed in gaps between the adapter and the filter. After introducing the usage of silicone gaskets (see Figure 6 C), no such particle accumulations were observed anymore, however, a mean RR of 83% was not surpassed. When looking at Figure 16, another issue becomes evident, which is the aggregation of particles, potentially leading to miscounting two or more particles as one. When counting under the stereomicroscope, however, particles in question were separated with the single-haired brush. Miscounting thus seems not as likely as actually losing the particles. For instance, it is possible that particles adhered to the filtration adapter even though it was rinsed thoroughly. To avoid cross-contamination between samples, the adapter and other filtration equipment was cleaned thoroughly as described in section 1.6.1.

For sample preparation procedures comprising  $n$  filtration steps, it would be expected that the final RR would amount  $RR^n$ . For instance, if 10% of particles get lost during each filtration step, the RR of three filtrations would amount  $0.9^3 = 73\%$ . However, it must be considered that the RRs determined during this thesis always comprise the final filtration on the analysis filter in addition to the studied sample preparation procedure. During a multi-step sample digestion, however, the filtration through the final filter is conducted only once at the very end. As the same set of filters was used from the first to the penultimate filtration, the accumulated recovery should thus be higher than  $RR^n$ . The  $84.5\% \pm 3.3\%$  recovery rate (bright red PS beads  $180\ \mu\text{m}$  to  $212\ \mu\text{m}$ ) achieved by Löder, Imhof *et al.* (2017) after a 7-step enzymatic and chemical treatment, however, surely was not reached with the methods employed in this work. Again, trapping of the irregularly shaped particles in filter meshes may explain the lower recovery. Further, Löder, Imhof *et al.* (2017) used one stainless steel filter only, while in this work, cascades of four filters needed to be used to avoid filter clogging. Consequently, more surface area that the particles could adhere to was present in comparison with their study, explaining the lower RR.

The highest RR was achieved for the bottle flushing process with  $86\% \pm 8\%$ . In all conscience, the only other study that reported an RR for a similar process is Li, Shi *et al.* (2020), stating  $94.9\% \pm 0.4\%$  recovery for  $2\ \mu\text{m}$  PS beads. The differences between the findings may be attributed to diverging bottle volumes, geometries, and materials. No further assumptions can be made as Li, Shi *et al.* (2020) did not report on size and geometry of the bottles examined.

A meta-analysis of MP studies by Way, Hudson *et al.* (2022) came to the conclusion that based on the RRs reported, MP is underestimated by 14% on average. RRs for bottle flushing and filtration through stainless steel sieves determined in this work are very close to this value. However, the other RRs determined show that MP were most likely underestimated at a greater extent than in average studies. However, as pointed out by Way, Hudson *et al.* (2022), the RR is strongly influenced by particle size, shape, polymer type, and reagents used. In turn, the standard deviations determined here show that the processes applied were reproducible within certain boundaries, underlining their suitability. According to the results presented, particle loss because of sample handling is a bigger issue than chemical damage of particles, as has already been described elsewhere (Dimante-Deimantovica, Suhareva *et al.* 2022). Extraction efficiency may be improvable further by employing ultra-sonication of filters and sieves. This was not considered here after contributing to the study by von der Esch, Lanzinger *et al.* (2020), where reference particles were produced from larger plastic pieces by ultrasonication. Meanwhile, however, another study found that ultrasonication does not fragment MP particles under absence of aggressive chemicals (Büks, Kayser *et al.* 2021).

Ultrasonication of filters may consequently still be a meaningful technique to enhance the RR of experiments.

Further, improved recovery is thinkable by spraying particles off with pressurized water-jets. It should be ensured, however, that splattering is avoided. Another possible procedure would be backwashing of filters, as employed here for the cartridge filters; yet, backwashing with EtOH may be more efficient than with air. When backwashing with air, particles need to be brought into suspension afterwards. In contrast, they would be suspended already when backwashing with a liquid. EtOH is especially suitable for this purpose because of its low polarity and low surface tension.

### **Analysis filters**

Even in combination with the customized filter holder, a maximum offset of 132  $\mu\text{m}$  was still to be expected when using Anodisc filters. This potentially led to overlooking of particles during FTIR imaging. In particular, results presented in Weisser, Beer *et al.* (2021) may underestimate MP concentrations because of the filters' unevenness. An additional drawback of the Anodisc filters is that when placing them in the holder, particles may roll off. In addition, contamination during mounting the upper part of the holder could not be ruled out, even though the sample was kept covered as far as possible during mounting.

Regarding filter flatness, the silicon filters were clearly preferable. Moreover, they can simply be placed on a BaF<sub>2</sub> window, minimizing contamination risks. The only downside to be noted is that they break relatively easy when falling or not being placed correctly into the adapter for filtration (see Figure 16).

To conclude, the silicon filters are favorable regarding QA of the FTIR measurements. If for some reason Anodisc or PC membranes are to be used, placing them in a holder is strongly recommended to minimize overlooking of particles outside of the microscope's focal plane.

### 4.3. Quality assurance and quality control in data analysis

The main strength of FTIR imaging for MP analysis is that a whole sample area can be measured relatively quickly. The identification of particles in the image, however, poses a major challenge because of the large amounts of spectra, their often-limited quality, and the diversity of target substances. The strengths and weaknesses of the DARs proposed until today were assessed on a theoretical level in Weisser, Pohl, Heinzinger *et al.* (2022) and are summarized in Table 6. The literature review reinforced the decision of choosing a supervised ML method for MP identification, but also revealed the worthiness of unsupervised ML (PCA, for example) for pre-filtering the data.

Table 6. Summary of strengths and weaknesses of Data Analysis Routine categories. MP = Microplastic.

| Database / Library Matching  | Machine Learning   |  |
|--|--|--|
|  | unsupervised   | supervised   |
| <ul style="list-style-type: none"> <li>+ High performance in class distinction</li> <li>+ Low to intermediate expert knowledge required</li> <li>+ Easy adding of new classes</li> </ul> | <ul style="list-style-type: none"> <li>+ Explore unknown data</li> <li>+ Dimensionality reduction</li> <li>+ MP – background separation</li> <li>+ Fast application</li> </ul> | <ul style="list-style-type: none"> <li>+ High performance in classification</li> <li>+ Little expert knowledge required for application</li> <li>+ Fast application</li> </ul>   |
| <ul style="list-style-type: none"> <li>- Careful selection of database, HQI calculation and HQI threshold</li> <li>- Rather slow on large datasets and large databases</li> </ul>        | <ul style="list-style-type: none"> <li>- Expert knowledge required</li> <li>- Limited suitability for class distinction</li> </ul>   | <ul style="list-style-type: none"> <li>- Expert knowledge required for model training and parameter tuning</li> <li>- Training can be time-consuming</li> <li>- New classes usually require model re-training</li> </ul> |

#### 4.3.1. QA/QC in database matching programs

Two other projects aimed to push forward the harmonization of DARs in the past years, called siMPLe (**S**ystematic **I**dentification of **M**icro**P**lastics in the **E**nvironment, Primpke, Cross *et al.* (2020)) and OpenSpecy (Cowger, Steinmetz *et al.* 2021). Both are database matching programs and are summarized including their up- and downsides in Weisser, Pohl, Heinzinger *et al.* (2022) and the corresponding supplementary information. The database of OpenSpecy was originally identical with the one published by Primpke, Wirth *et al.* (2018), but is augmented by its users over time. Only spectra passing a transparent QA/QC process are added to the database, which is vital for method harmonization, thus posing a significant enhancement compared to commercial databases. The most prominent drawback of OpenSpecy, however, is that it can be used only for single spectra and not for hyperspectral image classification.

The database by Primpke, Wirth *et al.* (2018) can be loaded in siMPLe to be used for both, single spectra and image classification. However, it comprises mostly ATR-FTIR spectra, limiting its usability for transmission and reflection IR spectra. Users may add their own spectra. Similarity between reference and query spectra is calculated based on a weighted score. The three weights for raw, first and second derivative spectra need to be specified by the user. In addition, the user needs to set two thresholds for each database entry (Primpke, Cross *et al.* 2020). Thresholds may depend on the type of sample and the quality of spectra, complicating the identification of the most suitable weights and scores. For the on-board database with 270

entries, this sums up to 540 thresholds to be set. The database is organized in 32 clusters (Primpke, Wirth *et al.* 2018), potentially reducing the number of thresholds to be set to 64. For the weights,  $3^3$  combinations are to be tested, at least (for weights of 0, 1, and 2). While this provides the user with high flexibility, they may be left overwhelmed as only few guidance is given on how to approach the optimization (Liu, Olesen *et al.* 2019). The program siMPle outputs a hit list for every particle identified, showing the similarity between the particle spectrum and the database entries, allowing to correct the assignments if necessary. This fulfills the basic requirements for QC. When launching siMPle, the assignment of 100 randomly selected spectra was rated by an expert, showing that > 90% of assignments were correct. This post-classification evaluation, however, may suffer from human bias. In contrast, specifying the ground truth before classification poses a less bias-prone approach. Moreover, it can be argued that a test dataset comprising 100 spectra is too small.

#### 4.3.2. Reference images for DAR evaluation

Another important QA measure for DARs is CV, such as MCCV, performed on a set of labelled spectra. These single, isolated spectra, however, do not reflect the full complexity of FTIR images. For instance, the RDF model employed for the study by Weisser, Beer *et al.* (2021), was evaluated on a set of 6,036 spectra by means of MCCV, resulting in an accuracy of 0.9545, close to the optimum of 1. Note that during this thesis, the ground truth was specified prior to classification, ensuring a low-bias evaluation of the results. MCCV was considered state-of-the-art at that time (Hufnagl, Steiner *et al.* 2019) and the accuracy reached was comparable with accuracies achieved by others (0.9766 in Hufnagl, Stibi *et al.* (2022) and 1.00 in Vinay Kumar, Löschel *et al.* (2021)). When reviewing the results generated by the model trained during the work Weisser, Beer *et al.* (2021), manual corrections were necessary at a much higher extent than expected based on the results from MCCV. These corrections implied both the class assignments and particle sizes. Depending on the number of particles identified, corrections took one to three hours per sample. Especially the fact that some particles were larger than identified by the model led to the question if particles may have been overlooked completely. To address this question, a reference FTIR image to serve as the ground truth was necessary.

Consequently, published FTIR images of MP were reviewed and assessed whether they were suitable to serve as a ground truth image. A summary is shown in Table 7. Xu, Hassellöv *et al.* (2020) allocated a reference transmission FTIR image comprising seven plastic particles made from polysulfone, PS, PP, PC, PET, and PE. The particles were rather large with sizes between ~1 mm and 5 mm (estimated from Figure 4 of the publication) and were cut from larger sheets. Thus, they do not represent the distortion of spectra due to scattering on particle surfaces, which is one of the most important factors impairing spectra quality. However, the data set covers detector over-saturation and mixed spectra as the particles partly overlaid each other.

Primpke, Wirth *et al.* (2018) published RefA to RefD, which are FTIR images comprising 33 synthetic and natural polymer types. Particles and fibers are much more realistic than in Xu, Hassellöv *et al.* (2020) in terms of sizes and shapes. With the same study, an FTIR image called Ref7P was published. It comprises a mixture of PE, copolyamide, polyester, polyurethane (PUR), quartz sand, cellulose, and diatomaceous earth (sizes 0 to 80  $\mu\text{m}$ ).

Table 7. Overview on publicly available reference Fourier-transform Infrared images containing MP = Microplastic.

| FTIR image                         | Number of intentionally added plastic types | Includes natural particles?   | Approximate particle sizes | No. of MP particles known? |     |
|------------------------------------|---|-------------------------------|----------------------------|----------------------------|-----|
| Xu, Hassellöv <i>et al.</i> (2020) | 6   | No                            | 1 – 5 mm                   | Yes                        |     |
| RefA                               | 8   | Yes                           | 0.65 – 2.2 mm              | Yes                        |     |
| RefB                               | 7   | Yes                           | 0.33 – 2.6 mm              | Yes                        |     |
| RefC                               | 7   | Yes                           | 0.18 – 0.93 mm             | Yes                        |     |
| RefD                               | Primpke, Wirth <i>et al.</i> (2018)         | 11                            | No                         | 0.47 – 2.5 mm              | Yes |
| Ref7P                              |   | 3                             | Yes                        | 0-80 µm                    | No  |
| RefEnv1                            |   | 0, but comprises 'natural' MP | Yes                        | 11 – 275 µm                | No  |
| RefEnv2                            | 0, but comprises 'natural' MP               | Yes                           | ≥ 11 µm                    | No                         |     |
| RefIMP                             | (Weisser, Pohl, Ivleva <i>et al.</i> 2022)  | 10                            | Yes                        | 11 – 1,890 µm              | Yes |

Additionally, the article was supplemented by RefEnv1, a real sample of marine sediments, and RefEnv2, a wastewater sample, both comprising natural matrix residues and weathered MP in environmentally relevant sizes. The dataset RefEnv1 has meanwhile been used as a reference for other studies (Hufnagl, Stibi *et al.* 2022; Primpke, Lorenz *et al.* 2017). A significant drawback is, however, that there no ground truth is available for Ref7P, RefEnv1, and RefEnv2, i.e., it is not known how many MP and non-MP particles are contained therein. Consequently, they can be used to compare the relative performance of DARs, however, they are not suitable to give insight into their absolute performance.

#### 4.3.3. DAR evaluation using RefIMP and MPVal

Because the datasets available were unsuitable to adequately address the question 'How many particles does my DAR overlook?', RefIMP was created and published. RefIMP is a fully evaluated FTIR image containing over 1,290 MP and non-MP particles (Weisser, Pohl, Ivleva *et al.* 2022). Together with the MatLab® script MPVal, a DAR's performance in classifying the particles of RefIMP can be evaluated, opening up a new standardized measure for the QA of DARs. This allows for both, intra- and inter-DAR evaluation. The concept can be applied to other imaging techniques and other analytes as well. Especially the normalized, modified confusion matrices, represented as heatmaps, provide class-specific details of the DAR's performance. Crucially, this comprises overlooked, over-segmented, and non-existing ('ghost') particles, as well as false type assignments. An example heatmap is shown in Figure 27. Rows represent the classes that the model predicted as well as an additional class 'overlooked'. Columns represent the ground truth classes with two extra columns for over-segmented and ghost particles. These extra row and columns added distinguish the heatmaps from standard confusion matrices that are symmetric, i.e., comprise as many rows as they comprise columns (see Figure 12). This way, the heatmaps can adequately illustrate a DAR's performance based on particle class assignments and counts.

## 4 - Discussion

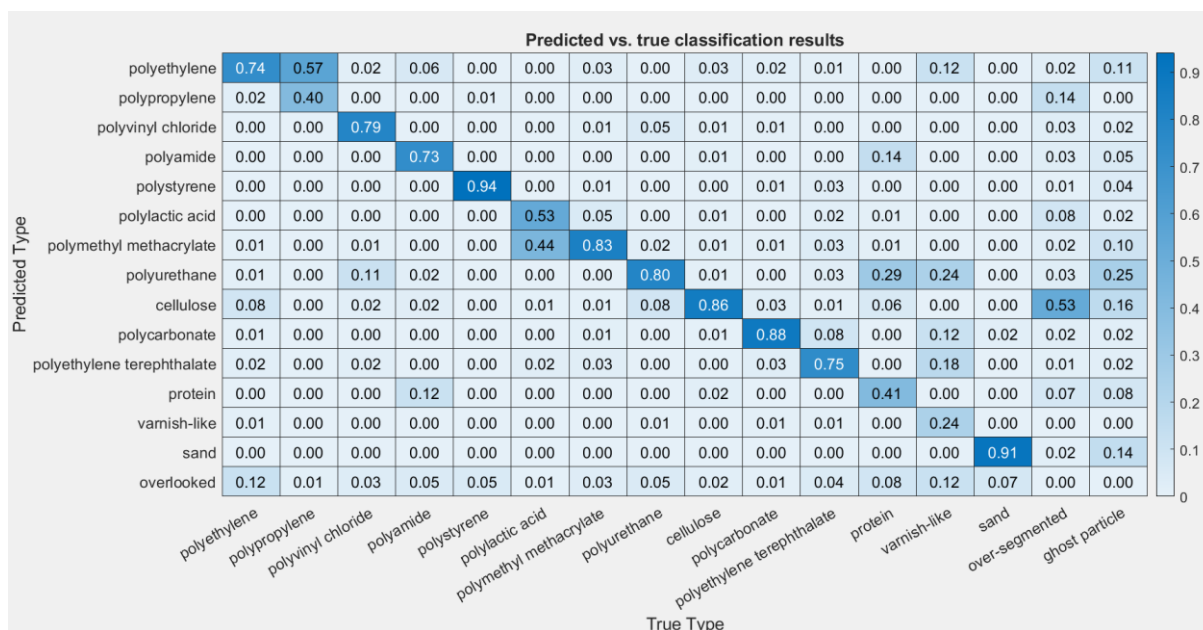


Figure 27. Heatmap of the results from evaluation of RefIMP with the best-performing model from Weisser, Pohl, Ivleva *et al.* (2022).

The values in the quasi-diagonal of the heatmap (excluding the row for overlooked and the columns for over-segmented and ghost particles) represent the share of correct assignments, based on the number of reference particles for the respective class. Importantly, the significance of high values in the quasi-diagonal raises with the size of the test set. For the best-performing model trained during the study Weisser, Pohl, Ivleva *et al.* (2022), the correct assignment rates range from 24% for varnish-like to 94% for PS when classifying RefIMP. Inspecting the last row, it becomes evident that even this best-performing model overlooked 12% of PE particles, 12% of varnish-like particles, and 8% of protein particles. Moreover, most class confusions were attributed to PP, PLA, *protein*, and *varnish-like*, despite yielding values  $> 0.95$  for  $Sn_g$ ,  $Sp_g$ , and  $Pr_g$  (formulae 6-8) with MCCV (with the exception of  $Sn_{\text{varnish-like}}$ ), see Table 8.

Table 8. Sensitivity =  $Sn_g$ , Specificity =  $Sp_g$ , and Precision =  $Pr_g$  for the classes PP = Polypropylene, Polyethylene = PE, Poly(lactic acid) = PLA, Polymethyl Methacrylate = PMMA, *protein*, *varnish-like*, and Polyurethane = PUR as determined through Monte-Carlo Cross Validation = MCCV on isolated spectra and through MPVal on RefIMP. Superscripts ( $\diamond$ ,  $\star$ ,  $\square$ ,  $\bullet$ ) indicate confused classes, where the first-mentioned class is underestimated because of the confusion. MCCV values are means from 5-fold MCCV on the 100% training data diversity set. MPVal results are based on the optimized Random Decision Forest model as described in Weisser, Pohl, Ivleva *et al.* (2022).

| Class                         | $Sn$   |        | $Sp$   |        | $Pr$   |        |
|-------------------------------|--------|--------|--------|--------|--------|--------|
|                               | MCCV   | MPVal  | MCCV   | MPVal  | MCCV   | MPVal  |
| PP $\diamond$                 | 0.9854 | 0.9437 | 0.9992 | 0.9959 | 0.9889 | 0.9306 |
| PE $\diamond$                 | 0.9873 | 0.8454 | 0.9986 | 0.8468 | 0.9818 | 0.3004 |
| PLA $\star$                   | 0.9739 | 0.8675 | 0.9991 | 0.9787 | 0.9882 | 0.7347 |
| PMMA $\star$                  | 0.9919 | 0.9516 | 0.9950 | 0.8966 | 0.9393 | 0.4876 |
| <i>protein</i> $\square$      | 0.9639 | 0.5783 | 0.9996 | 0.9556 | 0.9931 | 0.6531 |
| <i>Varnish-like</i> $\bullet$ | 0.5354 | 0.5000 | 1.0000 | 0.9961 | 0.9971 | 0.5000 |
| PUR $\square, \bullet$        | 0.9911 | 0.9223 | 0.9986 | 0.8307 | 0.9813 | 0.2978 |

When basing the evaluation on RefIMP and MPVal,  $Sn_g$ ,  $Sp_g$ , and  $Pr_g$  for these classes are lower. For instance,  $Sn_{\text{PLA}}$  reached 0.8675 opposed to 0.9739 based on MCCV, hinting at undetected PLA particles, either overlooked completely or falsely classified. The confusion of classes, importantly, is revealed only when additionally involving the classes that they were

confused with, which are PE, polymethyl methacrylate (PMMA), and PUR. Especially for  $Sn_g$  and  $Pr_g$ , there is a large discrepancy between the MCCV- and MPVal-based evaluation results. For example,  $Pr_{PE}$  based on MPVal is very low (0.3004) because of the high number of FPs among the total number of predictions for PE, as can be seen from the list of TPs, FPs, FNs, and TNs in generated by MPVal. This high number of FPs is caused mostly by the confusion for PP as the heatmap shows. Similarly,  $Sn_{protein}$  based on MPVal reaches only 0.5783, because of a combination of a high number of FNs and a low number of TPs for this class.

This interconnectivity between metrics and classes makes the evaluation of DARs very complex. A careful inspection from different perspectives and thorough analysis of errors are vital for understanding a model's behavior as the examples show.

### 4.3.4. Potential reasons for class confusion

The classes *varnish-like* and *protein* were underrepresented in the training data set. Therefore, it can be argued that this was the reason for the poor classification performance. This, however, is not the case for PE and PP, which were both well-represented in the training data. Nevertheless, 57% of PP particles were misclassified as PE. One reason for this may be the fact that the spectra quality of the training data cannot be guaranteed to perfectly represent the sample spectra. Training data were labelled manually and despite trying to label highly diverse spectra, this task remains somewhat subjective. In the case discussed here, however, training data diversity was assessed and the presence of high and low quality spectra assured (Weisser, Pohl, Ivleva *et al.* 2022).

The second reason for poor classification by an RDF model is the composition of the set of spectral descriptors. From a human point of view, IR spectra of PE and PP (shown in Figure 28) are well distinguishable, not only based on the height of the band at  $1,373\text{ cm}^{-1}$ , but also based on the CH-stretch band pattern ( $2,820 - 2,960\text{ cm}^{-1}$ ). For an RDF model, however, these differences become visible only when the set of spectral descriptors is designed adequately. If no descriptor describes a class' specific region(s), the model cannot be expected to be capable of correctly identifying this class. The spectral descriptors used in Weisser, Pohl, Ivleva *et al.* (2022) were generated systematically over the complete spectral range. Nevertheless, it seems that they should be improved further.

It could be expected that database matching does not suffer from overlooked spectral features, provided the matching is performed over the complete relevant spectral range. Surprisingly, class confusion is not unusual in database matching and related approaches, as outlined in the following.

Kedzierski, Falcou-Préfol *et al.* (2019) tested a k-nearest neighbor model for MP classification. This technique often is categorized as supervised ML, even though it is an advanced database matching procedure (Weisser, Pohl, Heinzinger *et al.* 2022). It provides the user with the k most similar database entries for each query spectrum.

Interestingly, the k-nearest neighbor model from Kedzierski, Falcou-Préfol *et al.* (2019) tended to confuse PE and PP (and related polymers), as well: their model falsely classified PP as PE, just like the RDF presented here. Based on the same dataset, the SVM by Back, Vargas Junior *et al.* (2022) was shown to confuse PE for PP, too.

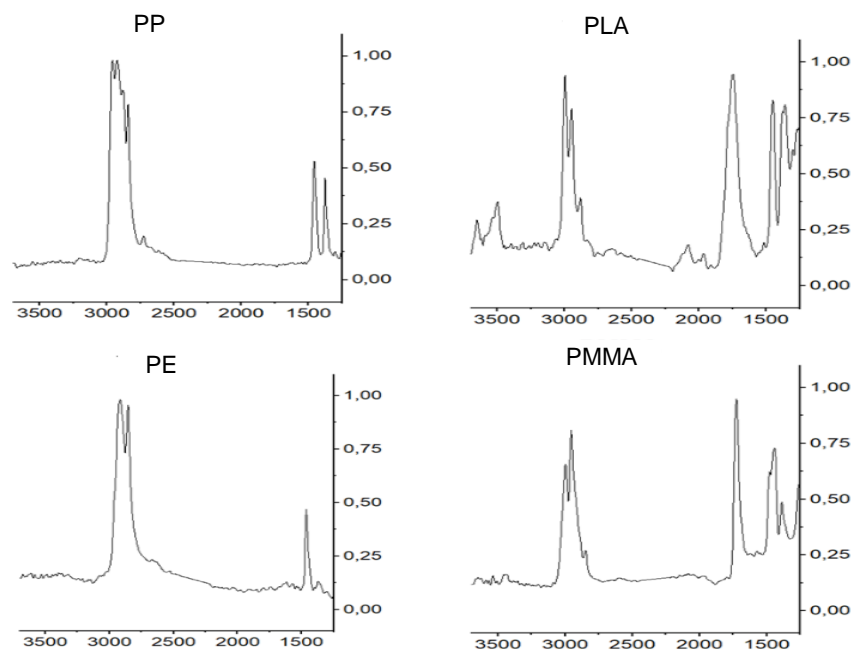


Figure 28. Normalized, dimensionless transmission IR spectra of PP = Polypropylene, PE = Polyethylene, PLA = Polylactic Acid, and PMMA = Polymethyl Methacrylate.

In Primpke, Godejohann *et al.* (2020), hierarchical cluster analysis of ATR-FTIR spectra resulted in confusing some PE spectra for PP (see supplementary information of the article). After augmenting the set with spectra generated by Quantum Cascade Laser-Based Hyperspectral Infrared Chemical Imaging, this confusion did not occur anymore. No explanation for this behavior was given as it was beyond the work's scope.

The risk of confusing PE and PP was further illustrated in Xu, Hassellöv *et al.* (2020), where spectral matching was performed using Pearson correlation. For both, PE and PP test spectra, the respective other received the second-highest hit. For spectra with worse quality, it can be assumed that the distance between the hits decreases further. Moreover, the matching procedure proposed by Morgado, Gomes *et al.* (2021) included three more steps to identify PE and PP than to identify PS and PET, showing that even though distinguishing their spectra seems simple, their computer-assisted interpretation is not.

The reason for this may lay in the relative simplicity of PE and PP spectra: the few bands that they exhibit are also present in many other plastic spectra, as most plastics comprise aliphatic C-H backbones. It may thus be the absence of more unique features (such as the aromatic C-H stretch of PS spectra, for instance, see Figure 7) that makes them hard to classify.

This explanation does not hold true for the spectra of PMMA and PLA, however, which should be well distinguishable in the range below  $1,800\text{ cm}^{-1}$  and based on the band at  $3,500\text{ cm}^{-1}$  that is present in the spectrum of PLA, but absent in the spectrum of PMMA. This is taken as another indicator that the set of spectral descriptors for the RDF model should be reassessed and augmented to enhance the distinction between PE and PP, but also between PLA and PMMA, and protein and PUR. Redesigning the spectral features may further reduce the number of ghost particles and overlooked particles.

#### 4.3.5. Up- and downsides of RefIMP and MPVal

Besides its strengths, RefIMP comes with certain limitations that should not be neglected, see Table 9. First, it contains engineered MP particles only, which are not weathered.

Consequently, it does not reflect all challenges inherent to environmental MP samples (Renner, Sauerbier *et al.* 2019). Second, only a chosen subset of plastic types and matrix residues is contained, limiting any evaluation to these types.

Table 9. Summary of the strengths and weaknesses of RefIMP and MPVal. PE = Polyethylene; PVC = Polyvinyl Chloride; PS = Polystyrene; PUR = Polyurethane; PMMA = Polymethyl Methacrylate; PET = Polyethylene Terephthalate; PA = Polyamide; PLA = Polylactic Acid; PC = Polycarbonate; PP = Polypropylene; MP = Microplastic; Dar = Data Analysis Routine; FTIR = Fourier-transform Infrared.

|               | Strengths  | Drawbacks   |
|---------------|--|---|
| <b>RefIMP</b> | <ul style="list-style-type: none"> <li>+ Represents a state-of-the-art MP analysis technique</li> <li>+ &gt; 1,200 reference particles</li> <li>+ Contains the most important plastic types: PE, PP, PS, PET, PA, PVC, PUR, PC, PMMA, PLA</li> <li>+ Contains the most important types of sample matrix residues: cellulose, protein, quartz sand</li> <li>+ Reference particles in a relevant size range: 11-666 <math>\mu\text{m}</math> for MP, 11-1,890 <math>\mu\text{m}</math> for non-MP</li> <li>+ Adaptable for new FTIR image tiles</li> <li>+ Well-accessible data format (.spe)</li> </ul> | <ul style="list-style-type: none"> <li>- Reference particles do not fully reflect the complexity of environmental MP, i.e., aging effects</li> <li>- Other matrix residues or plastic types may be relevant</li> <li>- Performance of a DAR on RefIMP does not necessarily equal the performance on other samples</li> <li>- Slight class imbalances</li> </ul> |
| <b>MPVal</b>  | <ul style="list-style-type: none"> <li>+ Easy-to-use</li> <li>+ Fully documented</li> <li>+ Global and class performance evaluation</li> <li>+ Heatmaps provide detailed insights</li> <li>+ Adjustable with basic programming knowledge</li> </ul>  | <ul style="list-style-type: none"> <li>- Particle sizes and shapes are not assessed</li> <li>- Association of found particles to reference particles based on bounding boxes and centers can lead to pessimistic outcomes</li> <li>- Runs on a commercial program (but can be adapted to free programs, e.g., Python, with few effort)</li> </ul>               |

Finally, it is important to understand that a high performance of a DAR on RefIMP does not automatically mean that the performance on any other MP sample will be just as high. Instead, the intention of creating RefIMP was to provide the MP research community with a fully transparent ground truth image. This image can serve as a common basis for DAR evaluation, delivering for the first time a low-bias way of directly comparing different DARs with each other. For this reason, RefIMP and MPVal are seen as key steps towards enhanced QA of the data analysis step in the MP analysis pipeline, thereby contributing to MP analysis method harmonization.

#### 4.3.6. Advanced recovery rates for improving DAR QA/QC

Once a computer-assisted DAR is established, it will yield reproducible results. This distinguishes computer-assisted DARs from manual data analysis (Esch, Kohles *et al.* 2020). Thus, it can be argued that the only QC measure necessary at this point is to manually assess the results for a given sample for their correctness. Doing so, it will very likely be experienced that a DAR performs differently on different sample types. Its performance can be expected to

be worse than on manually labelled reference data sets as the latter underlie human bias. Thus, it is proposed to employ advanced recovery rates for each type of sample as follows:

1. Spike in known numbers of MP particles of all types and sizes targeted
2. Prepare the sample as usual, e.g. enzymatic treatments
3. Measure the sample as usual, e.g. FTIR imaging
4. Detect MP as usual, e.g. with an RDF model
5. Compare the result with the known number of spiked-in particles

In contrast to classical recovery experiments, where usually brightly colored particles are counted under a visual microscope, this procedure would give a more realistic picture.

A drawback of this approach is that no conclusion can be drawn whether non-recovered particles got lost during sample preparation or are not detected by the DAR, for example because they are covered up by sample matrix residues. Nevertheless, an undetected particle remains an undetected particle and this advanced recovery rate enables to estimate the overall MP underestimation.

Importantly, a major challenge to be solved before conducting such experiments is the production of reference MP particles. In all conscience, no reproducible, clearly defined secondary MP particles of all relevant types and size classes are commercially available to date. Promising small-scale methods have been proposed, however (Seghers, Stefaniak *et al.* 2021; von der Esch, Lanzinger *et al.* 2020). To the best of the author's knowledge, the sole supplier for standardized MP particles is the German Bundesanstalt für Materialforschung und -prüfung (BAM); here, artificially aged PE and PS particles can be purchased. Moreover, even when commercially available, spiking a sample with decisive numbers of particles remains a challenge (see section 1.2 and Eitzen, Paul *et al.* (2019)).

The gold standard of QC, inter-laboratory tests, cover the whole analysis pipeline and give the opportunity of comparing different approaches in a standardized manner. In addition, the most suitable methods, i.e. those with most representative sample volumes, lowest LODs, and highest recovery rates can be identified. However, the bottleneck that currently limits the meaningfulness of inter-laboratory tests is the availability of adequate reference materials and of methods for the reproducible preparation of test samples (see section 1.2). Nevertheless, data analysis and the corresponding QA/QC should be advanced further to generate versatile, even quicker and robust DARs for MP research.

### **4.4. Entry paths for microplastics into beverages and food**

In the course of this thesis, beverages and a selection of foods were analyzed, aiming to identify the most important entry paths for MP. This included raw materials, processed foods, and packaged goods. Results were presented in section 3.5. The relevance of the entry paths identified is discussed in the following.

#### **4.4.1. Food preparation equipment**

The production of bread and fruit puree for infant feeding were chosen as examples for MP entry into processed foods.

##### **Bread production**

Rye flour, sea salt and dough from a bakery were sampled and examined. Compared with the corresponding LOD, the rye flour examined must be regarded free from MP, the dough, however, according to the results has experienced contamination during its fabrication. It was suspected that the sea salt added to the dough could be responsible for the high MP count. MP concentrations in the sea salt examined here were within the range reported elsewhere

(Peixoto, Pinheiro *et al.* 2019), so it can neither be classified as highly polluted nor as free from MP. Given the low amounts of salt used to prepare the dough (~1.0 to 1.5% (w/w)), however, its contribution can be neglected. Taking into account the RR of the density separation process that the salt samples underwent, however, the actual concentration may be twice as high. Nevertheless, the contaminated sea salt cannot explain the high MP concentration in the dough.

Most MP particles in the dough were classified as PP, PE, and EvOH (30.8%, 29.1%, and 19.1%, respectively). The PP dough scrapers used in the bakery seem to pose the most plausible source for the PP particles, as they need to be exchanged regularly because of high wear. The PE particles might stem from PE trays used in the bakery, but also from airborne particles. For example, opening of PE bags may generate particles that could get into the dough trays. Trays were open most of the time to allow the dough to rise (Hubin 2020). EvOH, in turn, is used as an oxygen barrier in food packaging (Domininghaus 2012) and thus might be present in the bakery in form of packaging materials, as well.

Some insecurity remains, however, due to the high blank values. They indicate that substantial contamination took place during sample preparation in the laboratory. The MP concentration in the dough was only 60% higher than the corresponding LOD. There are, however, no binding rules for acceptable blank or LOD values other than that they should be as low as possible (Schymanski, Oßmann *et al.* 2021).

### **Fruit puree production**

The MP concentrations determined in homemade and industrial apple puree were both below LOD. Note that the puree samples underwent a multi-step preparation process including four filtration steps. Taking into account the RR for sample filtration, the total RR for the process is approximately 47%. Therefore, the actual MP concentrations in both samples and the blanks may have been twice as high. The LOD here was relatively high, indicating non-negligible contamination during sample preparation. However, concluding that the samples were free of MP because they were below LOD, would be premature as a look at the plastic types reveals. While most plastic types detected in the samples were present in similar or higher amounts in the blank samples, as well, PS, EvOH, and PVC were more abundant in the samples than in the blanks. Among them, PVC is the only plastic type that may have its origin in the kitchen equipment used. More precisely, it might stem from a PVC sieve used to mash the cooked apples. During this process, the sieve experiences mechanical forces such as friction that can cause the generation of MP particles (Winkler, Santo *et al.* 2019). The origin of PS and EvOH could not be traced back (Eberl 2020). Especially the cutting board was expected to pose a source of MP contamination as found by others (Habib, Poulouse *et al.* 2022). However, the results indicate that the PP cutting board did not contribute significantly to the MP contamination. It should not be forgotten, that airborne contamination can play a major role, as well (Vianello, Jensen *et al.* 2019). It can thus be assumed that the PS and EvOH particles, and potentially also the PVC particles, were airborne rather than equipment-sourced.

It can be argued that the results presented here are of limited expressiveness because the sample sizes were rather small (3 × 6.5 g wet weight for each batch). In fact, only subsamples of 50-75% could be analyzed to avoid overloading the analysis filters. Using more or larger filters, however, would have led to disproportional high measurement and analysis times. Assessing larger samples would require further optimization of the sample preparation process, as especially cellulose-like structures were still present.

### Concluding remark

According to the results presented here, kitchen equipment could neither be confirmed as a source of MP in food, nor could it be excluded. It seems that a certain level of diffuse background contamination, most likely airborne MP, plays a major role (Vianello, Jensen *et al.* 2019). While the usage of a plastic cutting board and other plastic kitchen utensils did not result in noteworthy rises in MP concentrations in a so-produced apple puree, the results from dough analysis suggest that wear from PP scrapers was present in it. Moreover, sea salt can be a source for MP, but its contribution is negligible due to the low amounts consumed.

#### 4.4.2. Food packaging

In 2021, packaging accounted for 40.5% of the European demand for plastics (Plastics Europe's Market Research and Statistics Group 2021). The majority of food and beverages available for end consumers are packaged in plastic. The contribution of plastic packaging to human MP consumption, however, is not fully cleared yet.

#### Tea bags

Tea bags may pose a potential source for MP. Some tea bags on the market are completely made from plastic, usually PET, PA, or PLA, also known known as 'pyramid bags' because of their shape. Examining tea prepared from plastic tea bags, (Hernandez, Xu *et al.* 2019) claim to have detected billions of MP and NP particles. The results gained during this doctoral project differ substantially from their results. In the tea brewed in PLA bags, a maximum of 15 PLA items ( $\geq 11 \mu\text{m}$ ) were detected. The PLA detected was always fibrous and larger than  $100 \mu\text{m}$ . This lead to an atypical particle size distribution, where the number of particles did not rise with decreasing particle sizes, as is mostly the case. Instead, the class  $100\text{-}500 \mu\text{m}$  is the most represented with 35% of MP particles, while each of the other classes makes up for 20-23% of particles. All other MP types ranged in very low numbers ( $\leq 5$ ) or were below LOD.

The preparation of tea samples included four filtration steps. Consequently, the RR for this process amounts approximately  $0.83^4 \pm 47\%$ . The findings thus may underestimate MP concentrations by about half. Considering this, and even though more MP is to expected when choosing an analysis method that is able to identify particles  $< 11 \mu\text{m}$ , it is doubted whether such enormously high numbers as reported by Hernandez, Xu *et al.* (2019) would be reached. Their study faced strong criticism because they assumed that all particles visible in scanning electron microscopic images were MP or NP, respectively. The chemical analysis, however, did not support this assumption. Instead, the particles found may be crystallized oligomers, which are water-soluble and therefore do not fall into the definition of MP/NP (Busse, Ebner *et al.* 2020). In this doctoral project, in contrast, the chemical composition of each particle was assessed, ensuring that no non-MP particles were counted as MP. In fact, non-MP particles, mostly cellulose, were numerous.

In addition to the PLA tea bags, standard 'paper' bags were examined. Even though perceived as 'paper bags' by consumers, they contain plastic fibers, for example polyacrylamide, to make them stable during steeping in hot water (BfR 2022b). The German federal institute for risk assessment (Bundesinstitut für Risikobewertung, BfR) recommends to use paper additives based on vinyl chloride-vinyl acetate copolymers, PE, PP, or PEST. Depending on the additive chosen, between 0.015% and 6.1% can be used.

In the standard tea bags examined, PP was present in low numbers, potentially stemming from paper additives. Assessing the bags directly using  $\mu\text{ATR-FTIR}$ , however, only cellulose was detected. It is, however, possible that the cellulose covered other substances present in the

tea bag paper. The origin of the PP particles in the tea could thus not be resolved fully. No PLA was detected, indicating that no cross-contamination between the samples occurred.

### **Bottles for beverages**

While the presence of MP particles in bottled mineral water has been confirmed by others (Schymanski, Goldbeck *et al.* 2018; Oßmann, Sarau *et al.* 2018), the project presented here aimed to shed light on the origin of these (see section 3.4). As ground water was already known to be nearly free of MP (Mintenig, Löder *et al.* 2019), the cleaning process of reusable bottles was suspected to be the main entry path. However, MP findings in cleaned bottles from all four companies were < LOD. Cleaned and filled, but uncapped bottles were free of MP, as well. This shows that the bottle cleaning and fresh water jetting was successful at all four companies. It should be stressed that analyses of particles < 11 µm may have led to a different result. For instance, Oßmann (2020) detected up to  $487 \pm 257$  MP L<sup>-1</sup> > 10 µm in cleaned glass beer bottles. A comparison between their and our results remains difficult, as different methods for instrumental analysis and data analysis were pursued. For instance, the study by (Oßmann 2020) included phenoxy resin and styrene-butadiene-copolymer, which together accounted for up to 59% of MP particles detected.

The sharp rise of MP concentrations after bottle capping (see Figure 19) strongly indicates that the capping process was responsible for MP in bottled mineral water. With  $317 \pm 257$  MP L<sup>-1</sup>, the concentrations were relatively high when compared with studies employing spectroscopy and corrected for the particles > 10 µm ( $28 \pm 29$  MP L<sup>-1</sup> (Schymanski, Goldbeck *et al.* 2018) to  $212 \pm 175$  MP L<sup>-1</sup> (Oßmann, Sarau *et al.* 2018)). This may be because in Weisser, Beer *et al.* (2021), bottles were flushed three times after emptying them, which was not done in the other studies. The RR for the bottle flushing process was  $86 \pm 8\%$ . Without flushing, some MP may have remained in the bottle, so it can be argued that MP findings in both above-mentioned studies may be underestimated. They both did not report any RRs.

When inspecting the plastic types in (Weisser, Beer *et al.* 2021), PE dominated with 51-96% across samples from all four manufacturers. PE was among the most-represented plastic types in similar studies mentioned before, as well. As is known from Winkler, Santo *et al.* (2019), twisting of PE caps on PET bottles causes abrasion of plastic particles. They detected between 120 and 2,150 particles per mm<sup>2</sup> inner surface of bottle caps. As this statement was based only on the carbon content of the particles found, there remains some risk that the PE numbers were overestimated. Nevertheless, wear and abrasion of the caps can be seen clearly in their scanning electron microscope images. Most of the particles observed were smaller than 5 µm, however, particles > 10 µm were present, as well. In Weisser, Beer *et al.* (2021), glass bottles with aluminum screw caps were examined, however, the aluminum caps had a polymeric sealing layer on the inside. ATR-FTIR revealed that this sealing was made from a polymer whose spectrum was very similar to PE. Only a small additional band distinguished it from the reference PE spectrum, see Figure 29. This band at 1,648 cm<sup>-1</sup> hints at the presence of C=O groups in the sealing substance (Stuart 2004). Inspecting the spectra of MP particles classified as PE revealed that most of them comprised this band, as well. Yet, the spectra were similar enough to PE to be identified as such by the RDF model. The similarity between the cap sealing spectra and the PE-like MP spectra strongly indicated that the particles stemmed from the sealings and were most likely generated during opening the bottles in the laboratory.

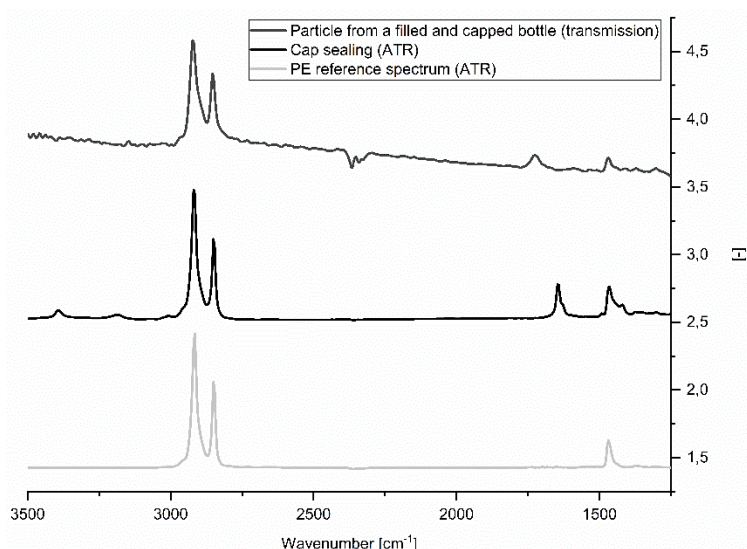


Figure 29. Example of transmission spectrum of a PE (polyethylene)-like particle from a filled and capped water bottle compared to Attenuated Total Reflection-Infrared spectra of cap sealing and PE reference material (reprinted from Weisser, Beer *et al.* (2021) under CC-BY license).

When trying to unravel the material precisely, the cap manufacturers did not give any information except that all sealings were made from a 'PVC-free polyolefin'. Interestingly, the mineral water brands with the highest MP concentrations were both supplied by the same cap manufacturer. This indicates that different additives in the sealings may influence the abrasion-proneness of the material.

Even though this study was conducted with mineral water, similar findings are to be expected for other bottled beverages. The findings in Shruti, Pérez-Guevara *et al.* (2020) seem to contradict the finding that bottle caps were responsible for most MP in bottled drinks, as the majority of MP identified were PA. The authors admit, however, that the pigments in colored particles masked the polymer spectrum in their RM analyses. As this was the case for 20-45% (estimated from Figure 3 in their publication), it can be suspected that these potentially stemmed from colored bottle caps.

The presence of other MP types, like PS, in Weisser, Beer *et al.* (2021), showed that the bottle caps are not the only source for MP contamination in bottled beverages. The caps seem to be, however, the most important one. Twisting the cap is, of course, inevitable to consume water from a bottle, meaning that MP in bottled drinks cannot be fully mitigated. Importantly, this does not only concern the bottles and caps used for commercial drinks, but also refillable bottles for private use. To minimize MP ingestion via drinks, bottles and especially their caps would need to be completely plastic-free. Natural materials, such as cork, in turn, may be problematic in terms of hygiene, especially when used over a long period of time.

### Concluding remark

Based on the data available to date, it seems hardly evitable to ingest MP with bottled drinks. There is, however, no proof for human health hazards caused by orally ingested MP (see section 1.1.3). Everybody therefore must evaluate the advantages and potential disadvantages of consuming bottled drinks for themselves.

## 5. Conclusions and future perspectives

Microplastics (MP) analysis is a challenging task and the methods applied are only partly harmonized until today. Strict measures for quality assessment (QA) and quality control (QC) during each step of the analysis pipeline are the cornerstones of harmonizing MP analysis as is summarized in Figure 30. Obeying to already established and developing new QA/QC measures, a high-performance pipeline for the analysis of MP in beverages and plant-based food was established during this doctoral research project. The main entry paths of MP into food and beverages were assessed. A special focus was put on the analysis of the data derived from spectroscopic imaging of MP samples.

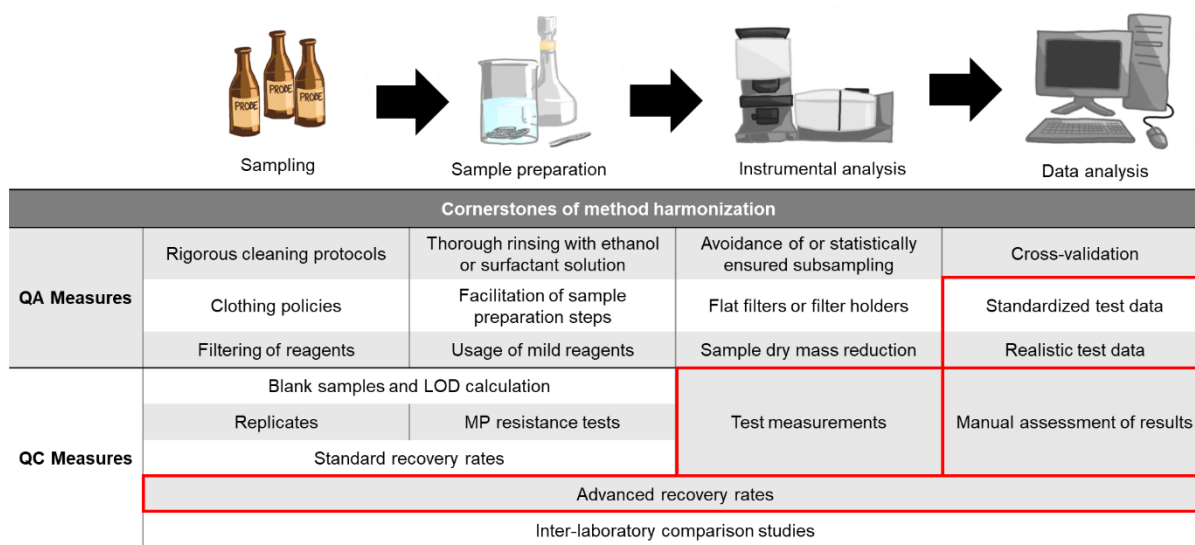


Figure 30. Quality Assurance (QA) and Quality Control (QC) measures as the cornerstones of method harmonization. All listed measures were applied during this doctoral research project, except for inter-laboratory tests (greyed out). Newly suggested measures within the scope of this thesis are highlighted in red. LOD = Limit Of Detection; DAR = Data Analysis Routine.

### Harmonization of MP sample preparation methods

Starting with sampling and sample preparation, blank samples and thereof deduced sample-specific limits of detection (LOD), MP chemical resistance tests and recovery rates (RR) were crucial for controlling the effectiveness of QA measures taken to avoid sample contamination and particle loss. The LODs and RRs achieved were compatible with other works and MP particle damage by the applied chemicals was marginal, showing the adequacy of the applied methods.

For isolating MP particles from various beverages and plant-based food matrices, the combination of chemical and enzymatic treatments is considered vital. According to the results, enzymes should be chosen carefully depending on the sample matrix and can be combined, when necessary. The well-established Fenton reaction was enhanced during this work by a) omitting the precipitation of iron oxides and b) by extending it with an ascorbic acid treatment, leading to increased matrix degradation. The enhanced Fenton protocol framed enzymatic degradations, enhancing the accessibility of complex structures for the enzymes and clearing up the products from enzymatic degradations.

Providing a good balance between the smallest detectable particle and analysis speed, it was decided to employ Fourier-transform Infrared (FTIR) imaging for the instrumental analysis of MP. Being the currently most-used MP analysis technique, comparability to many other studies

is complied with. As a prerequisite for successful imaging of a sample, it should be deposited on a flat filter with adequate pore widths. Silicon filters were found ideal for this purpose, and a 3D printed adapter for their usage with standard filtration devices was designed.

Some samples were unanalyzable despite high dry mass reduction. Therefore, it is suggested to assess the analyzability of a sample by spiking it with MP reference particles. This is called 'advanced RR'. The advanced RR can serve as a QC tool covering all analysis steps from sampling to data analysis.

The silver bullet in harmonizing MP analysis are inter-laboratory tests. However, the generation of adequate standard materials and methods to generate reproducible test samples still pose major challenges and hampers these tests.

### **Harmonization of MP detection in hyperspectral images**

Despite the advantages of FTIR imaging, the analysis of the thereby generated data posed a major challenge. The employed Random Decision Forest (RDF) model (a supervised machine learning, ML, technique) was fast in classifying MP particles and yielded high accuracies determined through the QA tool Monte Carlo cross validation (MCCV). However, during QC (manual evaluation of the classification), a discrepancy was experienced between the MCCV-based performance and the necessary extent of manual corrections of the results. Moreover, it remained unclear whether the model had overlooked any MP. This led to introducing a new QA measure, based on a reference FTIR image called RefIMP that serves as the ground truth. It enables low-bias evaluation of data analysis routines (DARs) such as RDF models or database matching. Along with an automatized MatLab® script, MPVal, that compares the DAR's results with the ground truth, a transparent and low-bias QA measure for DAR evaluation was created. MPVal provides access to all details of the DAR's performance. The performance is visualized using classification heatmaps and concise single-class and global performance metrics are calculated. Thereby, it was shown that the performance of a DAR can be overestimated considerably by MCCV. This illustrates the bias-proneness inherent to MCCV, as it relies on manually labelled spectra. RefIMP, in turn, covers typical issues in MP analysis in a more holistic way and at lower bias.

RefIMP of course cannot represent all conceivable sample types at once. Nevertheless, it can serve as a common baseline for evaluating DARs. Using RefIMP and MPVal, the question 'How many MP particles does my DAR overlook?' can be answered precisely for the first time. Moreover, the results from MPVal revealed which classes were most vulnerable to being overlooked or confused with other classes. In addition, over-segmentation of particles was introduced as a new type of error in MP classification. This knowledge is vital for further improving a DAR.

Three example hypotheses demonstrated how RefIMP (or an in-house reference image) and MPVal can be used for assessing the performance of a DAR. The first hypothesis pointed out to the danger of overlooking particles when using masks for filtering out background signals. The second hypothesis confirmed that RDF models benefit from training data that are highly diverse in terms of similarity to textbook-like reference spectra. Moreover, the importance of balanced classes was demonstrated. The third use case highlighted the role of model hyperparameters, an aspect that MCCV cannot cover as it does not include particle-level hyperparameters such as the correlation between neighboring pixels.

RefIMP and MPVal are intended as an impulse towards harmonizing DARs for MP analysis. If already existing or newly developed DARs are evaluated using this baseline, the comparability of results from various studies is enhanced considerably. It is hoped that more research groups

publish MP reference images, representing different sample types, more MP types and sizes to further push forward the harmonization of DARs.

### **Entry paths of MP into food and beverages**

Raw food ingredients, food preparation equipment, and packaging materials potentially pose sources of MP. Their relevance was examined based on the preparation of model foods. Flour, sea salt, and ground water were chosen as examples for raw food ingredients. Only in sea salt, relevant MP concentrations were detected. Nevertheless, its significance to human MP consumption is rather low because it is consumed in very small amounts.

During the industrial production of fruit purees, no MP contamination occurred, as the examined subsamples suggested. Samples of homemade fruit puree were not free from MP, but the plastic types identified did not match the plastic types of the kitchen equipment used. Accordingly, it seems that it is rather diffuse background contamination (e.g. airborne particles) than the kitchen equipment that contributes to MP in homemade foods.

Usage of plastic cutting boards and other plastic equipment commonly used in private kitchens paltry contributed to the overall MP concentration. It seems, however, that a certain background contamination was more relevant, potentially stemming from airborne contamination.

PLA fibers in tea could be traced back to the PLA tea bags. Concentrations were, however, very low. Standard 'paper' tea bags seemed to have leached small amounts of MP. They potentially stemmed from additives that enhance the paper's stability.

For mineral water and other beverages, the most important source for MP are the bottle caps, according to the findings presented here. The friction that the caps experience during twisting results in MP particles. Lamentably, cap twisting is inevitable for consummation.

### **Outreach of this work and future perspectives**

The harmonization of MP analysis has made large progress in the past five years. In 2017, no standards dealing with MP were available. As of today, ISO/DIS 24187 and ISO/TR 21960 describe the analysis of MP in the environment. ISO/NP 16094 and ISO/NP 5667-27 describe MP analysis in drinking and surface water. ISO/DIS 4484 deals with MP from textile sources. Lastly, DIN/TS 10068, a technical standard dealing explicitly with food samples, has been established. Experience and knowledge gained during this doctoral research project have contributed to the latter, aiming to give attention to suitable QA/QC measures for all steps of the analysis.

Additional contributions were made to joint projects aiming at harmonizing MP analysis in clean water samples (Schymanski, Oßmann *et al.* 2021) and sample preparation of complex matrices (Al-Azzawi, Kefer *et al.* 2020).

Entry paths of MP into food, such as kitchen equipment and packaging materials could partly be resolved: abrasion from kitchen equipment plays a role, as well as packaging materials. Especially, the work presented here has shed light on the previously unknown entry paths for MP particles into bottled mineral water. Accordingly, abrasion from bottle caps is responsible for 57-96% of MP particles therein.

Much progress has been made, but there is more to come in MP research: the development of enclosed devices for sample preparation that can be back-flushed could further minimize contamination and enhance recovery rates. Testing more enzymes and chemical sample matrix degrading agents may allow to scale up sample amounts.

Concerning the DARs, sweeping developments can be expected in the near future. Assessing the applicability of transfer learning could ease adding new classes to ML models. Moreover, techniques that do not require feature input from the user, like convolutional neural networks, seem promising to further reduce human bias. Ideally, future DARs can deal with a broad variety of sample types reaching from clean waters to complex environmental or biological samples. The here-presented MP reference image hopefully enhances the comparability and harmonization of upcoming DARs.

To conclude with, it is hoped that the suggestions made in this thesis for improving QA and QC will be picked up and help making methods for MP analysis more comparable in the future, ultimately leading to harmonized MP analysis methods. Once this is achieved, we can finally assess MP abundance in the environment, beverages, and food, which is crucial for meaningful risk assessments.

## 6. References

- 2009/54/EC, Directive. 2009. Directive 2009/54/EC of the European Parliament and of the Council of 18 June 2009 on the exploitation and marketing of natural mineral waters (Recast). edited by European Parliament and Council: European Parliament and Council.
- Abbasi, Sajjad, Mustafa Alirezazadeh, Nastaran Razeghi, Mahrooz Rezaei, Hanie Pourmahmood, Reza Dehbandi, Meisam Rastegari Mehr, Shirin Yavar Ashayeri, Patryk Oleszczuk, and Andrew Turner. 2022. "Microplastics captured by snowfall: A study in Northern Iran." *Science of The Total Environment* 822:153451. doi: <https://doi.org/10.1016/j.scitotenv.2022.153451>.
- Afrin, Sadia, Md Mostafizur Rahman, Md Ahedul Akbor, Md Abu Bakar Siddique, Md Khabir Uddin, and Guilherme Malafaia. 2022. "Is there tea complemented with the appealing flavor of microplastics? A pioneering study on plastic pollution in commercially available tea bags in Bangladesh." *Science of The Total Environment* 837:155833. doi: <https://doi.org/10.1016/j.scitotenv.2022.155833>.
- Al-Azzawi, Mohammed S. M., Simone Kefer, Jana Weißer, Julia Reichel, Christoph Schwaller, Karl Glas, Oliver Knoop, and Jörg E. Drewes. 2020. "Validation of Sample Preparation Methods for Microplastic Analysis in Wastewater Matrices—Reproducibility and Standardization." *Water* 12 (9):2445.
- Al-Kadhemy, Mahasin F. Hadi, Zahraa S. Rasheed, and Sanaa R. Salim. 2016. "Fourier transform infrared spectroscopy for irradiation coumarin doped polystyrene polymer films by alpha ray." *Journal of Radiation Research and Applied Sciences* 9 (3):321-331. doi: <https://doi.org/10.1016/j.jrras.2016.02.004>.
- Back, Henrique de Medeiros, Edson Cilos Vargas Junior, Orestes Estevam Alarcon, and Daphiny Pottmaier. 2022. "Training and evaluating machine learning algorithms for ocean microplastics classification through vibrational spectroscopy." *Chemosphere* 287:131903. doi: <https://doi.org/10.1016/j.chemosphere.2021.131903>.
- Ballabio, Davide, Francesca Grisoni, and Roberto Todeschini. 2018. "Multivariate comparison of classification performance measures." *Chemometrics and Intelligent Laboratory Systems* 174:33-44. doi: <https://doi.org/10.1016/j.chemolab.2017.12.004>.
- Bannick, Claus Gerhard, Regine Szewzyk, Mathias Ricking, Sara Schniegler, Nathan Obermaier, Anne Kathrin Barthel, Korinna Altmann, Paul Eisentraut, and Ulrike Braun. 2019. "Development and testing of a fractionated filtration for sampling of microplastics in water." *Water Research* 149:650-658. doi: <https://doi.org/10.1016/j.watres.2018.10.045>.
- Beer, Irina. 2019. "Identifizierung von Eintragspfaden für Mikropartikel in Getränke: Methodenentwicklung zur Probenahme, -aufbereitung und spektroskopische Untersuchung." Master of Science Master's Thesis, Lehrstuhl für Lebensmittelchemie und molekulare Sensorik, Technical University Munich.
- Belz, Susanne, Ivana Bianchi, Claudia Cella, Hakan Emteborg, Francesco Fumagalli, Otmar Geiss, Douglas Gilliland, Andrea Held, Ulf Jakobsson, Rita La Spina, Dóra Mehn, Yannic Ramaye, Piotr Robouch, John Seghers, Birgit Sokull-Kluettgen, Elzbieta Stefaniak, and Joerg Stroka. 2021. Current status of the quantification of microplastics in water - Results of a JRC/BAM inter-laboratory comparison study on PET in water. Luxembourg.
- Bender, Emily M., Timnit Gebru, Angelina McMillan-Major, and Shmargaret Shmitchell. 2021. "On the Dangers of Stochastic Parrots: Can Language Models Be Too Big?" Proceedings of the 2021 ACM Conference on Fairness, Accountability, and Transparency, Virtual Event, Canada.
- BfR, Bundesinstitut für Risikobewertung. 2022a. BfR Verbrauchermonitor 02 | 2022. Berlin: MKL Druck GmbH & Co. KG, Ostbevern.
- BfR, Bundesinstitut für Risikobewertung. 2022b. Empfehlung XXXVI/1. Koch- und Heißfilterpapiere und Filterschichten. edited by Bundesinstitut für Risikobewertung: Bundesinstitut für Risikobewertung.

- Bolobajev, Juri, Marina Trapido, and Anna Goi. 2015. "Improvement in iron activation ability ofalachlor Fenton-like oxidation by ascorbic acid." *Chemical Engineering Journal* 281:566-574. doi: <https://doi.org/10.1016/j.cej.2015.06.115>.
- Bourdages, Madelaine P. T., Jennifer F. Provencher, Julia E. Baak, Mark L. Mallory, and Jesse C. Vermaire. 2021. "Breeding seabirds as vectors of microplastics from sea to land: Evidence from colonies in Arctic Canada." *Science of The Total Environment* 764:142808. doi: <https://doi.org/10.1016/j.scitotenv.2020.142808>.
- Bowley, Jake, Craig Baker-Austin, Adam Porter, Rachel Hartnell, and Ceri Lewis. 2021. "Oceanic Hitchhikers – Assessing Pathogen Risks from Marine Microplastic." *Trends in Microbiology* 29 (2):107-116. doi: <https://doi.org/10.1016/j.tim.2020.06.011>.
- Braun, Thorsten, Loreen Ehrlich, Wolfgang Henrich, Sebastian Koepfel, Ievgeniia Lomako, Philipp Schwabl, and Bettina Liebmann. 2021. "Detection of Microplastic in Human Placenta and Meconium in a Clinical Setting." *Pharmaceutics* 13 (7):921.
- Braun, Ulrike. 2021. Status Report Analysis of Microplastics. Sampling, preparation and detection methods. edited by Ulf Stein and Hannes Schmitt. Berlin: BMBF research focus "Plastics in the Environment" Cross-cutting issue "analysis and reference materials".
- Breiman, Leo. 2001. "Random Forests." *Machine Learning* 45 (1):5-32.
- Büks, F., G. Kayser, A. Zieger, F. Lang, and M. Kaupenjohann. 2021. "Particles under stress: ultrasonication causes size and recovery rate artifacts with soil-derived POM but not with microplastics." *Biogeosciences* 18 (1):159-167. doi: 10.5194/bg-18-159-2021.
- Busse, Kristin, Ingo Ebner, Hans-Ulrich Humpf, Natalia Ivleva, Andrea Kaepler, Barbara E. Oßmann, and Darena Schymanski. 2020. "Comment on "Plastic Teabags Release Billions of Microparticles and Nanoparticles into Tea"." *Environmental Science & Technology*. doi: 10.1021/acs.est.0c03182.
- Carpenter, Edward J., and K. L. Smith. 1972. "Plastics on the Sargasso Sea Surface." *Science* 175 (4027):1240-1241. doi: 10.1126/science.175.4027.1240.
- Castro, Gleyson B., Aline C. Bernegossi, Fernanda R. Pinheiro, and Juliano J. Corbi. 2022. "The silent harm of polyethylene microplastics: Invertebrates growth inhibition as a warning of the microplastic pollution in continental waters." *Limnologica* 93:125964. doi: <https://doi.org/10.1016/j.limno.2022.125964>.
- Chareoansiri, Rin, and Ratchanee Kongkachuichai. 2009. "Sugar profiles and soluble and insoluble dietary fiber contents of fruits in Thailand markets." *International Journal of Food Sciences and Nutrition* 60 (sup4):126-139. doi: 10.1080/09637480802609376.
- Cole, M., P. Lindeque, E. Fileman, C. Halsband, R. Goodhead, J. Moger, and T. S. Galloway. 2013. "Microplastic ingestion by zooplankton." *Environ Sci Technol* 47 (12):6646-55. doi: 10.1021/es400663f.
- Comnea-Stancu, I. R., K. Wieland, G. Ramer, A. Schwaighofer, and B. Lendl. 2017. "On the Identification of Rayon/Viscose as a Major Fraction of Microplastics in the Marine Environment: Discrimination between Natural and Manmade Cellulosic Fibers Using Fourier Transform Infrared Spectroscopy." *Appl Spectrosc* 71 (5):939-950. doi: 10.1177/0003702816660725.
- Corami, F., B. Rosso, M. Roman, M. Picone, A. Gambaro, and C. Barbante. 2020. "Evidence of small microplastics (<100 µm) ingestion by Pacific oysters (*Crassostrea gigas*): A novel method of extraction, purification, and analysis using Micro-FTIR." *Marine Pollution Bulletin* 160:111606. doi: <https://doi.org/10.1016/j.marpolbul.2020.111606>.
- Cowger, W., A. Gray, S. H. Christiansen, H. DeFrono, A. D. Deshpande, L. Hemabessiere, E. Lee, L. Mill, K. Munno, B. E. Ossmann, M. Pittroff, C. Rochman, G. Sarau, S. Tarby, and S. Primpke. 2020. "Critical Review of Processing and Classification Techniques for Images and Spectra in Microplastic Research." *Applied Spectroscopy* 74 (9):989-1010. doi: 10.1177/0003702820929064.
- Cowger, Win, Zacharias Steinmetz, Andrew Gray, Keenan Munno, Jennifer Lynch, Hannah Hapich, Sebastian Primpke, Hannah De Frono, Chelsea Rochman, and Orestis Herodotou. 2021. "Microplastic Spectral Classification Needs an Open Source

- Community: Open Specy to the Rescue!" *Analytical Chemistry* 93 (21):7543-7548. doi: 10.1021/acs.analchem.1c00123.
- Dawson, Amanda L., Marina F. M. Santana, Michaela E. Miller, and Frederieke J. Kroon. 2021. "Relevance and reliability of evidence for microplastic contamination in seafood: A critical review using Australian consumption patterns as a case study." *Environmental Pollution* 276:116684. doi: <https://doi.org/10.1016/j.envpol.2021.116684>.
- De Frond, Hannah, Ronald Rubinovitz, and Chelsea M. Rochman. 2021. "μATR-FTIR Spectral Libraries of Plastic Particles (FLOPP and FLOPP-e) for the Analysis of Microplastics." *Analytical Chemistry* 93 (48):15878-15885. doi: 10.1021/acs.analchem.1c02549.
- Deutsches Institut für Normung e.V., DIN. 2022. DIN/TS 10068 Vornorm: 2022-09. Food - Lebensmittel - Bestimmung von Mikroplastik - Analytische Verfahren; Text Englisch Berlin: Beuth Verlag GmbH.
- Dimante-Deimantovica, Inta, Natalija Suhareva, Marta Barone, Ieva Putna-Nimane, and Juris Aigars. 2022. "Hide-and-see: Threshold values and contribution towards better understanding of recovery rate in microplastic research." *MethodsX* 9:101603. doi: <https://doi.org/10.1016/j.mex.2021.101603>.
- Dominghaus, Hans. 2012. *Kunststoffe Eigenschaften und Anwendungen*. 8 ed. Vol. 8. Heidelberg: Springer.
- Dunkel, Sandy Sylwestra. 2018. "Isolation von Mikroplastikpartikeln aus Lebensmitteln: Erprobung mechanisch-physikalischer Trennmethode in Ergänzung zu chemisch-enzymatischem Matrixabbau." B.Sc. Bachelor's Thesis, Chair of Food Chemistry and Molecular Sensory Science, Technical University Munich.
- Eberl, Theresa. 2020. "Vorkommen von Mikroplastik in hausgemachtem und industriell hergestelltem Apfelmus." B.Sc. Bachelor's Thesis, Chair of Food Chemistry and Molecular Sensory Science, Technical University of Munich.
- Eitzen, Lars, Sophia Paul, Ulrike Braun, Korinna Altmann, Martin Jekel, and Aki Sebastian Ruhl. 2019. "The challenge in preparing particle suspensions for aquatic microplastic research." *Environmental Research* 168:490-495. doi: <https://doi.org/10.1016/j.envres.2018.09.008>.
- Eriksson, Cecilia, and Harry Burton. 2003. "Origins and Biological Accumulation of Small Plastic Particles in Fur Seals from Macquarie Island." *AMBIO: A Journal of the Human Environment* 32 (6):380-384. doi: 10.1579/0044-7447-32.6.380.
- Ertel, Wolfgang. 2017. "Machine Learning and Data Mining." In *Introduction to Artificial Intelligence*, 175-243. Cham: Springer International Publishing.
- Esch, Elisabeth von der, Alexander Kohles, Philipp M. Anger, R. Hoppe, R. Niessner, M. Elsner, and N. Ivleva. 2020. "TUM-ParticleTyper: A detection and quantification tool for automated analysis of (Microplastic) particles and fibers." *PLoS ONE* 15.
- European Chemicals Agency, ECHA. 2018. "Microplastics." ECHA, European Chemicals Agency, accessed 01-05-2022. <https://echa.europa.eu/en/hot-topics/microplastics>.
- Fenton, H. J. H. 1894. "LXXIII.—Oxidation of tartaric acid in presence of iron." *Journal of the Chemical Society, Transactions* 65 (0):899-910. doi: 10.1039/CT8946500899.
- Fournier, Sara B., Jeanine N. D'Errico, Derek S. Adler, Stamatina Kollontzi, Michael J. Goedken, Laura Fabris, Edward J. Yurkow, and Phoebe A. Stapleton. 2020. "Nanopolystyrene translocation and fetal deposition after acute lung exposure during late-stage pregnancy." *Particle and Fibre Toxicology* 17 (1):55. doi: 10.1186/s12989-020-00385-9.
- Gray, Austin D., and John E. Weinstein. 2017. "Size- and shape-dependent effects of microplastic particles on adult daggerblade grass shrimp (*Palaemonetes pugio*)." *Environmental Toxicology and Chemistry* 36 (11):3074-3080. doi: <https://doi.org/10.1002/etc.3881>.
- Günzler, Helmut, and Hans-Ulrich Gremlich. 2003a. "Absorption und Molekülbau." In *IR - Spektroskopie*, 9-37. WILEY-VCH.
- Günzler, Helmut, and Hans-Ulrich Gremlich. 2003b. "Das Spektrometer." In *IR - Spektroskopie*, 39-71. WILEY-VCH.

- Günzler, Helmut, and Hans-Ulrich Gremlich. 2003c. "Einführung." In *IR - Spektroskopie*, 1-8. WILEY-VCH.
- Günzler, Helmut, and Hans-Ulrich Gremlich. 2003d. "Spezielle Untersuchungstechniken." In *IR - Spektroskopie*, 117-155. WILEY-VCH.
- Habib, Rana Zeeshan, Vijo Poulouse, Rana Alsaidi, Ruwaya al Kendi, Syed Haris Iftikhar, Abdel-Hamid Ismail Mourad, Wajeeh Fares Kittaneh, and Thies Thiemann. 2022. "Plastic cutting boards as a source of microplastics in meat." *Food Additives & Contaminants: Part A*:1-11. doi: 10.1080/19440049.2021.2017002.
- Hale, Robert C., Meredith E. Seeley, Mark J. La Guardia, Lei Mai, and Eddy Y. Zeng. 2020. "A Global Perspective on Microplastics." *Journal of Geophysical Research: Oceans* 125 (1):e2018JC014719. doi: <https://doi.org/10.1029/2018JC014719>.
- Hartmann, Nanna B., Thorsten Hüffer, Richard C. Thompson, Martin Hassellöv, Anja Verschoor, Anders E. Daugaard, Sinja Rist, Therese Karlsson, Nicole Brennholt, Matthew Cole, Maria P. Herrling, Maren C. Hess, Natalia P. Ivleva, Amy L. Lusher, and Martin Wagner. 2019. "Are We Speaking the Same Language? Recommendations for a Definition and Categorization Framework for Plastic Debris." *Environmental Science & Technology* 53 (3):1039-1047. doi: 10.1021/acs.est.8b05297.
- Hernandez, Laura M., Elvis Genbo Xu, Hans C. E. Larsson, Rui Tahara, Vimal B. Maisuria, and Nathalie Tufenkji. 2019. "Plastic Teabags Release Billions of Microparticles and Nanoparticles into Tea." *Environmental Science & Technology*. doi: 10.1021/acs.est.9b02540.
- Hou, Xiaojing, Xiaopeng Huang, Mengliang Li, Yunshang Zhang, Songhu Yuan, Zhihui Ai, Jincan Zhao, and Lizhi Zhang. 2018. "Fenton oxidation of organic contaminants with aquifer sediment activated by ascorbic acid." *Chemical Engineering Journal* 348:255-262. doi: <https://doi.org/10.1016/j.cej.2018.05.015>.
- Hu, Jinguang, Valdeir Arantes, and Jack N. Saddler. 2011. "The enhancement of enzymatic hydrolysis of lignocellulosic substrates by the addition of accessory enzymes such as xylanase: is it an additive or synergistic effect?" *Biotechnology for Biofuels* 4:36-36. doi: 10.1186/1754-6834-4-36.
- Hubin, Chloé. 2020. "Analysis of microplastics in bread." B.Sc. Bachelor's Thesis, Chair of Food Chemistry and Molecular Sensory Science, Technical University of Munich.
- Hufnagl, Benedikt, Dieter Steiner, Elisabeth Renner, Martin G. J. Löder, Christian Laforsch, and Hans Lohninger. 2019. "A methodology for the fast identification and monitoring of microplastics in environmental samples using random decision forest classifiers." *J. Anal. Meth.* 11 (17):2277-2285. doi: 10.1039/C9AY00252A.
- Hufnagl, Benedikt, and Michael Stibi. 2019. The Bayreuth Particle Finder: computer-assisted analysis of microplastics based on  $\mu$ FTIR imaging. edited by Vienna University of Technology.
- Hufnagl, Benedikt, Michael Stibi, Heghnar Martirosyan, Ursula Wilczek, Julia N. Möller, Martin G. J. Löder, Christian Laforsch, and Hans Lohninger. 2022. "Computer-Assisted Analysis of Microplastics in Environmental Samples Based on  $\mu$ FTIR Imaging in Combination with Machine Learning." *Environmental Science & Technology Letters* 9 (1):90-95. doi: 10.1021/acs.estlett.1c00851.
- Huppertsberg, Sven, and Thomas P. Knepper. 2018. "Instrumental analysis of microplastics—benefits and challenges." *Analytical and Bioanalytical Chemistry* 410 (25):6343-6352. doi: 10.1007/s00216-018-1210-8.
- Hurley, Rachel R., Amy L. Lusher, Marianne Olsen, and Luca Nizzetto. 2018. "Validation of a Method for Extracting Microplastics from Complex, Organic-Rich, Environmental Matrices." *Environmental Science & Technology* 52 (13):7409-7417. doi: 10.1021/acs.est.8b01517.
- Imhof, Hannes K., Johannes Schmid, Reinhard Niessner, Natalia P. Ivleva, and Christian Laforsch. 2012. "A novel, highly efficient method for the separation and quantification of plastic particles in sediments of aquatic environments." *Limnology and Oceanography: Methods* 10 (7):524-537. doi: <https://doi.org/10.4319/lom.2012.10.524>.

- International Organization for Standardization, ISO. 2021a. DIN CEN ISO/TR 21960. Plastics – Environmental aspects – State of knowledge and methodologies. Beuth Verlag GmbH.
- International Organization for Standardization, ISO. 2021b. ISO/DIS 4484-1. Textiles and textile products – Microplastics from textile sources –Part 1: Determination of material loss from fabrics during washing. Beuth Verlag GmbH.
- International Organization for Standardization, ISO. 2021c. ISO/DIS 24187:2021(E). Principles for the analysis of plastics and microplastics present in the environment. Berlin: Beuth Verlag.
- International Organization for Standardization, ISO. 2022a. ISO/NP 16094-2: Water quality — Analysis of plastics in water — Part 2: Water quality — Analysis of plastics in water — Part 2: Method using vibrational spectroscopy. Berlin: Beuth Verlag GmbH.
- International Organization for Standardization, ISO. 2022b. ISO/NP 16094-3. Water quality — Analysis of plastics in water — Part 3: Thermo-analytical methods for waters with low content of natural suspended solids. Berlin: Beuth Verlag GmbH.
- International Organization for Standardization, ISO. 2021d. ISO/NP 5667-27. Water quality – Sampling – Part 27: Guidance on sampling of microplastics in water: drinking water, surface waters, freshwater, seawater, wastewater-treated effluents, and untreated wastewater. Berlin: Beuth Verlag GmbH.
- International Organization for Standardization, ISO. 2022c. ISO/NP 16094-1: Water quality — Analysis of plastics in water — Part 1: General and sampling. Berlin: Beuth Verlag GmbH.
- Jani, Praful, Gavin W Halbert, John Langridge, and Alexander T Florence. 2011. "Nanoparticle Uptake by the Rat Gastrointestinal Mucosa: Quantitation and Particle Size Dependency." *Journal of Pharmacy and Pharmacology* 42 (12):821-826. doi: 10.1111/j.2042-7158.1990.tb07033.x.
- Japkowicz, Nathalie, and Shaju Stephen. 2002. "The class imbalance problem: A systematic study." *Intelligent Data Analysis* 6:429-449. doi: 10.3233/IDA-2002-6504.
- Je Yoo, Young, Yan Feng, Yong-Hwan Kim, and Camila Flor J. Yagonia. 2017. "Fundamentals of Enzyme Engineering." In: Springer Dordrecht. <https://doi.org/10.1007/978-94-024-1026-6>.
- Jung, Melissa R., F. David Horgen, Sara V. Orski, Viviana Rodriguez C, Kathryn L. Beers, George H. Balazs, T. Todd Jones, Thierry M. Work, Kayla C. Brignac, Sarah-Jeanne Royer, K. David Hyrenbach, Brenda A. Jensen, and Jennifer M. Lynch. 2018. "Validation of ATR FT-IR to identify polymers of plastic marine debris, including those ingested by marine organisms." *Marine Pollution Bulletin* 127:704-716. doi: <https://doi.org/10.1016/j.marpolbul.2017.12.061>.
- Kalogerakis, Nicolas. 2022. "Microplastics-A New Journal on the Environmental Challenges and Adverse Health Effects of Microplastics." *Microplastics* 1 (1):1-2.
- Käppler, Andrea, Frank Windrich, Martin G.J. Löder, Mikhail Melanin, Dieter Fischer, Matthias Labrenz, Klaus-Jochen Eichhorn, and Brigitte Voit. 2015. "Identification of microplastics by FTIR and Raman microscopy: a novel silicon filter substrate opens the important spectral range below 1300 cm<sup>-1</sup> for FTIR transmission measurements." *Anal Bioanal Chem* 407 (22):6791-801. doi: 10.1007/s00216-015-8850-8.
- Kedzierski, Mikaël, Mathilde Falcou-Préfol, Marie Emmanuelle Kerros, Maryvonne Henry, Maria Luiza Pedrotti, and Stéphane Bruzaud. 2019. "A machine learning algorithm for high throughput identification of FTIR spectra: Application on microplastics collected in the Mediterranean Sea." *Chemosphere* 234:242-251. doi: <https://doi.org/10.1016/j.chemosphere.2019.05.113>.
- Kedzierski, Mikaël, Benjamin Lechat, Olivier Sire, Gwénaél Le Maguer, Véronique Le Tilly, and Stéphane Bruzaud. 2020. "Microplastic contamination of packaged meat: Occurrence and associated risks." *Food Packaging and Shelf Life* 24:100489. doi: <https://doi.org/10.1016/j.fpsl.2020.100489>.
- Koelmans, Albert A., Nur Hazimah Mohamed Nor, Enya Hermsen, Merel Kooi, Svenja M. Mintenig, and Jennifer De France. 2019. "Microplastics in Freshwaters and Drinking

- Water: Critical Review and Assessment of Data Quality." *Water Research*. doi: <https://doi.org/10.1016/j.watres.2019.02.054>.
- Kooi, Merel, and Albert A. Koelmans. 2019. "Simplifying Microplastic via Continuous Probability Distributions for Size, Shape, and Density." *Environmental Science & Technology Letters*. doi: 10.1021/acs.estlett.9b00379.
- Lachenmeier, Dirk W., Jelena Kocareva, Daniele Noack, and Thomas Kuballa. 2015. "Microplastic identification in German beer – an artefact of laboratory contamination?" *Deutsche Lebensmittel-Rundschau: Zeitschrift für Lebensmittelkunde und Lebensmittelrecht* 111:437-440.
- Lasch, Peter, and Dieter Naumann. 2006. "Spatial resolution in infrared microspectroscopic imaging of tissues." *Biochimica et Biophysica Acta (BBA) - Biomembranes* 1758 (7):814-829. doi: <https://doi.org/10.1016/j.bbamem.2006.06.008>.
- Lenz, Robin, and Matthias Labrenz. 2018. "Small Microplastic Sampling in Water: Development of an Encapsulated Filtration Device." *Water* 10 (8). doi: 10.3390/w10081055.
- Lerch, Carolin. 2020. Sample preparation and data mining in beverage samples for microplastic analysis through  $\mu$ FTIR. In *Research Internship Report*. Chair of Food Chemistry and Molecular Sensory Science, Technical University of Munich.
- Leslie, Heather A., Martin J. M. van Velzen, Sicco H. Brandsma, A. Dick Vethaak, Juan J. Garcia-Vallejo, and Marja H. Lamoree. 2022. "Discovery and quantification of plastic particle pollution in human blood." *Environment International* 163:107199. doi: <https://doi.org/10.1016/j.envint.2022.107199>.
- Leslie, Heather. A., and Michael H. Depledge. 2020. "Where is the evidence that human exposure to microplastics is safe?" *Environment International* 142:105807. doi: <https://doi.org/10.1016/j.envint.2020.105807>.
- Li, Chengjun, Yan Gao, Shuai He, Hai-Yuan Chi, Ze-Chen Li, Xiao-Xia Zhou, and Bing Yan. 2021. "Quantification of Nanoplastic Uptake in Cucumber Plants by Pyrolysis Gas Chromatography/Mass Spectrometry." *Environmental Science & Technology Letters* 8 (8):633-638. doi: 10.1021/acs.estlett.1c00369.
- Li, Dunzhu, Yunhong Shi, Luming Yang, Liwen Xiao, Daniel K. Kehoe, Yurii K. Gun'ko, John J. Boland, and Jing Jing Wang. 2020. "Microplastic release from the degradation of polypropylene feeding bottles during infant formula preparation." *Nature Food*. doi: 10.1038/s43016-020-00171-y.
- Liebezeit, Gerd, and Elisabeth Liebezeit. 2013. "Non-pollen particulates in honey and sugar." *Food Additives & Contaminants Part A* (30:12):2136-2140. doi: 10.1080/19440049.2013.843025.
- Liebezeit, Gerd, and Elisabeth Liebezeit. 2014. "Synthetic particles as contaminants in German beers." *Food Addit Contam Part A Chem Anal Control Expo Risk Assess* 31 (9):1574-8. doi: 10.1080/19440049.2014.945099.
- Liebezeit, Gerd, and Elisabeth Liebezeit. 2015. "Origin of Synthetic Particles in Honeys." *Polish Journal of Food and Nutrition Sciences* 65 (2). doi: 10.1515/pjfn-2015-0025.
- Lipke, Peter N., and Rafael Ovalle. 1998. "Cell Wall Architecture in Yeast: New Structure and New Challenges." *Journal of Bacteriology* 180 (15):3735-3740. doi: 10.1128/JB.180.15.3735-3740.1998.
- Liu, Fan, Kristina Borg Olesen, Amelia Reimer Borregaard, and Jes Vollertsen. 2019. "Microplastics in urban and highway stormwater retention ponds." *Science of The Total Environment* 671:992-1000. doi: <https://doi.org/10.1016/j.scitotenv.2019.03.416>.
- Löder, Martin G. J., Hannes K. Imhof, Maïke Ladehoff, Lena A. Löschel, Claudia Lorenz, Svenja Mintenig, Sarah Piehl, Sebastian Primpke, Isabella Schrank, Christian Laforsch, and Gunnar Gerdts. 2017. "Enzymatic purification of microplastics in environmental samples." *Environmental Science & Technology* (51):14283-14292. doi: 10.1021/acs.est.7b03055.
- Löder, Martin G. J., Mirco Kuczera, Svenja Mintenig, Claudia Lorenz, and Gunnar Gerdts. 2015. "Focal plane array detector-based micro-Fourier-transform infrared imaging for

- the analysis of microplastics in environmental samples." *Environmental Chemistry* 12 (5):563-581. doi: <http://dx.doi.org/10.1071/EN14205>.
- Lopez-Vazquez, J., R. Rodil, M. J. Trujillo-Rodriguez, J. B. Quintana, R. Cela, and M. Miro. 2022. "Mimicking human ingestion of microplastics: Oral bioaccessibility tests of bisphenol A and phthalate esters under fed and fasted states." *Science of the Total Environment* 826:9. doi: 10.1016/j.scitotenv.2022.154027.
- Lusher, A. L., K. Munno, L. Hermabessiere, and S. Carr. 2020. "Isolation and Extraction of Microplastics from Environmental Samples: An Evaluation of Practical Approaches and Recommendations for Further Harmonization." *Applied Spectroscopy* 74 (9):1049-1065. doi: 10.1177/0003702820938993.
- Magri, Davide, Paola Sánchez-Moreno, Gianvito Caputo, Francesca Gatto, Marina Veronesi, Giuseppe Bardi, Tiziano Catelani, Daniela Guarnieri, Athanassia Athanassiou, Pier Paolo Pompa, and Despina Fragouli. 2018. "Laser Ablation as a Versatile Tool To Mimic Polyethylene Terephthalate Nanoplastic Pollutants: Characterization and Toxicology Assessment." *ACS Nano* 12 (8):7690-7700. doi: 10.1021/acsnano.8b01331.
- Masura, Julie, Joel Baker, Gregory Foster, and Courtney Arthur. 2015. "Laboratory Methods for the Analysis of Microplastics in the Marine Environment: Recommendations for quantifying synthetic particles in waters and sediments." *NOAA Technical Memorandum NOS-OR&R-48*.
- Microbeads in Toiletries Regulations. 2017. SOR/2017-111, CANADIAN ENVIRONMENTAL PROTECTION ACT, Microbeads in Toiletries Regulations. edited by Government of Canada.
- Mintenig, S. M., M. G. J. Löder, S. Primpke, and G. Gerds. 2019. "Low numbers of microplastics detected in drinking water from ground water sources." *Sci Total Environ* 648:631-635. doi: 10.1016/j.scitotenv.2018.08.178.
- Mintenig, S.M., I. Int-Veen, M.G.J. Löder, S. Primpke, and G. Gerds. 2017. "Identification of microplastic in effluents of waste water treatment plants using focal plane array-based micro-Fourier-transform infrared imaging." *Water Research* 108:365-372. doi: <http://dx.doi.org/10.1016/j.watres.2016.11.015>.
- Monteiro, Silvia S., Teresa Rocha-Santos, Joana C. Prata, Armando C. Duarte, Ana Violeta Girão, Pedro Lopes, Tiago Cristovão, and João Pinto da Costa. 2022. "A straightforward method for microplastic extraction from organic-rich freshwater samples." *Science of The Total Environment* 815:152941. doi: <https://doi.org/10.1016/j.scitotenv.2022.152941>.
- Morgado, Vanessa, Luís Gomes, Ricardo J. N. Bettencourt da Silva, and Carla Palma. 2021. "Validated spreadsheet for the identification of PE, PET, PP and PS microplastics by micro-ATR-FTIR spectra with known uncertainty." *Talanta* 234:122624. doi: <https://doi.org/10.1016/j.talanta.2021.122624>.
- Morgado, Vanessa, Carla Palma, and Ricardo J. N. Bettencourt da Silva. 2020. "Microplastics identification by infrared spectroscopy – Evaluation of identification criteria and uncertainty by the Bootstrap method." *Talanta*:121814. doi: <https://doi.org/10.1016/j.talanta.2020.121814>.
- Müller, Michelle. 2020. "Mikroplastik in Tee." B.Sc. Bachelor's thesis, Chair of Food Chemistry and Molecular Sensory Science, Technical University of Munich.
- Munno, Keenan, Hannah De Frond, Bridget O'Donnell, and Chelsea M. Rochman. 2020. "Increasing the Accessibility for Characterizing Microplastics: Introducing New Application-Based and Spectral Libraries of Plastic Particles (SLoPP and SLoPP-E)." *J. Anal. Chem.* 92 (3):2443-2451. doi: 10.1021/acs.analchem.9b03626.
- Oßmann, Barbara E. 2020. "Determination of microparticles, in particular microplastics in beverages." Dr. rer. nat. Dissertation, Naturwissenschaftliche Fakultät, Friedrich-Alexander-Universität Erlangen-Nürnberg.
- Oßmann, Barbara E. 2021. "Microplastics in drinking water? Present state of knowledge and open questions." *Current Opinion in Food Science*. doi: <https://doi.org/10.1016/j.cofs.2021.02.011>.

- Oßmann, Barbara E., George Sarau, Heinrich Holtmannspotter, Monika Pischetsrieder, Silke H. Christiansen, and Wilhelm Dicke. 2018. "Small-sized microplastics and pigmented particles in bottled mineral water." *Water Res* 141:307-316. doi: 10.1016/j.watres.2018.05.027.
- Oßmann, Barbara E., Darena Schymanski, Natalia P. Ivleva, Dieter Fischer, Franziska Fischer, Gerald Dallmann, and Frank Welle. 2019. "Comment on "exposure to microplastics (<10 µm) associated to plastic bottles mineral water consumption: The first quantitative study by Zuccarello et al. [Water Research 157 (2019) 365–371]".  
*Water Research* 162:516-517. doi: <https://doi.org/10.1016/j.watres.2019.06.032>.
- Paul, Maxi B., Valerie Stock, Julia Cara-Carmona, Elisa Lisicki, Sofiya Shopova, Valérie Fessard, Albert Braeuning, Holger Sieg, and Linda Böhmert. 2020. "Micro- and nanoplastics – current state of knowledge with the focus on oral uptake and toxicity." *Nanoscale Advances* 2 (10):4350-4367. doi: 10.1039/D0NA00539H.
- Peixoto, Diogo, Carlos Pinheiro, João Amorim, Luís Oliva-Teles, Lúcia Guilhermino, and Maria Natividade Vieira. 2019. "Microplastic pollution in commercial salt for human consumption: A review." *Estuarine, Coastal and Shelf Science* 219:161-168. doi: <https://doi.org/10.1016/j.ecss.2019.02.018>.
- Pérez-Guevara, Fermín, Priyadarsi D. Roy, Gurusamy Kuttralam-Muniasamy, and V. C. Shruti. 2022. "Coverage of microplastic data underreporting and progress toward standardization." *Science of The Total Environment* 829:154727. doi: <https://doi.org/10.1016/j.scitotenv.2022.154727>.
- Pivokonský, Martin, Lenka Pivokonská, Kateřina Novotná, Lenka Čermáková, and Martina Klimtová. 2020. "Occurrence and fate of microplastics at two different drinking water treatment plants within a river catchment." *Science of The Total Environment* 741:140236. doi: <https://doi.org/10.1016/j.scitotenv.2020.140236>.
- Plastics Europe's Market Research and Statistics Group, PEMRG. 2021. *Plastics - the Facts 2021*.
- Primpke, Sebastian, Silke H. Christiansen, Win Cowger, Hannah De Frond, Ashok Deshpande, Marten Fischer, Erika B. Holland, Michaela Meyns, Bridget A. O'Donnell, Barbara E. Ossmann, Marco Pittroff, George Sarau, Barbara M. Scholz-Böttcher, and Kara J. Wiggan. 2020. "Critical Assessment of Analytical Methods for the Harmonized and Cost-Efficient Analysis of Microplastics." *Applied Spectroscopy* 74 (9):1012-1047. doi: 10.1177/0003702820921465.
- Primpke, Sebastian, Richard K. Cross, Svenja M. Mintenig, Marta Simon, Alvis Vianello, Gunnar Gerds, and Jes Vollertsen. 2020. "Toward the Systematic Identification of Microplastics in the Environment: Evaluation of a New Independent Software Tool (siMPle) for Spectroscopic Analysis." *Applied Spectroscopy* 74 (9):1127-1138. doi: 10.1177/0003702820917760.
- Primpke, Sebastian, Philippe A. Dias, and Gunnar Gerds. 2019. "Automated identification and quantification of microfibrils and microplastics." *Analytical Methods* 11 (16):2138-2147. doi: 10.1039/C9AY00126C.
- Primpke, Sebastian, Marten Fischer, Claudia Lorenz, Gunnar Gerds, and Barbara M. Scholz-Böttcher. 2020. "Comparison of pyrolysis gas chromatography/mass spectrometry and hyperspectral FTIR imaging spectroscopy for the analysis of microplastics." *Analytical and Bioanalytical Chemistry*. doi: 10.1007/s00216-020-02979-w.
- Primpke, Sebastian, Matthias Godejohann, and Gunnar Gerds. 2020. "Rapid Identification and Quantification of Microplastics in the Environment by Quantum Cascade Laser-Based Hyperspectral Infrared Chemical Imaging." *Environmental Science & Technology*. doi: 10.1021/acs.est.0c05722.
- Primpke, Sebastian, C. Lorenz, R. Rascher-Friesenhausen, and Gunnar Gerds. 2017. "An automated approach for microplastics analysis using focal plane array (FPA) FTIR microscopy and image analysis." *Analytical Methods* 9 (9):1499-1511. doi: 10.1039/C6AY02476A.
- Primpke, Sebastian, Marisa Wirth, Claudia Lorenz, and Gunnar Gerds. 2018. "Reference database design for the automated analysis of microplastic samples based on Fourier

- transform infrared (FTIR) spectroscopy." *Analytical and Bioanalytical Chemistry* 410 (21):5131-5141. doi: 10.1007/s00216-018-1156-x.
- Ragusa, Antonio, Alessandro Svelato, Criselda Santacroce, Piera Catalano, Valentina Notarstefano, Oliana Carnevali, Fabrizio Papa, Mauro Ciro Antonio Rongioletti, Federico Baiocco, Simonetta Draghi, Elisabetta D'Amore, Denise Rinaldo, Maria Matta, and Elisabetta Giorgini. 2021. "Plasticenta: First evidence of microplastics in human placenta." *Environment International* 146:106274. doi: <https://doi.org/10.1016/j.envint.2020.106274>.
- Ramsperger, A. F. R. M., J. Jasinski, M. Völkl, T. Witzmann, M. Meinhart, V. Jérôme, W. P. Kretschmer, R. Freitag, J. Senker, A. Fery, H. Kress, T. Scheibel, and C. Laforsch. 2022. "Supposedly identical microplastic particles substantially differ in their material properties influencing particle-cell interactions and cellular responses." *Journal of Hazardous Materials* 425:127961. doi: <https://doi.org/10.1016/j.jhazmat.2021.127961>.
- Renner, Gerrit, Alexander Nellessen, Alexander Schwiers, Mike Wenzel, Torsten C. Schmidt, and Jürgen Schram. 2019. "Data preprocessing & evaluation used in the microplastics identification process: A critical review & practical guide." *TrAC Trends in Analytical Chemistry* 111:229-238. doi: <https://doi.org/10.1016/j.trac.2018.12.004>.
- Renner, Gerrit, Philipp Sauerbier, Torsten C. Schmidt, and Jürgen Schram. 2019. "Robust Automatic Identification of Microplastics in Environmental Samples Using FTIR Microscopy." *J. Anal. Chem.* 91 (15):9656-9664. doi: 10.1021/acs.analchem.9b01095.
- Renner, Gerrit, Torsten C. Schmidt, and Jürgen Schram. 2017. "Characterization and Quantification of Microplastics by Infrared Spectroscopy." In *Comprehensive Analytical Chemistry*, 67-118. Elsevier B.V.
- Renzi, Monia, and Andrea Blašković. 2018. "Litter & microplastics features in table salts from marine origin: Italian versus Croatian brands." *Marine Pollution Bulletin* 135:62-68. doi: <https://doi.org/10.1016/j.marpolbul.2018.06.065>.
- Ritchie, Hannah, and Max Roser. 2018. Plastic Pollution. online: OurWorldInData.org.
- Rochman, Chelsea M., Akbar Tahir, Susan L. Williams, Dolores V. Baxa, Rosalyn Lam, Jeffrey T. Miller, Foo-Ching Teh, Shinta Werorilangi, and Swee J. Teh. 2015. "Anthropogenic debris in seafood: Plastic debris and fibers from textiles in fish and bivalves sold for human consumption." *Scientific Reports* 5 (1):14340. doi: 10.1038/srep14340.
- Schwabl, Philipp, Sebastian Köppel, Philipp Königshofer, Theresa Bucsis, Michael Trauner, Thomas Reiberger, and Bettina Liebmann. 2019. "Detection of Various Microplastics in Human Stool." *Annals of Internal Medicine* 171 (7):453-457. doi: 10.7326/m19-0618
- Schymanski, Darena, Christophe Goldbeck, Hans-Ulrich Humpf, and Peter Fürst. 2018. "Analysis of microplastics in water by micro-Raman spectroscopy: Release of plastic particles from different packaging into mineral water." *Water Res* 129:154-162.
- Schymanski, Darena, Barbara E. Oßmann, Nizar Benismail, Kada Boukerma, Gerald Dallmann, Elisabeth von der Esch, Dieter Fischer, Franziska Fischer, Douglas Gilliland, Karl Glas, Thomas Hofmann, Andrea Käßler, Silvia Lacorte, Julie Marco, Maria E. L. Rakwe, Jana Weisser, Cordula Witzig, Nicole Zumbülte, and Natalia P. Ivleva. 2021. "Analysis of microplastics in drinking water and other clean water samples with micro-Raman and micro-infrared spectroscopy: minimum requirements and best practice guidelines." *Analytical and Bioanalytical Chemistry* 413:5969-5994. doi: 10.1007/s00216-021-03498-y.
- Seghers, John, Elzbieta A. Stefaniak, Rita La Spina, Claudia Cella, Dora Mehn, Douglas Gilliland, Andrea Held, Ulf Jacobsson, and Håkan Emteborg. 2021. "Preparation of a reference material for microplastics in water—evaluation of homogeneity." *Analytical and Bioanalytical Chemistry*. doi: 10.1007/s00216-021-03198-7.
- Shruti, V. C., Fermín Pérez-Guevara, I. Elizalde-Martínez, and Gurusamy Kutralam-Muniasamy. 2020. "First study of its kind on the microplastic contamination of soft drinks, cold tea and energy drinks - Future research and environmental considerations." *Science of The Total Environment* 726:138580. doi: <https://doi.org/10.1016/j.scitotenv.2020.138580>.

- Simon, Márta, Nikki van Alst, and Jes Vollertsen. 2018. "Quantification of microplastic mass and removal rates at wastewater treatment plants applying Focal Plane Array (FPA)-based Fourier Transform Infrared (FT-IR) imaging." *Water Research*. doi: 10.1016/j.watres.2018.05.019.
- Skansi, Sandro. 2018. "Machine Learning Basics." In *Introduction to Deep Learning: From Logical Calculus to Artificial Intelligence*, 51-77. Cham: Springer International Publishing.
- Sobhani, Zahra, Yongjia Lei, Youhong Tang, Liwei Wu, Xian Zhang, Ravi Naidu, Mallavarapu Megharaj, and Cheng Fang. 2020. "Microplastics generated when opening plastic packaging." *Scientific Reports* 10 (1):4841. doi: 10.1038/s41598-020-61146-4.
- Song, Young Kyoung, Sang Hee Hong, Mi Jang, Gi Myung Han, Manvir Rani, Jongmyoung Lee, and Won Joon Shim. 2015. "A comparison of microscopic and spectroscopic identification methods for analysis of microplastics in environmental samples." *Marine Pollution Bulletin* 93 (1-2):202-209. doi: 10.1016/j.marpolbul.2015.01.015.
- Stuart, Barbara H. 2004. *Infrared Spectroscopy: Fundamentals and Applications, Analytical Techniques in the Sciences*. Est Sussex, England: John Wiley & Sons, Ltd.
- Süssmann, Julia, Torsten Krause, Dierk Martin, Elke Walz, Ralf Greiner, Sascha Rohn, Elke Kerstin Fischer, and Jan Fritsche. 2021. "Evaluation and optimisation of sample preparation protocols suitable for the analysis of plastic particles present in seafood." *Food Control* 125:107969. doi: <https://doi.org/10.1016/j.foodcont.2021.107969>.
- Tagg, Alexander S., J. P. Harrison, Yon Ju-Nam, Melanie Sapp, E. L. Bradley, C. J. Sinclair, and Jesus Ojeda. 2017. "Fenton's reagent for the rapid and efficient isolation of microplastics from wastewater." *Chemical Communications* 53 (2):372-375. doi: 10.1039/C6CC08798A.
- Tang, Kuok Ho Daniel. 2021. "Interactions of Microplastics with Persistent Organic Pollutants and the Ecotoxicological Effects: A Review." *Tropical Aquatic and Soil Pollution* 1 (1):24-34. doi: 10.53623/tasp.v1i1.11.
- Tin Kam, Ho. 1998. "The random subspace method for constructing decision forests." *IEEE Transactions on Pattern Analysis and Machine Intelligence* 20 (8):832-844. doi: 10.1109/34.709601.
- Vianello, Alvise, Rasmus L. Jensen, Li Liu, and Jes Vollertsen. 2019. "Simulating human exposure to indoor airborne microplastics using a Breathing Thermal Manikin." *Scientific Reports* 9 (1):8670. doi: 10.1038/s41598-019-45054-w.
- Vinay Kumar, B. N., Lena A. Löschel, Hannes K. Imhof, Martin G. J. Löder, and Christian Laforsch. 2021. "Analysis of microplastics of a broad size range in commercially important mussels by combining FTIR and Raman spectroscopy approaches." *Environmental Pollution* 269:116147. doi: <https://doi.org/10.1016/j.envpol.2020.116147>.
- von der Esch, Elisabeth, Maria Lanzinger, Alexander J. Kohles, Christian Schwaferts, Jana Weisser, Thomas Hofmann, Karl Glas, Martin Elsner, and Natalia P. Ivleva. 2020. "Simple Generation of Suspensible Secondary Microplastic Reference Particles via Ultrasound Treatment." *Frontiers in Chemistry* 8. doi: 10.3389/fchem.2020.00169.
- Wander, Lukas, Alvise Vianello, Jes Vollertsen, Frank Westad, Ulrike Braun, and Andrea Paul. 2020. "Exploratory analysis of hyperspectral FTIR data obtained from environmental microplastics samples." *Anal. Meth.* 12 (6):781-791. doi: 10.1039/C9AY02483B.
- Wang, Feng, Zhongping Lai, Guyu Peng, Lan Luo, Kai Liu, Xianmei Huang, Yantian Xu, Qijing Shen, and Daoji Li. 2021. "Microplastic abundance and distribution in a Central Asian desert." *Science of The Total Environment* 800:149529. doi: <https://doi.org/10.1016/j.scitotenv.2021.149529>.
- Wang, Zhan, Stephen E. Taylor, Prabhakar Sharma, and Markus Flury. 2018. "Poor extraction efficiencies of polystyrene nano- and microplastics from biosolids and soil." *PLOS ONE* 13 (11):e0208009. doi: 10.1371/journal.pone.0208009.
- Way, Chloe, Malcolm D. Hudson, Ian D. Williams, and G. John Langley. 2022. "Evidence of underestimation in microplastic research: A meta-analysis of recovery rate studies."

- Science of The Total Environment* 805:150227. doi: <https://doi.org/10.1016/j.scitotenv.2021.150227>.
- Weber, F., J. Kerpen, S. Wolff, R. Langer, and V. Eschweiler. 2020. "Investigation of microplastics contamination in drinking water of a German city." *Science of the Total Environment* 755. doi: 10.1016/j.scitotenv.2020.143421.
- Weisser, Jana, Irina Beer, Benedikt Hufnagl, Thomas Hofmann, Hans Lohninger, Natalia P. Ivleva, and Karl Glas. 2021. "From the Well to the Bottle: Identifying Sources of Microplastics in Mineral Water." *Water* 13 (6):841.
- Weisser, Jana, Teresa Pohl, Michael Heinzinger, Natalia P. Ivleva, Thomas Hofmann, and Karl Glas. 2022. "The identification of microplastics based on vibrational spectroscopy data – A critical review of data analysis routines." *TrAC Trends in Analytical Chemistry* 148:116535. doi: <https://doi.org/10.1016/j.trac.2022.116535>.
- Weisser, Jana, Teresa Pohl, Natalia P. Ivleva, Thomas F. Hofmann, and Karl Glas. 2022. "Know What You Don't Know: Assessment of Overlooked Microplastic Particles in FTIR Images." *Microplastics* 1 (3):359-376. doi: 10.3390/microplastics1030027.
- Wiesheu, Alexandra C., Philipp M. Anger, Thomas Baumann, Reinhard Niessner, and Natalia P. Ivleva. 2016. "Raman microspectroscopic analysis of fibers in beverages." *Anal. Methods* 8 (28):5722-5725. doi: 10.1039/c6ay01184e.
- Winkler, Anna, Nadia Santo, Marco Aldo Orteni, Elisa Bolzoni, Renato Bacchetta, and Paolo Tremolada. 2019. "Does mechanical stress cause microplastic release from plastic water bottles?" *Water Research* 166:115082. doi: <https://doi.org/10.1016/j.watres.2019.115082>.
- Witzig, Cordula S., Corinna Földi, Katharina Wörle, Peter Habermehl, Marco Pittroff, Yanina K. Müller, Tim Lauschke, Peter Fiener, Georg Dierkes, Korbinian P. Freier, and Nicole Zumbülte. 2020. "When Good Intentions Go Bad—False Positive Microplastic Detection Caused by Disposable Gloves." *Environmental Science & Technology* 54 (19):12164-12172. doi: 10.1021/acs.est.0c03742.
- Wright, Stephanie L., Richard C. Thompson, and Tamara S. Galloway. 2013. "The physical impacts of microplastics on marine organisms: A review." *Environmental Pollution* 178:483-492. doi: <https://doi.org/10.1016/j.envpol.2013.02.031>.
- Xu, Jun-Li, Martin Hassellöv, Keping Yu, and Aoife A. Gowen. 2020. "Microplastic Characterization by Infrared Spectroscopy." In *Handbook of Microplastics in the Environment*, edited by Teresa Rocha-Santos, Mónica Costa and Catherine Mouneyrac, 1-33. Cham: Springer International Publishing.
- Xu, Jun-Li, Xiaohui Lin, Siewert Hugelier, Ana Herrero-Langreo, and Aoife A. Gowen. 2021. "Spectral imaging for characterization and detection of plastic substances in branded teabags." *Journal of Hazardous Materials* 418:126328. doi: <https://doi.org/10.1016/j.jhazmat.2021.126328>.
- Xu, Jun-Li, Kevin V. Thomas, Zisheng Luo, and Aoife A. Gowen. 2019. "FTIR and Raman imaging for microplastics analysis: State of the art, challenges and prospects." *TrAC Trends in Analytical Chemistry* 119:115629. doi: <https://doi.org/10.1016/j.trac.2019.115629>.
- Xu, Qing-Song, and Yi-Zeng Liang. 2001. "Monte Carlo cross validation." *Chemometrics and Intelligent Laboratory Systems* 56 (1):1-11. doi: [https://doi.org/10.1016/S0169-7439\(00\)00122-2](https://doi.org/10.1016/S0169-7439(00)00122-2).
- Yang, Ling, Yulan Zhang, Shichang Kang, Zhaoqing Wang, and Chenxi Wu. 2021. "Microplastics in soil: A review on methods, occurrence, sources, and potential risk." *Science of The Total Environment* 780:146546. doi: <https://doi.org/10.1016/j.scitotenv.2021.146546>.

## 7. Appendix A: Raw Data of unpublished data presented

| Initial sample wet weight [g] | Process  | Dry mass on filters [g] |        |        |        |        | Sum (g) | Dry mass after Treatment [g/g] | Initial Dry mass [g] | Degraded [%] | Mean [%] | Standard deviation [%] |
|-------------------------------|--|-------------------------|--------|--------|--------|--------|---------|--------------------------------|----------------------|--------------|----------|------------------------|
|                               |  | 5 µm                    | 10 µm  | 50 µm  | 100 µm |        |         |                                |                      |              |          |                        |
| 0.209                         | des.H2O 100ml/3,5h   | 0.0000                  | 0.0000 | 0.0010 | 0.0050 | 0.0060 | 0.0287  |                                |                      |              |          |                        |
| 5.905                         | Dest. H2O (300)/12h/Fenton(100/12,5)/2h/20-30C+Ask.S(25)/1h/cooled | 0.0001                  | 0.0030 | 0.0145 | 0.0645 | 0.0821 | 0.0139  | 0.1695                         | 91.80%               | 92.01%       | 0.004    |                        |
| 6.142                         | Dest. H2O (300)/12h/Fenton(100/12,5)/2h/20-30C+Ask.S(25)/1h/cooled | 0.0006                  | 0.0024 | 0.0101 | 0.0680 | 0.0811 | 0.0132  | 0.1763                         | 92.51%               |              |          |                        |
| 6.1832                        | Dest. H2O (300)/12h/Fenton(100/12,5)/2h/20-30C+Ask.S(25)/1h/cooled | 0.0002                  | 0.0034 | 0.0073 | 0.0801 | 0.0910 | 0.0147  | 0.1775                         | 91.71%               |              |          |                        |
| 6.026                         | Dest. H2O (300)/2h/Fenton(100/12,5)/3h/20-30C                      | 0.0000                  | 0.0121 | 0.0166 | 0.0890 | 0.1177 | 0.0195  | 0.1730                         | 88.71%               | 88.62%       | 0.002    |                        |
| 6.0222                        | Dest. H2O (300)/2h/Fenton(100/12,5)/3h/20-30C                      | 0.0003                  | 0.0097 | 0.0112 | 0.0947 | 0.1159 | 0.0192  | 0.1729                         | 88.87%               |              |          |                        |
| 5.9275                        | Dest. H2O (300)/2h/Fenton(100/12,5)/3h/20-30C                      | 0.0003                  | 0.0101 | 0.0132 | 0.0945 | 0.1181 | 0.0199  | 0.1702                         | 88.29%               |              |          |                        |
| 6.0032                        | Dest. H2O (300)/2h/buffer(100)&Cellulase(1)/24h/40C                | 0.0025                  | 0.0066 | 0.0024 | 0.0630 | 0.0745 | 0.0124  | 0.1723                         | 92.80%               | 92.52%       | 0.005    |                        |
| 6.0057                        | Dest. H2O (300)/2h/buffer(100)&Cellulase(1)/24h/40C                | 0.0016                  | 0.0075 | 0.0034 | 0.0607 | 0.0732 | 0.0122  | 0.1724                         | 92.93%               |              |          |                        |
| 6.0109                        | Dest. H2O (300)/2h/buffer(100)&Cellulase(1)/24h/40C                | 0.0014                  | 0.0097 | 0.0043 | 0.0694 | 0.0848 | 0.0141  | 0.1726                         | 91.82%               |              |          |                        |

Appendix Table 1. Raw data of chemical and enzymatic degradation of pear puree (see sections 1.3.2, 3.1.1, and 4.1). All numbers rounded to integers.

7 - Appendix A: Raw Data of unpublished data presented

| Initial sample wet weight [g] | Process  | Dry mass on filters [g] |        |        |        |         | Dry mass after Treatment [g/g] | Initial Dry mass [g] | Degraded [%] | Mean [%] | Standard deviation [%] |
|-------------------------------|--|-------------------------|--------|--------|--------|---------|--------------------------------|----------------------|--------------|----------|------------------------|
|                               |  | 5 µm                    | 10 µm  | 50 µm  | 100 µm | Sum (g) |                                |                      |              |          |                        |
| 0.2085                        | des.H2O 100ml/3,5h   | 0.0008                  | 0.0002 | 0.0004 | 0.0027 | 0.0041  | 0.0197                         |                      |              |          |                        |
| 6.0389                        | Dest. H2O (300)/12h/Fenton(100/12,5)/2h/20-30C+Ask.S(25)/1h/cooled | 0.0004                  | 0.0015 | 0.0057 | 0.0138 | 0.0214  | 0.0035                         | 0.1188               | 97.02%       | 97.24%   | 0.003                  |
| 6.0804                        | Dest. H2O (300)/12h/Fenton(100/12,5)/2h/20-30C+Ask.S(25)/1h/cooled | 0.0003                  | 0.0016 | 0.0073 | 0.0077 | 0.0169  | 0.0028                         | 0.1196               | 97.68%       |          |                        |
| 6.208                         | Dest. H2O (300)/12h/Fenton(100/12,5)/2h/20-30C+Ask.S(25)/1h/cooled | 0.0000                  | 0.0016 | 0.0049 | 0.0160 | 0.0225  | 0.0036                         | 0.1221               | 97.03%       |          |                        |
| 5.956                         | Dest. H2O (300)/2h/Fenton(100/12,5)/2h/20-30C                      | 0.0002                  | 0.0104 | 0.0156 | 0.0321 | 0.0583  | 0.0098                         | 0.1171               | 91.64%       | 91.61%   | 0.004                  |
| 5.9612                        | Dest. H2O (300)/2h/Fenton(100/12,5)/2h/20-30C                      | 0.0000                  | 0.0096 | 0.0144 | 0.0313 | 0.0553  | 0.0093                         | 0.1172               | 92.09%       |          |                        |
| 5.9824                        | Dest. H2O (300)/2h/Fenton(100/12,5)/2h/20-30C                      | 0.0000                  | 0.0058 | 0.0126 | 0.0443 | 0.0627  | 0.0105                         | 0.1176               | 91.09%       |          |                        |
| 6.0772                        | Dest. H2O (300)/2h/buffer(100)&Cellulase(1)/24h/40C                | 0.0015                  | 0.0076 | 0.0048 | 0.0125 | 0.0264  | 0.0043                         | 0.1195               | 96.36%       | 96.68%   | 0.002                  |
| 5.9744                        | Dest. H2O (300)/2h/buffer(100)&Cellulase(1)/24h/40C                | 0.0026                  | 0.0065 | 0.0057 | 0.0074 | 0.0222  | 0.0037                         | 0.1175               | 96.84%       |          |                        |
| 5.9884                        | Dest. H2O (300)/2h/buffer(100)&Cellulase(1)/24h/40C                | 0.0026                  | 0.0066 | 0.0051 | 0.0079 | 0.0222  | 0.0037                         | 0.1178               | 96.85%       |          |                        |
| 6.0086                        | Dest. H2O (300)/2h/buffer(100)&Xylanase(1g)/3,5h/40C               | 0.0030                  | 0.0193 | 0.0123 | 0.0078 | 0.0424  | 0.0071                         | 0.1182               | 94.03%       |          |                        |

Appendix Table 2. Raw data of chemical and enzymatic degradation of strawberry puree (see sections 1.3.2, 3.1.1, and 4.1). All numbers rounded to integers.

7 - Appendix A: Raw Data of unpublished data presented

|                       | Flour (dry mass content: 90.17%) |         |         |  |                                | Dough (dry mass content: 50.31%) |            |            |  |                                | blanks                             |                                    | LOD<br>(extrapolated<br>mean of<br>blanks + 3*<br>standard<br>deviation) |
|-----------------------|----------------------------------|---------|---------|--|--------------------------------|----------------------------------|------------|------------|--|--------------------------------|------------------------------------|------------------------------------|--|
|                       | flour 1                          | flour 2 | flour 3 | flour<br>mean,<br>extrapola<br>ted to 1 g<br>dry<br>weight | flour<br>standard<br>deviation | dough<br>1                       | dough<br>2 | dough<br>3 | dough<br>mean,<br>extrapolated<br>to 1 g dry<br>weight | dough<br>standard<br>deviation | blank from<br>flour<br>examination | blank from<br>dough<br>examination |  |
| sample mass (wet) [g] | 0.1500                           | 0.1500  | 0.1500  |  |                                | 0.1500                           | 0.1500     | 0.1500     |  |                                | 0.1500                             | 0.1500                             |  |
| examined subpart      | 100%                             | 100%    | 100%    |  |                                | 100%                             | 100%       | 100%       |  |                                | 100%                               | 100%                               |  |
| PP                    | 6                                | 0       | 9       | 37   | 28                             | 15                               | 21         | 40         | 336  | 141                            | 4                                  | 8                                  | 114  |
| PS                    | 0                                | 0       | 0       | 0  | 0                              | 7                                | 0          | 0          | 31   | 44                             | 0                                  | 0                                  | 0  |
| PE                    | 13                               | 11      | 18      | 104  | 22                             | 24                               | 19         | 29         | 318  | 54                             | 5                                  | 13                                 | 199  |
| PA                    | 9                                | 24      | 12      | 111  | 48                             | 8                                | 15         | 8          | 137  | 44                             | 5                                  | 0                                  | 95   |
| PET                   | 0                                | 0       | 0       | 0  | 0                              | 0                                | 0          | 0          | 0  | 0                              | 0                                  | 3                                  | 57   |
| EvOH                  | 7                                | 0       | 5       | 30   | 22                             | 11                               | 20         | 16         | 208  | 49                             | 2                                  | 6                                  | 95   |
| PVC                   | 0                                | 0       | 12      | 30   | 42                             | 0                                | 9          | 5          | 62   | 49                             | 7                                  | 0                                  | 133  |
| PLA                   | 3                                | 0       | 4       | 17   | 13                             | 0                                | 0          | 0          | 0  | 0                              | 0                                  | 3                                  | 57   |
| PTFE                  | 0                                | 0       | 3       | 7  | 10                             | 0                                | 0          | 0          | 0  | 0                              | 0                                  | 0                                  | 0  |
| sum                   | 38                               | 35      | 63      | 335  | 93                             | 65                               | 84         | 98         | 1091   | 179                            | 23                                 | 33                                 | 408  |

Appendix Table 3. Raw data from examination of flour and dough (see sections 3.5 and 4.4) from Hubin (2020). All numbers rounded to integers.

7 - Appendix A: Raw Data of unpublished data presented

---

|                           | sea salt |        | blank | LOD<br>(estimated as<br>blank * 1.75) |
|---------------------------|----------|--------|-------|---------------------------------------|
|                           | salt 1   | salt 2 |       |                                       |
| sample mass (wet=dry) [g] | 1000     | 1000   | 1000  |                                       |
| examined subpart          | 100%     | 100%   | 100%  |                                       |
| PP                        | 32       | 56     | 1     | 2                                     |
| PS                        | 8        | 28     | 4     | 7                                     |
| PE                        | 52       | 88     | 3     | 5                                     |
| PA                        | 32       | 16     | 0     | 0                                     |
| PET                       | 24       | 16     | 1     | 2                                     |
| EvOH                      | 20       | 24     | 4     | 7                                     |
| PVC                       | 56       | 32     | 6     | 11                                    |
| PLA                       | 36       | 20     | 0     | 0                                     |
| PTFE                      | 0        | 0      | 0     | 0                                     |
| sum                       | 260      | 280    | 19    | 33                                    |

Appendix Table 4. Raw data from examination of flour and dough (see sections 3.5 and 4.4) from Hubin (2020). All numbers rounded to integers.

7 - Appendix A: Raw Data of unpublished data presented

|   | homemade apple puree (dry mass content 9.57%) |                      |                      |   |                                   | industrial apple puree (dry mass content 11.72%) |                        |                        |   |                                     | blanks      |             | LOD<br>(extrapolated<br>mean of blanks<br>+ 3* standard<br>deviation) |
|---|---|----------------------|----------------------|---|-----------------------------------|--|------------------------|------------------------|---|-------------------------------------|-------------|-------------|---|
|   | homemade<br>1 (AM10)                          | homemade<br>2 (AM11) | homemade<br>3 (AM12) | mean<br>homemade,<br>extrapolated<br>to 1 g dry<br>weight | standard<br>deviation<br>homemade | industrial<br>1 (AM13)                           | industrial<br>2 (AM14) | industrial<br>3 (AM15) | mean<br>industrial,<br>extrapolated<br>to 1 g dry<br>weight | standard<br>deviation<br>industrial | blank<br>P1 | blank<br>P2 |   |
| sample<br>mass<br>(wet) [g]                   | 6.5003  | 6.5005               | 6.5007               | n/a   | n/a                               | 6.5002   | 6.5004                 | 6.5002                 | n/a   | n/a                                 | 6.5005      | 6.5004      | n/a   |
| examined<br>subpart<br>(see page<br>24 of BT) | 64%   | 75%                  | 82%                  | n/a   | n/a                               | 50%  | 70%                    | 50%                    | n/a   | n/a                                 | 100%        | 100%        | n/a   |
| PP  | 3   | 4                    | 0                    | 5   | 4                                 | 0  | 3                      | 4                      | 4   | 3                                   | 10          | 9           | 16  |
| PS  | 2   | 2                    | 3                    | 5   | 1                                 | 6  | 3                      | 0                      | 5   | 4                                   | 0           | 0           | 0   |
| PE  | 23  | 10                   | 23                   | 41  | 15                                | 30   | 29                     | 0                      | 32  | 22                                  | 19          | 11          | 39  |
| PA  | 1   | 0                    | 0                    | 1   | 1                                 | 0  | 0                      | 0                      | 0   | 0                                   | 3           | 2           | 6   |
| EvOH  | 17  | 1                    | 0                    | 15  | 20                                | 0  | 0                      | 0                      | 0   | 0                                   | 0           | 0           | 0   |
| PVC   | 2   | 0                    | 0                    | 2   | 2                                 | 0  | 0                      | 0                      | 0   | 0                                   | 0           | 0           | 0   |
| PTFE  | 3   | 5                    | 7                    | 11  | 3                                 | 2  | 15                     | 7                      | 13  | 9                                   | 11          | 31          | 74  |
| PET   | 0   | 1                    | 2                    | 2   | 2                                 | 5  | 0                      | 0                      | 3   | 4                                   | 3           | 2           | 6   |
| sum   | 51  | 23                   | 35                   | 82  | 33                                | 43   | 50                     | 11                     | 56  | 27                                  | 46          | 55          | 92  |

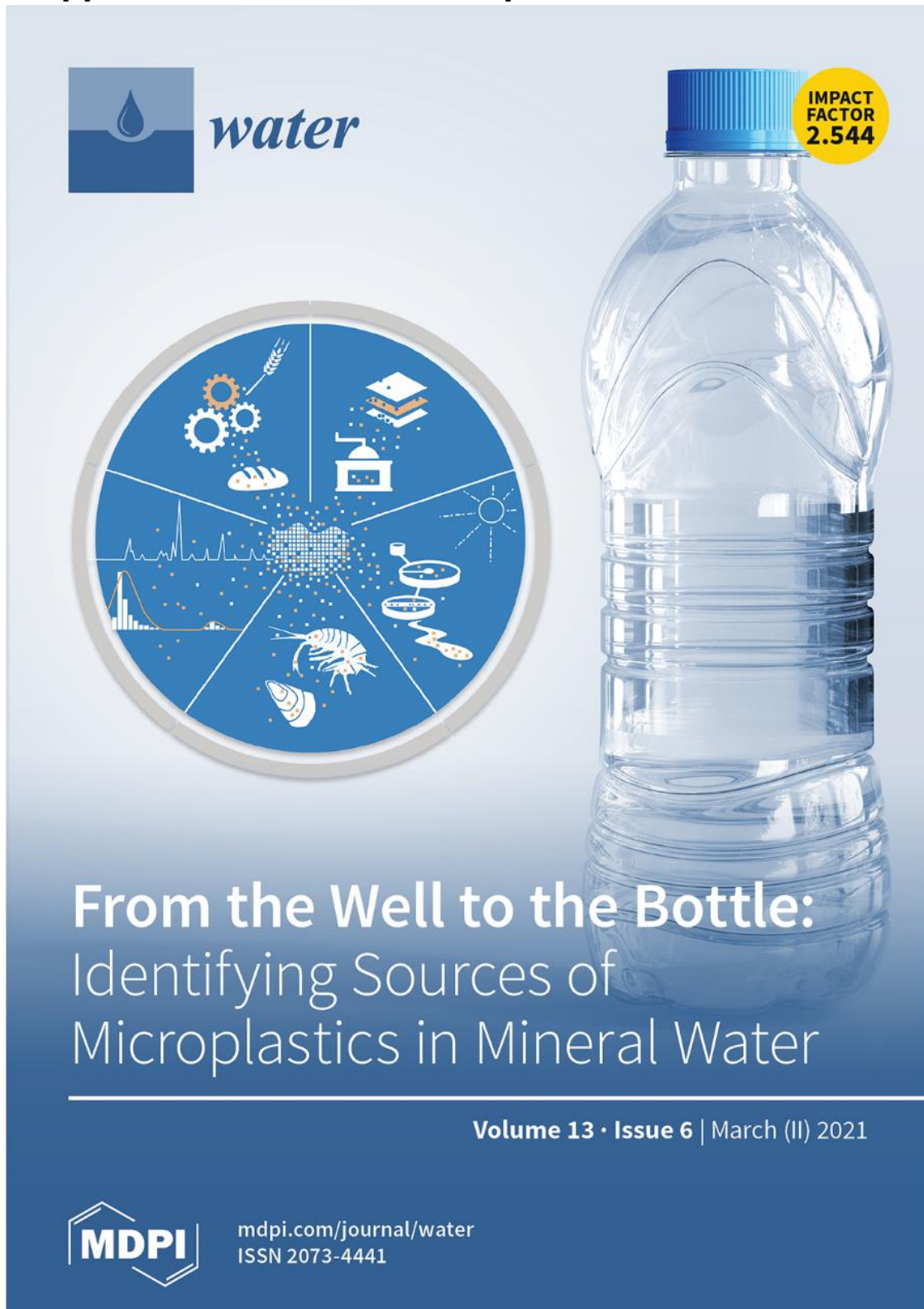
Appendix Table 5. Raw data from examination of homemade and industrially made apple puree (see sections 3.5 and 4.4) from Eberl (2020). All numbers rounded to integers.

7 - Appendix A: Raw Data of unpublished data presented

|                  | PLA tea bags |       |       |      |                    | standard tea bags |            |            |      |                    | blanks         |                     | LOD (mean blanks + 3* standard deviation) |
|------------------|--------------|-------|-------|------|--------------------|-------------------|------------|------------|------|--------------------|----------------|---------------------|---|
|                  | PLA 1        | PLA 2 | PLA 3 | mean | standard deviation | standard 1        | standard 2 | standard 3 | mean | standard deviation | blank PLA bags | blank standard bags |   |
| teabags examined | 1            | 1     | 1     |      |                    | 1                 | 1          | 1          |      |                    | 1              | 1                   |   |
| examined subpart | 100%         | 100%  | 100%  |      |                    | 100%              | 100%       | 100%       |      |                    | 100%           | 100%                |   |
| PP               | 1            | 5     | 1     | 2    | 2                  | 2                 | 3          | 6          | 4    | 2                  | 0              | 1                   | 2   |
| PS               | 0            | 1     | 0     | 0    | 0                  | 0                 | 1          | 0          | 0    | 0                  | 0              | 0                   | 0   |
| PE               | 4            | 1     | 1     | 2    | 1                  | 2                 | 2          | 0          | 1    | 1                  | 0              | 1                   | 2   |
| PA               | 4            | 5     | 0     | 3    | 2                  | 1                 | 0          | 0          | 0    | 0                  | 4              | 3                   | 5   |
| PET              | 2            | 4     | 4     | 3    | 1                  | 0                 | 4          | 3          | 2    | 2                  | 1              | 1                   | 1   |
| EvOH             | 0            | 0     | 0     | 0    | 0                  | 0                 | 0          | 0          | 0    | 0                  | 0              | 0                   | 0   |
| PVC              | 3            | 0     | 0     | 1    | 1                  | 0                 | 0          | 0          | 0    | 0                  | 0              | 0                   | 0   |
| PLA              | 7            | 2     | 17    | 9    | 6                  | 0                 | 0          | 0          | 0    | 0                  | 0              | 0                   | 0   |
| PTFE             | 1            | 3     | 4     | 3    | 1                  | 5                 | 5          | 6          | 5    | 0                  | 6              | 6                   | 6   |
| sum              | 22           | 21    | 27    | 23   | 3                  | 10                | 15         | 15         | 13   | 2                  | 11             | 12                  | 13  |

Appendix Table 6. Raw data from examination of tea in PLA and standard 'paper' tea bags (see sections 3.5 and 4.4) from Müller (2020). All numbers rounded to integers.

## 8. Appendix B: Peer-reviewed publications



Appendix Figure 1. One publication from this project was chosen as the cover story by the editorial board of *water*